Analytical and Data driven Strategies to Advance Operational Flexibility of Smart Grids with Bulk System Renewables and Distributed Energy Resources

by

Mohammad Ghaljehei

A Dissertation Presented in Partial Fulfillment
of the Requirements for the Degree
Doctor of Philosophy

Approved April 2022 by the
Graduate Supervisory Committee:

Mojdeh Khorsand, Chair
Vijay Vittal
Meng Wu
Yang Weng

ARIZONA STATE UNIVERSITY

May 2022

ABSTRACT

Due to the new and old challenges, modern-day market management systems continue to evolve, including market reformulations, introducing new market products, and proposing new frameworks for integrating distributed energy resources (DERs) into the wholesale markets. Overall, questions is regarding how to reflect these essential changes in the market models (design, reformulation, and coordination frameworks), design market-based incentive structures to adequately compensate participants for providing ancillary services, and assess these impacts on market settlements.

First, this dissertation proposes the concept of securitized-LMP to solve the issue of how market participants should be compensated for providing N-1 reliability services. Then, pricing implications and settlements of three state-of-art market models are compared. The results show that with a more accurate representation of contingencies in the market models, N-1 grid security requirements are originally captured; thereby, the value of service provided by generators is reflected in the prices to achieve grid security.

Also, new flexible ramping product (FRP) designs are proposed for different market processes to (i) schedule day-ahead (DA) FRP awards that are more adaptive concerning the real-time (RT) 15-min net load changes, and (ii) address the FRP deployability issue in fifteen-minute market (FMM). The proposed market models performance with enhanced FRP designs is compared against the DA market and FMM models with the existing FRP design through a validation methodology based on California independent system operator (ISO) RT operation. The proposed FRP designs lead to less expected final RT operating cost, higher reliability, and fewer RT price spikes.

Finally, this dissertation proposes a distribution utility and ISO coordination framework to enable ISO to manage the wholesale market while preemptively not allowing aggregators to cause distribution system (DS) violations. To this end, this coordination framework architecture utilizes the statistical information obtained using different DS conditions and data-mining algorithms to predict the aggregators qualified maximum capacity. A validation phase considering Volt-VAr support provided by distributed PV smart inverters is utilized for evaluate the proposed model performance. The proposed model produces wholesale market awards for aggregators that fall within the DS operational limits and, consequently, will not impose reliable and safety issues for the DS.

ACKNOWLEDGMENTS

First and foremost, sincere thanks and appreciation must be given to my supervisor, Professor Mojdeh Khorsand, for her continual guidance and support throughout the entire process. Her passion and insights in cutting-edge research while being as close as possible to the industry practice have been genuinely inspirational, the impact of which cannot be easily stated on my academic experience and professional career. To Dr. Mojdeh Khorsand, I sincerely thank you for your time, the interdisciplinary knowledge you shared for this project, and the opportunities you provided for me in my life. To the rest of the professors throughout the courses of the curriculum of the Electrical Engineering Program, I want to thank you for your commitment to education, dedication, and practice in teaching the courses. Special thanks to Dr. Kory Hedman for being a truly inspirational teacher in the Energy Market and Operation research fields. I gained unprecedented knowledge during multiple meetings with him for the Power Systems Engineering Research Center (PSERC) project and his Electric Energy Markets course. Also, I would like to thank Dr. Yang Weng sincerely; I first got familiar with the data-mining field during his Machine Learning for Smart Grid course. I learned a lot and benefited greatly from his course for performing this project. Last but not least, I also want to thank Dr. Adolfo Escobedo for his outstanding and diligently-designed courses that I took at the Industrial Engineering department at Arizona State University in the Operation Research field. Furthermore, I would like to thank the great ECEE staff at Arizona State University, who work effortlessly to support us to smoothly research and study. In particular, I appreciate Toni Mengert, who was always knowledgeable and prompt on many occasions I sought her help.

I would also like to express my appreciation to the New York Independent System Operator (NYSIO) for giving me the opportunity to serve as an intern at the Energy Market team. I gained valuable insights into the Energy Market industry over the six months during which I did two internships at NYISO. I want to thank Muhammad Marwali, shubhrajit Bhattacharjee, and especially Hossein Lotfi for their dedication, the valuable knowledge they shared, and patience while mentoring me.

I would also like to extend my genuine gratitude to my committee members, Professor Vijay Vittal, Dr. Meng Wu, and Dr. Yang Weng, for your willingness to serve on my committee and their contribution and support in the search process. Thank you for all of your comments and suggestions, which helped me enrich the content of my thesis.

The Ph.D. life abroad would be tedious and complicated without the presence of friends who understand you. I have been privileged enough to have my dear Friends, Zahra Soltani, Mohammad Mousavi, Behrouz Azimian, Amir Pouladvand, Rana Pourmohamad, Reza Khalili, Hoda Shokrollahzadeh, Amirali Sabzehparvar, AmirHossein Tavakoli, Ramin Kaviani, Nima Taghipourbazargani and other friends beside me. My friendship with Mohammad and Behrouz goes back to our undergrad school, Iran University of Science and Technology (IUST). We started a long journey together from IUST. With all we could, being supportive in our personal and professional life or giving advice, we helped each other reach this level to finish our last course of study program here at the U.S. at Arizona State University, far from our home county. Zahra and I met before starting our master's program. During these years, she always has been there for me, considering all the complications her life has been through; I’m deeply grateful for almost everything I’ve experienced with her alongside this journey we started together

several years ago. If it wasn't for her, I might not have been the person with more passion for life who I am now.

Last but certainly not least, I must say my immense gratefulness to my family for their unending support; my parents, Zahra and Ebrahim, are why I got this far. Apart from the immense care they have had for me always, with all they had, they provided for my education and also taught me the highest levels of commitment and dedication. Furthermore, my bond with my sister, Fatemeh, cannot be described in words. She has always been a source of peace for me, and I always have been appreciative of her presence in my life.

TABLE OF CONTENTS

Page

CHAPTER Page

LIST OF TABLES

Table Page

Table Page

Table Page

LIST OF FIGURES

Figure Page

Figure Page

Figure Page

NOMENCLATURE

Acronyms

CAISO	California Independent System Operator
DA	Day-ahead
DDP	Desired dispatch point
EMS	Energy management system
FERC	Federal Energy Regulatory Commission
FRP	Flexible ramping product
ISO	Independent system operator
ISO-NE	ISO New England
KKT	Karush-Kuhn-Tucker
MILP	Mixed-integer linear programming
MISO	Midcontinent Independent System Operator
MMS	Market management system
NERC	North American Electric Reliability Corporation
NREL	National Renewable Energy Laboratory
NAE	National Academy of Engineering
LP	Linear programming
MILP	Mixed-integer linear programming
OMC	Out-of-market correction
PTDF	Power transfer distribution factor
RT	Real-time
UC	Unit commitment
SCUC	Security-constrained unit commitment

VOLL	Value of lost load
CS	Complementary slackness
NN	Neural networks
FMM	Fifteen-minute market
DER	Distributed energy resources
ESCUC	Extend security-constraint unit commitment
DS	Distribution system
PV	photovoltaics
RTD	Real-time dispatch

Sets and Indices

c	Index of operating state; 0 for the base-case, non-zero for contingencies.
g	Index of generators, $g \in G$.
k, ℓ	Index of transmission lines, $k, \ell \in K$.
n	Index for buses, $n \in N$.
t	Index for time periods, $t \in T$.
i	Index of solar power generations, $i \in I$.
w	Index of training scenarios for data-mining algorithm, $w \in W$.
s	Index of deployment scenarios, $s \in S$.
b	Index of blocks in linearized operating cost of generation resource, $e \in B$.
a	Index of aggregators, $a \in A$.
l	Index of lines in distribution system, $l \in \mathcal{K}$.
it	Index of iteration in the IVACOPF.

ni, nj	Index of buses in distribution system, $ni, nj \in \mathcal{P}$.
x	Index of phases in distribution system, $x \in \phi$.
e	Index of PV units without volt-VAr controller in distribution system, $e \in F2$.
f	Index of PV units without volt-VAr controller in distribution system, $e \in F1$.
sb	Index of substation in distribution system.
kc	Index of capacitors bank units, $kc \in \mathcal{C}$.
C_0, C_g, C_k	Set of scenarios representing base-case, generator, and line contingencies, respectively.
$g(n)$	Set of generators connected to node *n.*
$i(n)$	Set for solar power generations connected to node *n.*
$n(g)$	Set for the node of generation resource g.
$n(i)$	Set for the node of solar power generation i.
$sb(ni)$	Set of substations connected to bus ni in distribution system.
$a(ni)$	Set of aggregators connected to bus ni in distribution system.
$f1(ni)$	Set of PV units with Volt-VAr controller connected to bus ni in distribution system.
$f2(ni)$	Set of PV units without Volt-VAr controller connected to bus ni in distribution system.
$d(ni)$	Set of loads connected to bus ni in distribution system.
$\hbar(ni)$	Set of lines connected to bus ni in distribution system.

G^F Set for fast-start generation resource.

G^M Set for must-run generation resources in FMM.

Parameters and Constants

$c_g^{NL}, c_g^{SD}, c_g^{SU}$ No-load, shutdown, and startup costs of unit g.

$Load_{nt}$ Load at bus n at time period t.

$\bar{P}_g, \bar{u}_g, \bar{r}_g$ Day-ahead scheduled power output, commitment, and contingency reserve of unit g.

P_g^{max}, P_g^{min} Maximum output and minimum output of unit g.

$PTDF_{cnk}^{ref}$ Power transfer distribution factor during operating state c for line k for an injection at n.

$LODF_{k\ell}^{ref}$ Line outage distribution factor representing the change in flow on line k for the outage of line l.

c_g^p Variable cost of unit g ($/MWh).

$N1_k$ N-1 contingency indicator of transmission line k; 0 for a contingency on line k; otherwise, 1.

$N1_g$ N-1 contingency indicator of generator g; 0 for a contingency on generator g; otherwise, 1.

R_g^{HR}, R_g^{10} Hourly and 10-min ramp rates of unit g.

R_g^{SU}, R_g^{SD} Startup and shutdown ramp rates of unit g.

UT_g, DT_g Minimum up time and down time of unit g.

π_{BC} Probability of base-case operating state.

π_c	Probability of contingency operating state c.
P_k^{max}	Thermal rating of transmission line *k.*
η	Percentage of demand in proxy reserve requirements.
R_g^{15}	15-min ramp rates of unit g.
$FRup_{t,(.)}^{ih}$	15-min flexible ramping up requirement in period t.
$FRdown_{t,(.)}^{ih}$	15-min flexible ramping down requirement in period t.
NL_t	Hourly system net load in period t.
$NL_{t,(.)}^{ih}$	15-min system net load in period t.
NL_t^{max}	Maximum hourly system net load in period t.
$NL_{t,(.)}^{ih,max}$	Maximum 15-min system net load in period t.
NL_t^{min}	Minimum hourly system net load in period t.
$NL_{t,(.)}^{ih,min}$	Minimum 15-min system net load in period t.
$PTDF_{nk}$	Power transfer distribution factor for line k for an injection at bus n.
$Load_{nt}$	Load at bus n at time period t.
η	Percentage of demand in regulation reserve requirements.
$FRup_t$	Flexible ramping up requirement in period t.
$FRdown_t$	Flexible ramping down requirement in period t.
$Load_{nt}^{nodal}$	Nodal load at bus n at period t.
$\underline{F_g}$	Minimum operating cost of generation resource g for being committed with minimum power.
B_{gb}	Slope of block b in linearized operating cost of unit g.

c_g^{UR}, c_g^{DR}	Cost of upward and downward FRP of unit g.
$\overline{u_{gt}^h}$	Commitment status of generation resource g at period. t.
P_{ge}^{max}	Maximum power generation of block b in linearized operating cost of generation resource g at period t.
$Load_t^f$	Total forecasted load at period t.
$Load_t^{f,min}$	Minimum of total forecasted load at period t.
$Load_t^{f,max}$	Maximum of total forecasted load at period t.
P_{it}^{solar}	Power output of solar generation i at period t.
$P_{it}^{solar,min}$	Minimum power output of solar generation i at period t.
$P_{it}^{solar,max}$	Maximum power output of solar generation i at period t.
$P_{itw}^{solar,train}$	Power output of solar generation i at period t at training scenario w.
$Load_{ntw}^{train}$	Nodal load at bus n at period t at training scenario w.
$Load_{ts}^{f,dep}$	Total load at period t at deployment scenario s.
$P_{its}^{solar,dep}$	Power output of solar generation i at period t at deployment scenario s.
ζ_{gts}	Ramping response set factor of generation resource g at period t at deployment scenario s.
ΔNL_{ts}	Difference of netload of deployment scenario s at period $t+1$ compared to forecasted netload at period t.
$\overline{ur_{gt}}, \overline{dr_{gt}}$	Scheduled FMM upward and downward FRP awards of generation resource g in period t.

$\overline{f_{kts}^{dep,ur}}$, $\overline{f_{kts}^{dep,dr}}$ Calculated flow of transmission line k for post-deployment of FRPs at period t at deployment scenario s.

$c_a^A, c_a^{Res,A}$ Bid of energy and reserve of aggregator a.

R_a^{HR}, R_a^{10} Hourly and 10-min ramp rates of aggregator a.

R_a^{SU}, R_a^{SD} Startup and shutdown ramp rates of aggregator a.

$P_{a,t}^{max}, P_{a,t}^{min}$ Available maximum and minimum capacity of aggregator a at period t.

$P_{a,x}^{max}$ Available maximum capacity of aggregator a at phase x.

$P_{a,t}^{max,qualified}$ Qualified maximum capacity of aggregator a at period t.

$\overline{P_a^A}$ Independent system operator dispatch signal to aggregator a during a transmission-level uncertain event.

$y_l^{x,m}/Z_l^{x,m}$ Shunt admittance/impedance between phases x and m of line l in distribution system.

$R_l^{x,m}/X_l^{x,m}$ Resistance/Reactance between phases x and m of line l in distribution system.

$D_{d,x}^P/D_{d,x}^Q$ Active/Reactive load d at phase x in distribution system.

M A large positive number.

$I_l^{max,x}$ Maximum current of line l at phase x in distribution system.

$P_{f,x}^{PVV,av}$ Available active power of PV f with Volt-VAr at phase x in distribution system.

$Q_{f,x}^{PVV,max}$ Maximum reactive power of PV f with Volt-VAr at phase x in distribution system.

$S_{f,x}^{PVV}$ Apparent power rating of PV f with Volt-VAr at phase x in distribution system.

$P_{e,x}^{PV,av}$ Available active power of PV e without Volt-VAr at phase x in distribution system.

Variables

P_{gct} Output of unit g for operating state c at period t.

P_{nct}^{inj} Net power injection at bus n for operating state c at period t.

$FL^{0}{}_{\ell t}$ Flow on transmission line l at period t.

r_{gt} Contingency reserve of unit g at period t.

u_{gt} Unit commitment variable for unit g at period t.

v_{gt}, w_{gt} Startup and shutdown variables for unit g at period t.

d_{nt} Demand at bus n at period t.

λ_{nct} Locational marginal price at bus n for operating state time c at period t.

P_{gt} Power output of unit g at period t.

P_{nt}^{inj} Net power injection at bus n at period t.

$ur_{gt}^{ih}, dr_{gt}^{ih}$ Intra-hour ramping up and down auxiliary variables of unit g in period t.

r_{gt}^{u}, r_{gt}^{d} Up and down regulation reserve awards of unit g in period t.

δ_t Dual variable related to the nodal power balance constraint at period t.

λ_{nt} Dual variable related to the system-wide power balance constraint at bus n at period t.

α_{gt}^{+}, α_{gt}^{-} Dual variable related to the power output limit constraints of unit g at period t.

F_{kt}^{-}, F_{kt}^{+} Dual variable related to flow limit constraints of transmission line k at period t.

γ_{gt}^{+}, γ_{gt}^{-} Dual variable related to the hourly ramping limit constraints of unit g at period t.

β_{gt}^{+}, β_{gt}^{-} Dual variable related to the hourly up and down FRP constraints of unit g at period t.

π_{t}^{+}, π_{t}^{-} Dual variable related to the hourly ramping up and down requirement constraints at period t.

$\pi_{t}^{ih,+}$, $\pi_{t}^{ih,-}$ Dual variable related to the intra-hour 15-min ramping up and down requirement at period t.

ω_{gt}^{+}, ω_{gt}^{-} Dual variable related to the constraints of connection between up and down hourly and intra-hour ramp capabilities of unit g at period t.

$\beta_{gt}^{ih,+}$, $\beta_{gt}^{ih,-}$ Dual variable related to the intra-hour ramping up and down auxiliary variables constraints of unit g at period t.

$OC_{g}^{Rup,new}$ Total opportunity cost of unit g for providing proposed up FRP.

$OC_{g}^{Rdown,new}$ Total opportunity cost of unit g for providing proposed down FRP.

OC_{g}^{Rup} Total opportunity cost of unit g for providing general up FRP.

OC_{g}^{Rdown} Total opportunity cost of unit g for providing general down FRP.

ur_{gt}, dr_{gt} Upward and downward FRP awards of generation resource g in period t.

P_{gtb}	Power generation of block b in linearized operating cost of generation resource g at period t.
ur_{gts}^{a}	Upward ramping auxiliary variable of generation resource g at period t at deployment scenario s.
ur_{gts}^{a}	Downward ramping auxiliary variable of generation resource g at period t at deployment scenario s.
P_{at}^{A}	Power output of aggregator a at period t.
$P_{a,x}^{A}$	Power output of aggregator a at phase x.
r_{at}^{A}	Reserve award of aggregator a at period t.
u_{at}^{A}	Unit commitment variable for aggregator a at period t.
v_{at}^{A}, w_{at}^{A}	Startup and shutdown variables for aggregator a at period t.
$I_{l}^{r,x}/I_{l}^{im,x}$	Real/Imaginary part of current flow at phase x of line l in distribution system.
V_{ni}^{x}	Voltage magnitude at bus ni and phase x in distribution system.
$V_{ni}^{r,x}/V_{ni}^{im,x}$	Real/Imaginary part of voltage at bus ni and phase x in distribution system.
$I_{ni}^{r,x}/I_{ni}^{im,x}$	Real/Imaginary part of current injection at bus ni and phase x in distribution system.
$P_{f,x}^{PVV}/Q_{f,x}^{PVV}$	Active/Reactive power of PV f with Volt-VAr at phase x in distribution system.
$P_{sb,x}^{B}/Q_{sb,x}^{B}$	Active/Reactive power of substation sb at phase x in distribution system.
$Q_{kc,x}^{C}$	Reactive power of capacitor kc at phase x in distribution system.

Chapter 1.

INTRODUCTION

1.1. Motivation

Constantly changing system operating conditions, combined with the uncertainty and variability caused by amplified penetration of new resource-mix, such as solar generation, impose new challenges to the electric transmission and distribution systems. As a result, ancillary services are acquired in the electricity market to address these challenges so that a continuous supply of electricity is maintained. The ancillary services based on the Federal Energy Regulatory Commission (FERC) is defined as "those services necessary to support the transmission of electric power from seller to purchaser, given the obligations of control areas and transmitting utilities within those control areas, to maintain reliable operations of the interconnected transmission system" [1]. Also, distributed energy resources (DERs) are overgrowing in the US, most of which are smaller than 10 MW and are connected to the local distribution grids (DSs) [2]. This rapid growth can lead to significant challenges for independent system operators (ISOs) and distribution utilities, such as adding complexities in the energy and market management systems and potentially posing reliability and safety concerns to the transmission systems and DSs.

Due to the mentioned challenges, new and old, existing modern-day market management systems (MMSs) continue to evolve, including market reformulations, introducing new market products, and proposing new frameworks for integrating DERs into the wholesale markets. For example, there are proposals to transition the market auction models from a deterministic structure to a stochastic structure to better reflect the

impact of uncertain events such as contingencies. As another example, in recent years, ISOs have introduced new market products, i.e., flexible ramping products (FRPs), to account for extreme ramp events imposed on the system due to the evolving resource mix (e.g., renewables). It is pertinent to note that conventional ancillary service products comprise regulation (reserves to respond to small forecast deviations that frequently occur), 10-minute spinning and non-spinning reserves (to respond to contingencies), and 30-minute reserves (to replace other fast-response reserves after they are depleted). The final example is that FERC required all ISOs in the US to allow the participation of DER aggregations in the wholesale markets through Order No. 2222. Overall, questions remain regarding how to reflect these essential changes in the market models (design, reformulation, and coordination frameworks), design market-based incentive structures and pricing schemes to adequately compensate market participants for providing ancillary services, and assess these impacts on market settlements.

1.2. Representation of Uncertain Contingency Events in the Electric Energy Market Models

Electric systems are considered the greatest achievement of the 20th century by the National Academy of Engineering [3]. Operational scheduling of this sophisticated engineering system necessitates consideration of both economic and reliability aspects. However, due to its complexity, it is non-trivial to model all system components, capture detailed characteristics of all system assets, and satisfy all reliability requirements altogether. Hence, existing operational scheduling models are designed with approximations, e.g., DC approximation of power flow and approximations of the *N*-1 reliability mandate (i.e., loss of a single element, e.g. a generator or a non-radial

transmission asset, should not cause involuntary load shedding [4]). This mandate makes the underlying market model stochastic in nature.

Some of the existing electricity market operators solve day-ahead (DA) security-constrained unit commitment (SCUC) models with an approximation of the *N*-1 reliability mandate via a proxy reserve requirement [5], where the total of contingency reserves across the power system is forced to be greater than a certain threshold. Such SCUC models do not account for and guarantee post-contingency reserve deliverability.

Furthermore, some other operators have the model of zonal reserve requirements [6], e.g., Midcontinent independent system operator (MISO). This model cannot differentiate the generators within each zone regardless of their ability or inability to deploy reserve due to transmission system congestion. To compensate for the approximations in market models, the operator may intervene and make adjustments in the market solutions. Such interventions are referred to as out-of-market corrections (OMC) [7] or exceptional dispatches [8], which include committing additional generation units, or redispatching committed units. After an *N*-1 reliable dispatch solution is obtained, the settlements are calculated. The existing practice to calculate market settlements is to use the locational marginal prices (LMPs) from the DA SCUC (which have not been affected by the OMC) and the modified *N*-1 reliable dispatch solution [8]. Such market models are unable to account for the true value of reserve provided by each generator on a nodal basis. Consequently, they might not incentivize resources to do as directed by the market. These inabilities to impact market prices will lead to a *missing money* problem (i.e., insufficient compensation received by generators) and cause a natural unfairness as market participants might not be dispatched fairly with these pricing schemes.

In the electricity markets, compensation mechanisms are still a subject of debate. Some ISOs have capacity market auctions with estimated peak load and peak period prices in an attempt to compensate market participants for providing reliable services during peak periods [9]. Others, such as MISO, use convex hull pricing, which is an alternative pricing scheme in non-convex markets to clear the market while also minimizing the total uplift payments [10]. While these approaches are developed in an attempt to improve compensation mechanisms, the issue still persists; existing pricing schemes do not sufficiently reflect the true value of providing energy during contingencies, as these uncertain events are not explicitly included in the market models.

Explicit representation of the contingencies via a two-stage stochastic extensive-form SCUC (ESCUC) enables the inclusion of the value of reliability services into the LMPs and can reduce the *missing money* problem. ESCUC optimizes the recourse decision variables (or corrective actions) while explicitly considering the network constraints for the post-contingency state, which ensures nodal reserve deployment considering physical network limitations.

In addition, prior work proposed approaches based on the estimated post-contingency states using *pre-determined* participation factors. These approaches fill the gap between the traditional deterministic and the stochastic models by explicitly representing contingencies without any second-stage recourse decisions. For instance, line outage distribution factors (LODFs) can be used to model the transmission line contingencies [11] explicitly. Another example is CAISO, which intends to explicitly enforce the post-contingency transmission constraints for the generator contingencies using generator loss distribution factors (GDF) [11]. With the explicit modeling of contingency events within

the state-of-the-art market auction models, the industry is actually moving from the deterministic market models to a stochastic model. With such stochastic modeling, it is desirable for LMPs to reflect the value and quality of services provided by market participants in response to contingencies. However, there are unsolved issues regardless of the choice of uncertainty modeling: *generators compensation for providing N-1 reliability services as well as the impact of contingency modeling on prices.*

Apart from the above issue, in the context of stochastic market designs, the majority of prior work adopt an objective function that optimizes the base-case along with the expected cost of the post-contingency states [12]–[16]. However, there are a number of reasons why optimizing over an expected cost may not be the best choice. Firstly, during emergency conditions in real-time (RT), the operator may not exactly follow the proposed corrective actions since the intention during an emergency condition is not to minimize cost; rather, the goal is to recover from the event as quickly as possible to prevent future unforeseen problems that could lead to cascading outages. Furthermore, it is difficult to accurately predict the probability of outages, which itself can lead to different pricing implications and market solutions. There are other studies [17], [18], and [19] that minimize the base-case costs as their objective functions, while the model is still a stochastic two-stage SCUC with explicit representation of post-contingency states. References [12]–[19] aim to improve stochastic market models, whereas the proper design of objective function for these models has neither been analyzed nor included in prior work.

Thus, the main outcomes of this dissertation, with respect to transitioning the market auction models from the deterministic structure to the stochastic structure, are:

- to present the concept of securitized-LMP to capture the value of providing *N*-1 services.
- to inform market stakeholders about the impacts of contingency modeling approaches in the DA process and their implications on pricing and settlements. To do so, the pricing implication and settlements of the existing proxy serve policies, the state-of-the-art market auction models with estimated post-contingency states, and the ESCUC model with second-stage optimal recourse are compared.
- to analyze the choices of the objective function for the stochastic market models; it is beneficial to minimize the cost for all potential *N*-1 scenarios in the stochastic SCUC market model or if it is better to only minimize the base-case (or no contingency) cost.

1.3. Augmenting DA and RT Energy Markets with FRPs

The recent rapid integration of variable energy resources, such as wind and solar, causes new operational challenges for power systems. For example, 26 percent of the total generation of CAISO in 2018 was served by non-hydro renewable, an increase from 24, 22, and 18 percent in 2017, 2016, and 2015, respectively [20]. Due to this trending increase, one emerging challenge is the growth of variability and uncertainty in the system net load (i.e., actual system load minus total renewable generation), which has resulted in system ramp capability shortage [21]. Generally, there are two main ways to improve ramp responsiveness in the system. The first way is through improving the operational models and market design, e.g., more explicit representation of the uncertain

events in the model and introducing new market products. The second way is to incorporate new flexible resources, e.g., energy storage systems and demand response programs, into the electric system. Following the first procedure, some ISOs, e.g., CAISO [22] and midcontinent ISO (MISO) [23], have been augmenting their market models with ramping products in order to meet the net load variability and uncertainty and attain higher ramping responsiveness from existing flexible resources. In this dissertation, such products are referred to as FRP, although they are also called "flexiramp" in CAISO [22] and "ramp capability" in MISO [23].

Two new market design variables, i.e., flexible ramp up and flexible ramp down capabilities, are introduced to the operating market models by implementing the FRPs. The FRPs withhold the ramp capabilities from the flexible resources in a way that better reposition them at time interval t to be able to respond to the net load's variations and uncertainty at time $t+1$. The upward and downward ramping requirements are illustrated in Fig. 1.1. The ramp capability product has been implemented in the CAISO's RT market since Fall 2016, where requirements are set to manage the net load variations and uncertainty 5-min ahead [24]. For MISO, the ramp capability product has been implemented in its RT market since Spring 2016. For this market, requirements are set to manage net load variations and uncertainty 10-min ahead, while the RT dispatch is performed for 5-min intervals [25].

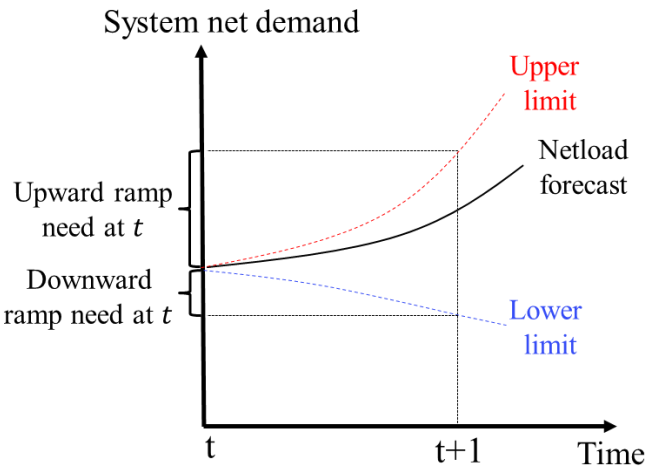

Fig. 1.1. The Concept of Ramping Requirement [26].

FRP differs from the other ancillary services, namely regulation and contingency reserves, in a couple of ways. First, contingency reserves (i.e., spinning and non-spinning reserves) are called mainly during contingency conditions, specifically during generation contingencies, according to the current practices of most ISOs, i.e., contingency reserves are not deployed frequently unless for outage events [27], [28]. Also, the regulation product is dispatched after the last market processes (i.e., RT dispatch) through the automatic generation control (AGC). However, the FRP is ramp capability reserved at one period to respond to net load changes (in both directions, up and down) in the next period to improve the system dispatch flexibility inside the RT operational scheduling processes (i.e., RT unit commitment and RT dispatch). Thus, FRP is deployed continuously in the RT scheduling processes [22], [27]. Some markets, including CAISO, acknowledge that traditional regulation and contingency-based reserve products cannot provide sufficient ramp capability; therefore, new market products (i.e., FRP) are necessary [29]. Furthermore, increasing the system ramp capability through increased

regulation requirements or using contingency reserve capacity was not selected based on the studies carried out by MISO [30].

1.3.1. Introducing FRPs to the DA Energy Markets

There have been intentions of modeling and procuring FRP in the DA market in order to ensure resource adequacy for meeting the ramping needs in the RT markets. For example, CAISO has started market initiatives to add FRP to its DA market to correctly position and commit resources to address uncertainty and variability in the net load, especially meeting the ramping needs in the fifteen-minute market (FMM), i.e., the next closest market to DA [31] and [32]. In previous work and existing industry proposals [33]–[36] and [22], the DA FRP is designed in such a way that resultant added ramp capabilities must be able to respond to variability (foreseen) and uncertainty (unforeseen) changes in net load between hour t and next hour, $t+1$. However, this FRP design (called general FRP design in this dissertation) does not consider the magnitude of intra-hour net load changes in the following RT market processes with shorter scheduling granularity (e.g., 15-min scheduling granularity). An essential goal of modeling the hourly FRP is to increase the system ramp capability to follow the realized net load in the next RT market processes (i.e., FMM) [22]. In this situation, the general FRP may not be able to accommodate the steep realized RT 15-min net load changes as they happen in shorter periods of time, and their effects are not considered when the hourly FRP decisions are made in DA. Two examples of such cases are shown through cases I and II in Fig. 1.2. CAISO also acknowledges the necessity of meeting 15-min ramping needs by hourly reserved ramp capabilities and DA schedules as specified in [31], [32]: "*Steep net load differences between 15-minute intervals (granularity differences) may result in 15-*

minute ramp infeasibility due to mid-point to mid-point hourly scheduling". It is worth noting that if there are insufficient ramp capabilities in the system, the ISOs may not be able to serve the demand totally; there may not be ready-to-action ramp-responsive generation resources in the system to follow the net load changes, which potentially can jeopardize system reliability. Moreover, such system ramp capability shortage can cause high penalty prices during the RT market processes and consequently create market inefficiency in the long run [28], [37]. With the above discussion, there is a need for a detailed design of the FRP in the DA market in order to ensure that enough ramp capabilities are available from ramp-responsive and yet non-expensive units; an effective FRP modeling in DA operation prepositions and commits the generation units and enables them to respond to sharp transitions of RT 15-min net load.

Although it is vital to evaluate both the efficiency and reliability, it is also necessary to evaluate the incentive structure for the resources that provide FRPs. Generally, the ancillary services can be dispatched and priced based on two different market models [38]: sequential or co-optimized market designs. In the sequential market design, one of the commodities (i.e., energy or ancillary service) is dispatched and cleared first. Then the remaining commodity is optimized in the subsequent market, considering the results of the first market. Both commodities are optimized simultaneously and cleared in the same process in the co-optimized market design. Among these two market designs, generally, the latter has better performance [39]. Note that all the electric energy markets in the United States have adopted co-optimization of energy and ancillary services. Thus, this dissertation follows the same structure of co-optimization of energy and ancillary services.

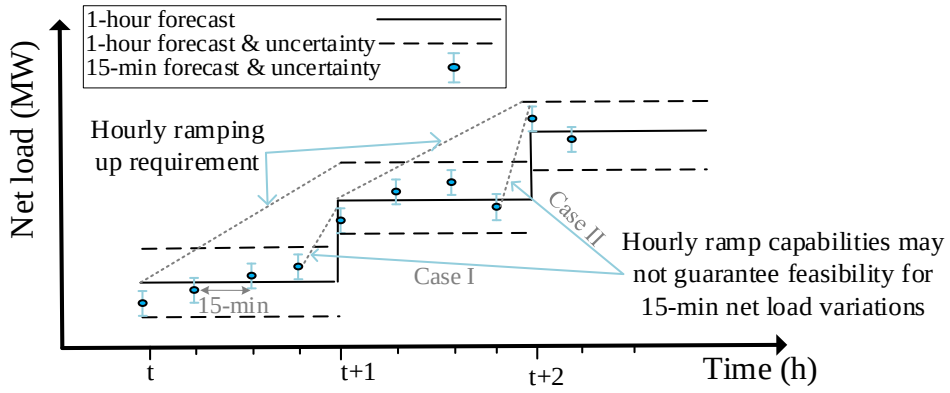

Fig. 1.2. Hourly FRP Versus 15-Min Variability and Uncertainty.

It is pertinent to note that when the energy and an ancillary service product are co-optimized, and no bids are submitted for the ancillary service product, the resources are compensated for procuring the ancillary service based on the lost opportunity cost (i.e., lost net profit from the energy market due to out of merit dispatch) [28], [40]. Similarly, in the context of FRP, the ramp-responsive resources are dispatched out of merit to provide the ramp capabilities, while generally no bids/offers are submitted for FRP [28]. For example, a generation unit with less operating cost but higher flexibility, e.g., ramp rate, may be held back from producing more due to allocating its capacity and ramping capability to FRP. Thus, the lost opportunity cost should be provided to the ramp-responsive resources for being dispatched out of merit to make the FRP available. This market-based payment has already been well developed for the general FRP design and the RT FRP; the cost is generally calculated through the shadow price (dual variable) of the FRP requirement constraint multiplied by the FRP quantity [28]. For example, [37] introduces the FRP in the RT market to manage ramping shortage and settles this product based on the above general FRP market payment structure. Also, [40] compares a time-coupled multi-period market (TCMPM) model against a single-period market (SPM)

model with FRP, wherein the SPM is settled based on the above general FRP market payment structure, and TCMPM has only the first interval economically binding. Then, cross interval marginal price (CIMP) is proposed to settle RT multi-period market models with only one economically binding interval, but since all the intervals in the DA market are economically binding, there is no need for the CIMP in the DA market [40]. Nevertheless, if the FRP design is modified, the market-based incentives and/or compensations in terms of the lost opportunity cost based on the above common approach may not be enough and need to be calculated differently to encourage ramp-responsive resources to follow market decisions. However, this step (i.e., market-based incentive analyses for FRP) often is ignored in the majority of studies with DA FRP design.

One of the goals of this dissertation is to complement proposed efforts by industry and previous work to more precisely schedule DA FRP without adding too much complexity to the DA operational scheduling models so that the dispatch flexibility in the FMM increases. Furthermore, appropriate market-based incentives are designed for ramp-responsive resources to make the ramp capabilities (awarded based on the corresponding enhanced FRP design) available.

The main outcomes of this dissertation, with respect to introducing FRPs to the DA markets, are:

- to propose a novel FRP requirement for the DA market to preposition and commit ramp-responsive resources to respond to sharp transitions in the RT 15-min net load.

- to design corresponding market payment policies using primal-dual market formulations that accurately reflect the value of awarded ramp capabilities through the proposed FRP design.
- to create a validation methodology that mimics the RT market operation of CAISO in order to evaluate both efficiency and reliability of the proposed FRP design against the general FRP design.
- to conduct comprehensive analyses and comparisons of the DA market structure based on the proposed FRP design with (i) the DA market model incorporating only regulation reserve, and (ii) the DA market model with general FRP design. These analyses include their impacts on market efficiency, settlements, and system reliability.

1.3.2. FRPs Deployability Issue in the FMMs

Since the FRP requirements implemented by industry or other work are based on the proxy system-wide or zonal requirements, there is no guarantee that awarded FRPs will actually be deployable without violating transmission line limits. Please note that with deployability issues, we mean that we should assign FRP awards to qualified ramp-responsive resources that are not behind the transmission bottlenecks. The reason can simply be associated with the fact that the FRP post-deployment deliverability within the transmission line limits is disregarded when making decisions on the FRP awards. More advanced techniques to deal with the uncertainty imposed on the power system include, but are not limited to, (i) stochastic programming (e.g., two-stage stochastic models), wherein the uncertainties are explicitly represented and simultaneously solved in the

model [41] and (ii) robust optimization, which mitigates worst-case consequences [42]. The independent system operators (ISOs) in the U.S. do not utilize the stochastic programming and the robust optimization in their day-ahead (DA) and real-time (RT) market processes since (i) these approaches have implementation complexity and computational requirements for the real-world scheduling problems [43], and (ii) market pricing and settlement based on these approaches are not well-acceptable by stakeholders.

Therefore, an approach is desirable in this situation to create a proper balance between decisions efficiency (i.e., deployable FRP awards) and complexity while being practically implementable. In this dissertation, statistical information and knowledge of the market outcomes under the possible realization of scenarios, data-mining algorithms, and enhanced FRP policies are leveraged efficiently to enhance the decisions on FMM FRP awards, without adding too much disruption to the existing energy market practices and compromising computational efficiency. The final goal is to award the ramp capabilities to the potential generation resources which could deploy them in the RT operation. This goal also has been perused by CAISO to reduce the ad-hoc and out-of-market corrections to create additional ramp capabilities [26] and [44].

The main outcomes of this dissertation, with respect to FRPs deployability performance in the FMMs, are:

- to propose an offline stage to predict the generation recourse ramping response to a ramping event. Then, a new FMM FRP design is presented to allocate the ramp capability awards more effectively within the market model while accounting for the effects of the post-employment of FRP awards on the transmission line limits.

- to introduce a ramping response set model upon the existing industry practices to enhance the deployability of the FRPs. The ramping response set factors are obtained through the data-mining algorithm performed in the offline stage for a set of deployable scenarios.
- to develop an out-of-sample validation methodology that mimics the RT market operation of CAISO in order to evaluate both efficiency and reliability of the proposed data-driven FRP policy against proxy FRP policy. The analyses of this methodology can be translated into the ad-hoc and out-of-merit operator actions, which can be potentially expensive for procuring additional ramp capabilities to meet changes in the netload

1.4. DERs Participation in the Wholesale Markets

The penetration of distributed energy resources (DERs) is overgrowing due to their cost-effective and environmental benefits. Generally, the DERs are placed in the DS; due to the minimum size requirement, they are not allowed to participate in the wholesale market individually. However, as one potential approach, aggregators that satisfy the minimum wholesale market size requirements can be used to manage and/or owe a number of DERs and participate in the wholesale market. Recently, FERC order No. 2222 requires ISOs to propose new operation and market rules for aggregators to participate in the wholesale markets, namely, capacity, energy, and ancillary services markets [45]. Essentially, this order attempts to encourage competition in the wholesale markets by removing the barriers that prevent DERs aggregators from wholesale market participation.

To this end, ISOs are mandated to modify their procedures to consider DERs aggregation for market participation. Among different challenges ISOs are facing (e.g., DERs eligibility to participate in ISO markets through aggregators, single-node or multi-node aggregation of DERs, as well as data and metering requirements), proposing proper coordination frameworks between the ISO, aggregator, and distribution utility is regarded a very prominent matter for safe power system operation [45]. More specifically, in the Notice of Proposed Rulemaking (NOPR) [45], it is suggested to propose new market and operational rules to address the coordination framework needed between the ISO, aggregator, and distribution utility. These rules should ensure the aggregators participation stays within DS operational limits to prevent creating reliability and safety concerns for the DS and transmission system. The DS hosting capacity is defined as "The maximum DER penetration for which a distribution grid (from substation through feeder) can operate safely and reliably is the hosting capacity" by Lawrence Berkeley National Laboratory [46]. Three main engineering factors that constrain the DS hosting capacity are thermal, voltage, and relay protection limits [46]. The DS hosting capacity usually represents the total injection that can be obtained from the distribution system (in the planning horizon) before doing an upgrade with PV units. However, in this dissertation, this concept is developed to represent operational short-term nodal (OSTN) hosting capacity aspect which is time-varying and changes with DS conditions.

Generally, one potential coordination framework is that ISO manages the wholesale market incorporating DS aggregators without visibility over DS limitations. However, the actual amount of products (e.g., energy and reserve) produced by aggregators to the ISO during an uncertain event depends on the DS limits (e.g., voltage limits, equipment

thermal limits, and supply-demand imbalance). This issue, i.e., not being able to respond to ISO dispatch instructions without posing any major risk to the DS, was also raised by the commission in the FERC order NO. 2222 [45]. Therefore, in the FERC order, a need is stated for creating an effective framework for the distribution utility to coordinate such concerns or issues with the ISO before allowing aggregator to participate in the organized wholesale electric market. It is necessary to mention that this coordination framework would be effective and practical if the associated proposals preemptively and dynamically consider time-varying DS OSTN hosting capacity (due to the ever-changing aggregators bid, DS conditions, and network configuration change).

Also, apart from the DS limits, the actual amount of deployable products by aggregators in response to the ISOs dispatch signals during a transmission-level uncertain event is dependent on the available flexibility inside the DS. The DS flexibility can come from various sources: Volt/VAR support from DERs smart inverters, DS reconfiguration, DS services provided by aggregators, etc. If these flexibilities are used and managed correctly, it can help mitigate violation in the DS even if aggregators are allowed to participate in the wholesale market beyond minimum DS OSTN hosting capacity limits. Thus, two questions that this part is seeking to answer is: (i) *how much ISOs can rely on the aggregators in the wholesale market to provide a certain amount of product considering the DS OSTN hosting capacity, and (ii) how the DS flexibility can be utilized to increase the deployability of the aggregators promised awards to the ISOs.*

Based on the above discussion, one of the goals of this dissertation is to create a coordination framework using statistical information of the DS and data-mining algorithms to provide ISOs and distribution utilities with a dynamic DS OSTN hosting

capacity that limits total active power services (e.g., energy and reserve) provided by aggregators to the wholesale market. The limit presented per this coordination framework can capture various voltage and thermal line limits in the feeders or substation while considering the effect of the Vol-VAr support from the distributed photovoltaics (PV) units.

The primary outcomes of this dissertation concerning the DERs participation in the wholesale markets are:

- to propose an offline stage before the DA wholesale market to predict the DS hosting to a given DS condition. Then, a new coordination framework is proposed for the ISO and distributions utility based on this hosting capacity to award services to aggregators without posing any major risk to the DS. To this end, the concept of the maximum qualified aggregation capacity is proposed to determine the level of qualification and disqualification of the total services provided by aggregators. Then, using the maximum qualified aggregation capacity (translatable into the DS OSTN hosting capacity), the wholesale market can award any combination of services to an aggregator located in the relevant DS region as long as the total amount falls within the limit stated by this function.
- to propose the mixed-integer linear programming model of Volt-VAr droop controller of the distributed PV smart inverters inside a detailed unbalanced ACOPF based on current and voltage (IVACOPF) formulation [47].
- to develop a validation phase that represents transmission and distribution management during uncertain events. The validation phase mimics the ISOs dispatch instructions to aggregators during transmission-level uncertain events. It also

includes the IVACOPF with the objective function of minimizing voltage and thermal limits violation while avoiding the aggregators curtailment.

- to consider and assess the effects of Volt-VAr support from distributed PV units on the DS OSTN hosting capacity, and mitigating the voltage and thermal violations caused by aggregators meeting their obligations to ISOs during transmission-level uncertain events.

1.5. Overview of the Dissertation

This dissertation is structured as follows. Chapter 2 provides a literature review. Firstly, a review of contemporary industry-based contingency modeling approaches, which are currently embedded within the DA optimization models in an attempt to ensure the *N*-1 mandate, is presented. Then, a literature survey on ramp capability procurement in the DA and RT market is presented. Finally, a literature review is elaborated on DERs participation in the wholesale markets and different coordination frameworks for ISOs, distribution system operators, and aggregators.

In chapter 3 the impacts of uncertainty modeling strategies on electricity market outcomes, pricing, and settlements are analyzed. The LMP comprises three components, i.e., energy, congestion, and loss components. This compressive exam report uses a method based on the duality theory to shed light on the LMP calculation in a stochastic market model; this theoretical method confirms that the value of providing *N*-1 reliability services can be reflected in the LMPs of such stochastic market models. This pricing scheme is then compared to the two state-of-the-art market auction models, where the corrective actions to achieve an *N*-1 reliable solution are postponed to OMC. Also, the market settlements of these models are calculated and compared. With these analyses,

this dissertation seeks to inform market stakeholders about the impacts of contingency modeling approaches in the DA process and their implications on pricing and settlements. Furthermore, this dissertation analyzes the choices of the objective function for the stochastic market models; a stochastic market design with an expected cost objective function is examined and compared with the base-case cost minimization objective function from two aspects: (i) realized cost during *N*-1 contingencies and (ii) effects of inaccurate calculation of the probabilities on market outcomes.

Chapter 4, firstly, presents the formulation of a DA market model with general FRP constraints. Then, it sheds light on a subtle issue that can potentially happen in the next market processes after the DA market, as a result of procurement of DA ramp capabilities only based on the hourly ramping requirements. Then, a new FRP design is proposed to address this issue. In the proposed formulation, the DA FRP design is modified to accommodate the 15-min net load variability and uncertainty while scheduling hourly FRPs in the DA market. The proposed approach overcomes the concerns raised by CAISO in [9] and [14] regarding the 15-min ramp infeasibility. Furthermore, the DA market models with different FRP designs are developed by incorporating the regulation reserve into the market formulation. Then, coordination among these market products is evaluated to see how they can affect the system operation efficiency in the FMMs against steep 15-min net load changes. Finally, new market-based incentivizing policies are driven for the proposed FRP design to properly encourage the ramp-responsive resources that provide the enhanced ramp capability. To effectively evaluate different FRP designs from reliability and market efficiency points of view, a validation methodology is proposed similar to the RT unit commitment (RTUC) processes of the CAISO. This

validation phase plays a pivotal role in evaluating the performance of DA FRP in the view of how the system ramp capability is improved in RT operation (e.g., FMM); however, this step has been ignored in most of the work in the literature [33]–[36], [48], [49].

In chapter 5, to address the deployability issue of FRPs, a computationally tractable data-driven policy is proposed for FRPs awarded in FMMs, which improves upon the existing industry models. The key idea is to allocate the FRPs to the resources that can effectively deploy their ramping capabilities in the corresponding locations when needed without violating transmission line limits. To do so, the proposed approach uses data-mining algorithms to specify ramping response factor sets for generation resources that have higher responsiveness given a set of ramping deployment events. Furthermore, the impacts of the FRPs post-deployment on the transmission line flows are considered so that the ramp capabilities are allocated to the potentially deployable locations. Finally, the performance of the enhanced FMM market model, modified to include the proposed FRP design, is compared against the FMM market model with proxy FRP design through an out-of-sample validation methodology. This validation methodology mimics RT unit commitment (RTUC) of CAISO's FMM, results of which can be translated into the ad-hoc and out-of-merit operator action to increase the ramping capabilities.

In chapter 6, two distribution system operator and ISO coordination frameworks (architectures I and II) are presented. The latter enables the ISO to have visibility over the DS limits and accordingly allows the aggregators to participate in the organized wholesale electric market based on the DS OSTN hosting capacity. Architecture II utilizes the statistical information obtained using different distribution system conditions

and data-mining algorithms to predict the hosting capacity of the DS. Also, a validation phase is proposed to compare the performance of the architectures I and II. The validation phase, which mimics the DS condition during an uncertain event, utilizes an IVACOPF formulation. Also, the Volt-VAr support provided by distributed PV smart inverters is leveraged to increase the DS flexibility to improve the deployability of the aggregators promised awards in the DS. The Q-V curve of Volt-VAr controllers of distributed PVs is based on the IEEE 1547-2018 standard and formulated as proposed mixed-integer linear constraints using the Big-M method.

Finally, chapter 7 presents a discussion on potential future work.

Chapter 2.

LITERATURE SURVEY

Energy markets are ever-evolving due to operational complexities and complications due to changing resource mix (e.g., renewable resources and distributed energy resources, DERs). The ISOs are introducing reformulations, new market products, and market participation architectures to better represent the inherent complexity of electricity production, transmission, and consumption; and integrate the new resource mix. Different contingency modeling approaches and flexible ramping products are examples of reformulations and market products. It is worth noting that uncertainties in the power systems are caused by discrete disturbances (e.g., generator, transmission line, and transformer outages) or continuous disturbances (e.g., forecasting error of loads and renewable resources).

This chapter reviews state-of-the-art approaches of contingency modeling inside the market auction models, including an overview of existing deterministic reserve policies included in present-day SCUC formulations, stochastic programming, and state-of-the-art market auction models with estimated post-contingency states. Then, this chapter presents a literature review on the DA and RT FRPs, followed by a literature review on DERs participation in the wholesale markets.

2.1. Contingency Modeling Approaches

The basic UC model, disregarding contingencies, is well-studied; related efforts were overviewed by [50], [51], and more recently by [52]. After the 2003 Northeast blackout

in North America, the SCUC models with enhanced contingency constraints have received increasing attention from both industry and academics.

Different approaches for the SCUC problem in the context of managing uncertain contingencies can be mainly categorized into three subgroups. The first subgroup is the SCUC problem with proxy reserve policies that implicitly determine reserve requirements to respond to the contingencies. The second subgroup for meeting the *N*-1 reliability mandate is through using the stochastic programming approaches, e.g., the two-stage stochastic SCUC or the ESCUC, wherein the two stages represent the pre-contingency and post-contingency states. Finally, the third subgroup is associated with estimating the post-contingency state of line flows due to the contingencies. A literature survey related to these approaches is presented in the following subsections.

2.1.1. Existing Proxy Reserve Policies

Proxy reserve requirement and reserve zones are predominantly employed by a majority of the system operators in their DA SCUC market model in an attempt to achieve the *N*-1 reliability criteria. Today, the existing reserve policies mostly make some approximations in the market model. The above contingency reserve requirements are a result of approximating the *N*-1 reliability criteria. They focused on the quantitative aspects of reserves, rather than explicitly modeling the N-1 contingency events within the SCUC market model.

2.1.1.1. Proxy Reserve Requirements

The proxy reserve requirements simply entail the contingency reserve to be greater than a certain percentage of the peak load and/or to be adequate to compensate for the

loss of any single generation unit. Moreover, there are some other rules, such as the 3+5 rule suggested by the National Renewable Energy Laboratory (NREL), which simply suggests that the system-wide reserve should not be less than 5% of the short-term forecasted wind power or less than 3% of the load [53].

Although the proxy reserve criteria are generally easy to implement, they ignore the intrinsic stochastic nature of such models and rely on approximations of the *N*-1 mandate. With such approximations, where post-contingency operating states are not taken into account when making the scheduling decisions, there is no guarantee that procured reserves by the market will be deliverable without violating transmission constraints. After the market is cleared, the operator may change the market solutions to ensure the *N*-1 reliability criterion. In the industry, these specific actions which happen outside the market are referred to as out-of-merit energy/capacity [54], manual dispatches [55], security corrections [56], uneconomic adjustments [57], and exceptional dispatches [58]. These actions for making the market solution *N*-1 reliable are called the OMC [59] in this dissertation. Newly committed units during OMC do not directly influence LMPs, and they are either compensated based on the market LMP or based on their market bid. If needed, the operator will compensate them with an uplift payment. This inability to impact market prices will cause a natural unfairness as market participants might not be dispatched fairly with this mechanism.

2.1.1.2. Regional Reserve Requirements

As discussed in section 2.1.1.1., the proxy reserve policies may not guarantee reliable operations because they are only based on quantitative rules. To enhance the deliverability issue associated with the contingency-based reserve, the zonal reserve

model is being adopted by some ISOs (e.g., MISO) [6]. However, this zonal reserve model still includes approximations, such as treating all the locations inside a zone as the same. Consequently, it is unable to differentiate the generators within each zone regardless of their ability or inability to deploy reserve due to system congestion. It is pertinent to note that discounting intra-zonal congestion can itself lead to inaccurate inter-zonal flow calculations; potentially causing nodal reserve deliverability issue. Thus, the ISOs are usually forced to perform the OMC actions, such as manually disqualifying generators or turning on additional units in local areas to account for modeling approximations and inaccuracies. Accordingly, such a market model is also unable to properly account for the value of reserve provided by each generator.

2.1.2. Stochastic Programming

A more accurate solution to handle the uncertain disturbances is to solve stochastic programming. Stochastic programming has been utilized in the optimization market models (e.g., SCUC) to address discrete disturbances (e.g., asset outages) and continuous disturbances (e.g., renewable resources and demand uncertainty). For example, in the context of discrete disturbances, uncertain contingency events are explicitly captured in a two-stage stochastic SCUC model, where the two stages are the representation of the pre-contingency and post-contingency states [60], [61]. For the modeled events, the contingency-based reserves are guaranteed to be deliverable since the network constraints and corrective actions are explicitly formulated. It is pertinent to note that no pre-defined reserve requirements are necessary because of the endogenous acknowledgment of uncertainty and more accurate modeling of the pre-contingency and post-contingency operating states.

A two-stage stochastic SCUC model that includes uncertain contingencies is presented in [60], wherein the focus is on the stochastic programming formulation and effective numerical methods. Reference [61] proposes a two-stage stochastic program approach to handle uncertain contingencies. Then, the benefits of combining both stochastic methods and reserve requirements are assessed in efficiently managing uncertainty in the stochastic model. However, in [60], [61], it has not been discussed how generators should be compensated for their procured energy and *N*-1 reliability services in such models.

Pricing analyses for stochastic security-constrained approaches in the energy and reserve markets are presented in [17], [12], [62], [13]. Reference [17] investigates a method to compensate generators for the energy and reserve they provide through an optimization problem. The model accounts for the UC, corrective security actions, and the transmission line limits, where both generation units and loads offer reserves. The authors in [17] derive a pricing mechanism where the generators are compensated for the modeled *N*-1 scenarios. However, results are shown for only a single time interval while the formulated model allows load shedding. It is worth noting that the fixed cost of load shedding is hard to estimate since: (1) it is not necessarily proportional to bids submitted to the market as energy bids, and (2) it is not the same (fixed cost) for different sectors (industry, domestic, commercial). Furthermore, [17] does not consider other complex constraints, such as minimum-up and minimum-down time constraints.

The authors in [12], [62] formulate a multi-period stochastic SCUC model that takes into account the post-contingency states for pre-selected contingencies. The authors state that there is a "set of random generator and line outages with known historical failure rates." The proposed stochastic program optimizes the base-case along with the expected

cost of the post contingency states. However, their model allows for load-shedding and "pre-selected" contingencies. In [13], the authors utilize a two-stage stochastic linear program to propose different methods to compensate generators. The authors use a linear programming formulation, not mixed-integer linear programming. The models presented in [12], [13], [62] allow for load-shedding through the value-of-lost-load (VOLL); however, this approach is subjective since the obtained results are sensitive to the choice of VOLL.

A SCUC auction model for energy and contingency-based ancillary services is presented in [18] to optimize reserve requirements by explicitly simulating contingencies rather than implementing the fixed reserve requirements. The original auction problem is decomposed into a master problem and subproblems to address the computational complexity.

However, a comprehensive economic evaluation for the stochastic two-stage SCUC and its comparison with other contingency modeling approaches have neither been included nor analyzed in the studies [12], [13], [17], [18], [60]–[62]. Specifically, this evaluation can include an assessment of the generation cost, generation revenue, generation rent, load payment, and congestion rent.

Apart from economic evaluation, it is also essential to assess the performance of the stochastic market formulation. Generally, multiple scenarios are modeled in the two-stage stochastic SCUC models, wherein the objective function is an expected cost of the base-case along with the expected cost for corrective actions (or recourse decisions). The base-case is a high probability scenario, wherein "the power system is in normal steady-state operation, with all components in service that are expected to be in service" [19].

Traditionally, two-stage stochastic programs are formulated in a way that the objective function is optimized over an expectation [12]–[16], [60]–[62]. There are several reasons why optimizing over an expected cost may not be preferred. First, it is difficult to accurately predict the probabilities of outages. Second, the amount of discretionary, ad-hoc corrections made between the day-ahead and real-time markets is not accurately captured. Third, there is also the issue that market operators in real-time may not implement the proposed corrective actions; fast recovery of the system security is more of a concern than the least-cost path to recovering the system security. Finally, when the objective function is modified to include the probabilities and optimize over the expected cost, there are different pricing implications than when the system optimizes only over the base-case cost. There are other studies [17]–[19] that minimize the base-case cost as their objective functions, while the model is a stochastic two-stage SCUC problem including explicitly modeling of the post-contingency constraints. References [12]–[19] aim to improve stochastic market models, whereas the proper design of objective function for these models has neither been analyzed nor included in prior work. Therefore, a comprehensive study is needed to examine the implications of an expected cost objective function versus what is commonly used today in the industry, which only optimizes the base-case cost.

2.1.3. State-of-the-art Market Auction Models with Estimated Post-Contingency States

The gap between the traditional deterministic and future stochastic models is filled by the use of market models with pre-determined participation factors. These approaches aim to explicitly represent generator and/or non-radial line contingencies without any second-stage recourse decisions.

In [63], line outage distribution factors (LODFs) are used to explicitly model the transmission line contingencies in the DA SCUC models. Another example is the CAISO, which intends to enhance its scheduling model to explicitly enforce the post-contingency transmission constraints for the generator contingencies using generator loss distribution factors (GDF) [11].

Reference [64] proposes a set of *G*-1 security constraints; thereby, contingency reserves are allocated more efficiently in the system concerning post-contingency dispatch feasibility. The proposed model disqualifies the undeliverable contingency-based reserves in the post-contingency states and assigns those reserves at other locations to guarantee a market solution that is *G*-1 reliable on a locational basis. A reserve response set model to enhance existing proxy reserve policies is proposed in [65]. This model is aimed to address the deliverability issues related to proxy reserves by modeling the estimated post-contingency impacts of nodal reserve deployment for a few critical transmission elements. The performance of the proposed reserve model is compared against an ESCUC model and contemporary proxy reserve policies from only operating costs and reliable points of view. Also, [66] have proposed a set of *G*-1 security constraints; thereby, contingency reserves are allocated more efficiently in the system with respect to post-contingency dispatch feasibility.

Among the above models, transmission line contingencies within state-of-art market models based on LODFs have been well implemented in industry practice; however, there have been limited efforts for investigating its pricing implications and market settlements compared to other contingency modeling approaches. With the explicit modeling of contingency events within the state-of-the-art market auction models, the

industry is moving from the deterministic market models to a stochastic model. With such stochastic modeling, LMPs should reflect the value and quality of services provided by market participants in response to contingencies. However, there are unsolved issues regardless of the choice of uncertainty modeling: *generators compensation for providing N-1 reliability services as well as the impact of contingency modeling on prices.*

2.2. Ramp Capability Products

The new resource mix, e.g., renewable resources, are imposing operational complexities on modern power systems by intensifying the uncertainty and variability in the system net load. As a result, energy markets are evolving in order to overcome such operational challenges. For instance, the ISOs have been motivated to institute and implement a new ancillary service product, ramping products, to handle variations in the forecasted net load (foreseeable changes), as well as uncertainties (unforeseeable changes). While ISOs may use different terms to refer to ramping products (e.g., ramp capability in the MISO and flexiramp in the CAISO [28]), the concept and motivations behind these new ramping requirements are essentially the same.

2.2.1. FRPs in Real-time Markets

Several works on the area [28], [29], [37], [40], [67]–[72] have been focused on the FMMs and real-time dispatch (RTD) markets since the main purpose of the FRPs is to improve the ramping capabilities in RT. The FRP for an RTD market was introduced in [37], wherein the ramp capability requirement is set based on the system-wide requirement. Reference [29] compares the dispatch, prices, settlements, and market efficiency of a deterministic market model, including the FRPs constraints (similar to

ISO operations), with a stochastic market model in the RT economic dispatch problem. A simplistic case study is employed to fundamentally evaluate the performance of FRP markets. A similar study with the same intentions is conducted in [28]; however, the comparisons are made for a real-time unit commitment (RTUC) market model with 15-min granularity. It is concluded that including FRP in FMM and RT markets enhances the dispatch flexibility, but stochastic market models have better performance. A single-period market model with FRP is compared with a time-coupled multi-period market model in [40] from efficiency, reliability, and incentive compatibility points of view. Reference [67] discussed the FRP design for the RT economic dispatch in the MISO market, wherein the ramping requirements are set 10-min ahead to manage net load variations and uncertainty. In contrast, the RT dispatch is performed every 5-min. It has been shown that the 10-min ramping capabilities may be depleted in the first 5-min dispatch, so the system may not be able to follow the variability and uncertainty of the net load in the second 5-min dispatch. Therefore, a new FRP design is proposed in [67] to address this subtle issue and maintain the system reliability and efficiency. Reference [73] includes the FRPs constraints into a risk-limiting RT economic dispatch problem, wherein risk has been defined as the "loss-of-load probability." The FRP requirement and market design based on system-wide policy were improved for the RTUC problems in [68], [69]. A new solar FRP was proposed in [70] for a multi-interval RTD market model, wherein, for estimation of FRP requirement, a Gumbel copula-based joint probability distribution of load and wind forecasting errors was used. However, the RT FRP model presented in [28], [29], [37], [40], [67]–[70] is based on the system-wide requirements

without considering which generation resources are more qualified for ramp capability products and/or the effects of transmission lines on the FRP awards.

To address the deliverability issue of FRP, a distributionally-robust multi-interval optimal power flow is proposed in [71] while considering the spatiotemporal correlations among demand uncertainties and wind power. Furthermore, reference [72] has proposed a robust FRP design for the RTD markets to address the FRP deliverability issues. Also, the corresponding pricing scheme was developed to value the generation resources that provide the FRP. Still, as mentioned earlier, applications of these advanced optimization models for real-world market models are limited due to the scalability and pricing barriers. Overall, to address the deployability issue, FRP awards should be given to the generation resources that can deploy them during ramping shortages, and these FRP decisions are made while considering their effects on the transmission line limits.

2.2.2. FRPs in the Day-ahead Market

There have also been intentions in some works [34]–[37] toward implementing and procuring some of the ramp capability in the DA market to ensure resource adequacy for meeting ramping requirements in the RT market processes. Furthermore, the CAISO intends to add the FRPs to their DA market to address uncertainty and variability in the net load previously left to the RT market [24].

Reference [33] has proposed an optimization model for energy storage aggregators to maximize profit by bidding for and procuring FRP in the DA energy and reserve markets. However, it is pertinent to note that the FRP is considered a not-biddable product [28]. A wind power ramping product (WPRP) has been proposed by [34] to allow wind resources to participate in the FRP market. The WPRP is designed to respond to the needed

ramping requirements in order to ensure sufficient ramp capabilities in the RT operations. However, due to their relatively low operational costs, wind units may not be good options to procure the ramp capability product [68]. In [48], the business models and fundamentals for an aggregator managing different flexible resources, such as energy storage system, distributed generation, and a controllable load of customers in demand response programs, are discussed. One of the characteristics of the aggregator assessed in [48] is its ramping performance in the DA market; however, the focus has been on the business models and fundamentals for the aggregator, rather than proposing new operational models to increase the system ramp capability. Reference [35] has proposed an integrated stochastic DA scheduling model to allocate FRP for managing the variability and uncertainty of the renewable energy system. A non-deterministic FRP design is proposed in [36] to adequately allocate the ramp capacities in the DA market. The proposed model, which is an affinely adjustable robust UC model, is based on a cost-free ramp capacity procurement procedure. An optimal robust bidding strategy model has been proposed in [49] for a micro-grid that manages distributed energy resources (DERs), namely, photovoltaic systems, wind turbines, energy storage systems, and micro-turbines, to maximize its revenue from the DA markets. The proposed model also aims to assess the microgrid ramping capability in day-ahead joint energy and ancillary service markets. The results showed that proper coordination of the DERs can considerably increase the microgrid ramp capability. Despite appealing results, [35], [36], and [49] have utilized stochastic programming and robust optimization methods, both of which are under the umbrella of advanced stochastic programming techniques [52]. However, due to scalability and pricing issues, the FRP was initially designed to keep the market models

close to the existing practice while addressing variability and uncertainty [29]. Furthermore, in compliance with common practice, proper market-based incentive policies corresponding to the modified FRP designs should be developed for the flexible resources that participate in the FRP market; however, this step is ignored in [33]–[36], [48], [49]. Overall, such structural changes, i.e., the inclusion of FRP in DA market formulation, require detailed analyses and design in order to ensure adequate operational flexibility, market efficiency, and pricing. In the same direction as the proposal of CAISO [22], the focus of this dissertation will be on the efficient design of DA FRP and associated market-based incentivizing policies.

2.2.3. Different Options for Increasing System Ramp Capability

Generally, there are two main ways to improve ramp responsiveness in the system. The first way is through improving the operational models and market design, e.g., more explicit representation of the uncertain events in the model and introducing new market products. The second way is to incorporate new flexible resources, e.g., energy storage systems and demand response programs, into the electric system. Following the second procedure, some studies have attempted to procure flexible ramp capabilities through the emerging techniques including, but not restricted to, electrical vehicles [74], [75], demand response programs [35], [75], and energy storage systems [33], [75]. However, the lowest cost option for improving the flexibility is associated with the improved market and operational design, such as improved weather forecasting, the shorter granularity for market processes, and enhanced designs of ancillary service products [76], as shown in Fig. 2.1. It is cheaper because this option makes the relatively small market and operational changes while utilizing the existing infrastructures [77]. In some other

studies, wind generators themselves participate in providing ramp capabilities [34], [78]; however, as mentioned in the previous section, wind resources may not be good choices for providing FRPs.

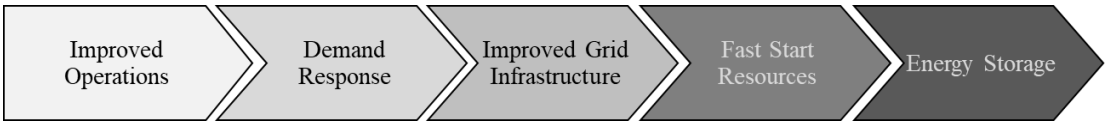

Fig. 2.1. Cost Comparison Between Different Options to Improve Operational Flexibility from Lower Cost on the Left to Higher Cost on the Right [77].

2.3. DERs Participation in the Wholesale Markets

Generally, DERs participation in the wholesale markets can be categorized into three subgroups. The first subgroup is DERs directly (without aggregation) participating in the wholesale markets to provide capacity, energy, and ancillary services products (ideal case) [79]. However, the main problem with this participation model is that due to the minimum size requirement, they may not be allowed to participate in the wholesale market individually, which will prevent the ISOs from utilizing numerous benefits of these resources [80]. Furthermore, a substantial number of DERs participation in the wholesale market can potentially cause huge computational complexities for different ISOs market processes, namely, DA SCUC, RTUC, and RTD [81].

The second subgroup is developing the new concept of distribution system operators (DSOs), which has some functional capabilities over today's utility distribution operators and is fully responsible for aggregating and dispatching DERs within its distribution system (DS) region [82], [83]. Generally, in this subgroup, ISOs run the market engine for aggregated pricing nodes (i.e., DSOs incorporating corresponding DERs and DS network) and other conventional market participants. It is pertinent to mention that the

DSO is defined as “the entity responsible for planning and operational functions associated with a DS that is modernized for high levels of DERs” by Lawrence Berkeley National Laboratory [46]. Although there is some literature work on the second subgroup [81], [83]–[87], DSO implantation in practice is still in the very initial stages [45]. Furthermore, if an independent aggregator inside the DS is willing to directly participate in the wholesale market, there should be clear and transparent market rules for the DSOs to keep a neutral position and not practice market power. The reason is that DSO is also a market participant in the wholesale market and at the same time manages the DS network.

Finally, the third subgroup includes DERs directly participate in the wholesale market through the role of aggregators. In this case, the distribution utility is primarily responsible for the safe and reliable operation of the DS network while the ISO manages and dispatches aggregators directly. Since the aggregators participate in the transmission-level wholesale market and locate at the DS while receiving dispatch instructions directly from ISOs, a coordination framework between ISO and distribution utility becomes essential for the safe and reliable operation of the DS network. This subgroup is a more compatible option with the current ISOs market.

2.3.1. Aggregators Directly Participate in the Wholesale Market

There is some work in the literature [88]–[95] on DERs participating in the wholesale markets by aggregators. The role of aggregator was presented in [88] to enable a portfolio of DERs, which store and convert a set of energy carriers (i.e., solar energy, gas, thermal energy, and electricity), to maximize the expected aggregator profit by finding the its optimal bidding strategy. Using stochastic optimization, the optimal bidding strategy of

an electric vehicles aggregator was determined in the DA energy and regulation reserve markets [89]. The uncertainties associated with the electric vehicle characteristic and price signals were also considered. A similar study was presented in [90], in which the aggregator manages electric vehicles only based on their grid-to-vehicle charging characteristics. A bi-level mixed-integer linear problem was proposed to assess the aggregator ability to affect the clearing market prices. The bi-level model has two levels; in the first level, the aggregator minimizes the charging cost of the electric vehicles, while in the second level, the wholesale market is run. A risk-averse optimal bidding formulation was proposed in [91] to manage a set of flexible demand-side resources, namely, plug-in electric vehicles and distributed generation, through the role of an aggregator. The conditional value-at-risk (VaR) theory was used to risk-averse aggregator optimal bidding under the uncertainty of renewable generation, electricity demand, and real-time price.

An aggregator model managing commercial compressed air energy storage and wind power aggregator was proposed in [92] to simultaneously participate in different market processes, including DA, intraday, and balancing markets. The proposed model was formulated as a three-stage stochastic optimization problem, wherein the VaR model was utilized to control the financial risks. However, in [88]–[92], aggregators participate in the wholesale market without considering the DS OSTN hosting capacity, which could be problematic for the DS security and reliability.

A robust optimization model for an aggregator managing electrochemical batteries, PV, and thermal energy storage was proposed in [93] to participate in the wholesale DA energy and emerging local flexibility markets. The robust optimization also considered

the energy, electrical demand, and PV production uncertainty. In this work [93], so-called local constraint support in terms of the maximum allowed net exchange at the point of common coupling with the distribution grid was considered for the aggregator to ensure that its local portfolio will not cause DS operational issues. However, the maximum allowed net exchange was based on the assumption that the distribution utility knows and provides it to the aggregator without presenting a framework for calculating it.

A prequalification process was proposed in [94] to modify the bids of the aggregators before submitting them to the ISO wholesale market. However, the model is an iterative process that uses sensitivity analyses and power flow to modify the bid instead of optimally determining the DS OSTN hosting capacity. Furthermore, after solving the DA wholesale market and during a transmission-level uncertain event, the effects of the proposed model were not investigated on the deployability of the ISOs dispatch signals to the aggregators concerning the DS limitations. A service-centric methodology and cooperation of the aggregator and the distribution utility were proposed in [95] to consider the DA wholesale market participation of the DERs through the aggregator while providing congestion relief service to the DS in the intraday scheduling process. However, in [95], the aggregator Kw bid effects submitted to the wholesale market were not considered on the safe and reliable operation of the DS. Instead, after the DA wholesale market and in the intraday scheduling process, power flow analyses followed by optimal adjustment of active and reactive power of aggregator is presented as a solution to address network constraints for congestion management in the distribution network. Also, overvoltage issues were not considered in [95]. Furthermore, the proposed

models and simulation results in [94], [95] were performed only based on the small-scale balanced distribution DS networks.

Chapter 3.

REPRESENTATION OF UNCERTAINTY IN ELECTRIC ENERGY MARKET MODELS: PRICING IMPLICATION AND FORMULATION

3.1. Introduction

Modern-day market management systems continue to evolve due to the intention to improve system security and reliability. This evolvement leads to a transition of the market auction models from a deterministic structure with approximations on the reliability criteria (e.g., acquirement of contingency reserve through proxy reserve policies) to the explicit representation of contingencies (e.g., estimation of post-contingency states via participation factors and stochastic program). The literature survey presented in Chapter 2 reveals a few gaps that need additional attention and further work. To the best of the authors' knowledge, very limited efforts have been done on how various choices of modeling contingency events affect the potential operational efficiency, incentive compatibility, market transparency, and market settlement policies in the markets with inherent stochastic nature. In addition, no prior work has been conducted about how to formulate the objective function that maintains efficiency for stochastic markets with uncertain contingency events. The primary contributions of this work are as follows:

- Impacts of contingency modeling strategies on electricity market outcomes, pricing, and settlements are analyzed. This chapter leverages the duality theory to calculate LMP in a stochastic market model; this theoretical method confirms that the value of providing *N*-1 reliability services can be reflected in the LMPs of such stochastic market models. This pricing scheme is then compared to two state-of-the-art market

auction models, where achieving *N*-1 reliable dispatch is postponed to OMC. Also, the market settlements of these models are calculated and compared. With these analyses, this chapter seeks to inform market stakeholders about the impacts of contingency modeling approaches in the DA market process and their implications on pricing and settlements.

- The choices of the objective function for the stochastic market models are analyzed; a stochastic market design with an expected cost objective function is examined and compared with the base-case costs minimization objective function from two aspects: (i) realized cost during *N*-1 contingencies and (ii) effects of inaccurate calculation of the probabilities on market outcomes.

It is worth noting that the aim of this chapter is not to develop a new market design; it is rather to propose a framework to evaluate existing market models and stochastic market models in terms of potential operational efficiency, incentive compatibility, fair pricing, and transparency.

The rest of the chapter is organized as follows. Section 3.2 presents model formulation. Section 3.3 focuses on the pricing implication of contingency modeling approaches. Section 3.4 evaluates choices of the objective function for stochastic market frameworks. Finally, Section 3.5 concludes this chapter.

3.2. Model Formulation

Previous studies in the area of managing discrete uncertain events (i.e., contingencies) in the SCUC problem can be categorized as follows: (i) proxy reserve policies, (ii) modeling system response via participation factors, e.g. LODF and GDF, (iii) stochastic programming approaches, e.g., ESCUC, and (iv) chance-constrained optimization and

robust optimization. The main focus of this work is on managing uncertainty through (i), (ii), and (iii) above. In the following three subsections, model formulations related to these approaches are presented.

3.2.1. SCUC with Deterministic Proxy Reserve Requirement

A SCUC market model with deterministic proxy reserve requirement is presented in (1)-(19), which is similar to the model in [66]. The objective function, minimizing total operating costs, is presented in (3.1). In this formulation, constraints (3.2) and (3.3) model the relationship of the unit commitment variables with the startup and shutdown variables, respectively. Constraints (3.4)-(3.7) model the binary commitment (u_{gt}) decision and the startup (v_{gt}) and shutdown (w_{gt}) decisions, respectively. Minimum up and down time constraints are enforced by (3.8) and (3.9). Constraints (3.10) and (3.11) ensure ramp rate limits. Constraint (3.12) guarantees a balance between the power injection and withdrawal at every bus and constraint (3.13) ensures the energy balance between load and generation across the system. Constraint (3.14) models the transmission line limits. The generator output limits are presented by (3.15) and (3.16), while constraint (3.17) limits the spinning reserve to the 10-minute generators' ramp rate capability. Proxy reserve requirements are modeled through (3.18)-(3.19). Based on the constraints (3.18) and (3.19), the system must withstand the loss of any single bulk power generation at any time interval, and the total system proxy reserve must be greater than a particular percentage (η) of the demand at each time interval, respectively.

$$minimize \sum_g \sum_t (c_g^p P_{g0t} + c_g^{NL} u_{gt} + c_g^{SU} v_{gt} + c_g^{SD} w_{gt}) \quad (3.1)$$

Subject to

$$v_{gt} \geq u_{gt} - u_{gt-1}, \forall g, t \geq 2 \quad (3.2)$$

$$w_{gt} \geq u_{gt-1} - u_{gt}, \forall g, t \geq 2 \quad (3.3)$$

$$v_{gt} \geq u_{gt}\,, w_{gt} = 0, \forall g, t = 1 \quad (3.4)$$

$$0 \leq v_{gt} \leq 1\,, \forall g, t \quad (3.5)$$

$$0 \leq w_{gt} \leq 1\,, \forall g, t \quad (3.6)$$

$$u_{gt} \in \{0,1\}, \forall g, t \quad (3.7)$$

$$\sum_{s=t-UT_g+1}^{t} v_{gs} \leq u_{gt}, \forall g, \mathrm{t} \geq UT_g \quad (3.8)$$

$$\sum_{s=t-DT_g+1}^{t} w_{gs} \leq 1 - u_{gt}, \forall g, t \geq DT_g \quad (3.9)$$

$$P_{g0t} - P_{g0t-1} \leq R_g^{HR} u_{gt-1} + R_g^{SU} v_{gt}, \forall g, t \quad (3.10)$$

$$P_{g0t-1} - P_{g0t} \leq R_g^{HR} u_{gt} + R_g^{SD} w_{gt}, \forall g, t \quad (3.11)$$

$$\sum_{g \epsilon g(n)} P_{g0t} - Load_{nt} = P_{n0t}^{inj}, \forall n, t \quad (3.12)$$

$$\sum_n P_{n0t}^{inj} = 0, \forall c, t \quad (3.13)$$

$$-P_k^{max} \leq \sum_n P_{n0t}^{inj}\, PTDF_{0nk}^{ref} \leq P_k^{max}, \forall k, t \quad (3.14)$$

$$P_{g0t} + r_{gt} \leq P_g^{max} u_{gt}, \forall g, t \quad (3.15)$$

$$P_g^{min}\, u_{gt} \leq P_{g0t}, \forall g, t \quad (3.16)$$

$$0 \leq r_{gt} \leq R_g^{10} u_{gt}, \forall g, t \quad (3.17)$$

$$\sum_j r_{jt} \geq P_{g0t} + r_{gt}, \forall g, t \quad (3.18)$$

$$\sum_g r_{gt} \geq \eta\% \sum_n Load_{nt}, \forall t \quad (3.19)$$

3.2.2. SCUC with Line Contingency Modeling Using LODF

Today, some ISOs use LODF to explicitly model non-radial line contingencies in the DA SCUC model without adding any second-stage recourse variables [63]. The LODFs

are participation factors, which indicate redistribution of flow on the transmission lines (e.g., line k) after outage of a line (e.g., line ℓ) [7]. The SCUC model that incorporates explicit representation of the transmission contingency using LODF is presented in (3.20)-(3.23).

$$minimize \sum_g \sum_t (c_g^p P_{g0t} + c_g^{NL} u_{gt} + c_g^{SU} v_{gt} + c_g^{SD} w_{gt}) \quad (3.20)$$

Subject to

Constraints (2)-(19) (3.21)

$$-P_k^{max,c} \leq \sum_n P_{n0t}^{inj} PTDF_{0nk}^{ref} + LODF_{k\ell}^{ref} FL^0{}_{\ell t} \leq P_k^{max,c}, \forall k \neq \ell, t \quad (3.22)$$

$$FL^0{}_{\ell t} = \sum_n P_{n0t}^{inj} PTDF_{0n\ell}^{ref}, \forall \ell, t \quad (3.23)$$

Detailed explanations on how to calculate LODF are given in Appendix A.

3.2.3. ESCUC Market Models

The ESCUC problem is formulated as a two-stage stochastic program. The scenarios represent the base-case pre-contingency scenario and contingency scenarios (i.e., the loss of non-radial transmission line and generator) with their corresponding probabilities. This market model is defined by (3.24)-(3.35).

$$minimize \sum_g \sum_t \pi_{BC} c_g^p P_{g0t} + \sum_g \sum_t \left(c_g^{NL} u_{gt} + c_g^{SU} v_{gt} + c_g^{SD} w_{gt}\right) +$$

$$\sum_g \sum_{c \neq C_0} \sum_t \pi_c c_g^p P_{gct} \quad (3.24)$$

Subject to

Constraints (2)-(11) and (15) (3.25)

$$\sum_{g \epsilon g(n)} P_{g0t} - d_{nt} = P_{n0t}^{inj}, \forall n, t \qquad [\lambda_{n0t}] \quad (3.26a)$$

$$\sum_{g \epsilon g(n)} P_{gct} - d_{nt} = P_{nct}^{inj}, \forall n, c \in C_g, t \qquad [\lambda_{nct}] \quad (3.26b)$$

$$\sum_{g\epsilon g(n)} P_{gct} - d_{nt} = P_{nct}^{inj}, \forall n, c \in C_k, t \qquad [\lambda_{nct}] \tag{3.26c}$$

$$d_{nt} = Load_{nt}, \forall g, [\lambda_{nt}^{securitized}] \tag{3.27}$$

$$\sum_n P_{nct}^{inj} = 0, \forall c, t \tag{3.28}$$

$$-P_k^{max} \leq \sum_n P_{nct}^{inj} PTDF_{0nk}^{ref} \leq P_k^{max}, \forall k, c \neq C_k, t \tag{3.29}$$

$$-P_k^{max,c} N1_k \leq \sum_n P_{nct}^{inj} PTDF_{cnk}^{ref} \leq P_k^{\max,c} N1_k, \forall k, c \in C_k, t \tag{3.30}$$

$$P_g^{min} u_{gt} N1_g \leq P_{gct} \leq P_g^{max} u_{gt} N1_g, \forall g, c, t \tag{3.31}$$

$$P_{gct} - P_{g0t} \leq R_g^{10} u_{gt}, \forall g: g \neq c, c, t \tag{3.32}$$

$$P_{g0t} - P_{gct} \leq R_g^{10} u_{gt}, \forall g: g \neq c, c, t \tag{3.33}$$

$$P_{gct} - P_{g0t} \leq r_{gt}, \forall g: g \neq c, c, t \tag{3.34}$$

$$P_{g0t} - P_{gct} \leq r_{gt}, \forall g: g \neq c, c, t \tag{3.35}$$

In the above formulation, the objective is to minimize the expected operating cost over a set of uncertain scenarios as presented in (3.24). The node balance constraint (see (3.26a-c)) is separated to distinguish when the constraint represents the base-case (3.26a), *G*-1 generation contingency scenarios (3.26b), and finally *T*-1 transmission contingency scenarios (3.26c). Constraint (3.28) enforces the energy balance between the supply and the demand at the system level. The transmission line capacity limit for the base-case scenario and the *G*-1 generation contingency scenarios is constrained by (3.29), whereas that for *T*-1 transmission contingency scenarios is imposed by (3.30). The generator output limit constraint is represented by (3.31). Finally, deviation of an online generator output level (see (3.32)-(3.35)) from the base-case dispatch to the post-contingency dispatch is limited by its reserve (r_{gt}) and by its 10-minute ramp rate (R_g^{10}). Note that for

each scenario, only one of $N1_k$ and $N1_g$ is set to 0 while the rest is set to 1. Detailed explanations on how to calculate PTDF in different scenarios are given in Appendix A.

ESCUC model presented by (3.24)-(3.35) minimizes the expected cost of all scenarios (called ESCUC-*expected* model in rest of this chapter), as presented in (3.24). An alternative option for ESCUC is to minimize only the base-case costs including generator production costs, the startup costs, and the shutdown costs as shown in (3.36), with the same set of constraints as (3.25)-(3.35).

$$minimize \sum_g \sum_t \left(c_g^p P_{g0t} + c_g^{NL} u_{gt} + c_g^{SU} v_{gt} + c_g^{SD} w_{gt}\right) \quad (3.36)$$

The above model for the stochastic market is called the ESCUC-*base* market model throughout this chapter. This model minimized (3.36) while searching for a feasible solution for pre- and post-contingency states.

3.3. Pricing Implications of Contingency Modeling Approaches

The market model presented in Sections 3.2.1 and 3.2.2 give market solutions that may not be *N*-1 and *G*-1 reliable, respectively. To achieve *N*-1 reliable solutions, the market operators implement OMC on their market solutions [8]. To replicate this practice, this chapter implements OMC on the output of market models from Sections 3.2.1 and 3.2.2. The OMC approach used in this work is similar to [8], [66], and [22]. In this approach, the generation units that are committed in the DA SCUC market model are not allowed to be de-committed, and their dispatches are limited to the original approximated DA solution by their 10-minute ramp rate limit. However, modifying the dispatch and the commitment of additional units is allowed in order to ensure reliable operation.

After an *N*-1 reliable dispatch solution is obtained through the OMC approach, the settlements are calculated using DA market LMP [8]. However, these settlements may not reflect the true value of *N*-1 reliability services due to the discrepancy between LMP calculation and final dispatch solution. Thus, such practice may not be incentive compatible for market participants, especially those who provide reliability services.

On the other hand, since all contingencies are represented endogenously in the ESCUC market model (Section 3.2.3), the obtained solution is expected to be *N*-1 reliable. For this model, a pricing mechanism can be obtained to properly incentivize all market participants for providing energy and contingency reserve. In this chapter, the concept of s*ecuritized LMP* (SLMP) is presented to better capture the value of reliability services. The SLMP is the dual variable of (3.27), i.e., $\lambda_{nt}^{securitized}$. Since the ESCUC model is a mixed-integer linear program, its dual formulation is not well-defined. However, after fixing the binary variables to their values at the best solution found, the linear model of ESCUC is achieved, which has a well-defined dual formulation. Equation (3.37) is obtained by deriving the dual formulation from the ESCUC linear primal problem, which shows the relationship between LMPs from the base-case (3.26a), contingency scenarios (3.26b)-(3.26c), and the SLMP.

$$\lambda_{nt}^{securitized} = \lambda_{n0t} + \sum_{c\in C_g} \lambda_{nct} + \sum_{c\in C_k} \lambda_{nct}, \forall n, t \tag{3.37}$$

It is worth mentioning that to obtain the relation presented in (3.37), the demand is treated as a variable in (3.26a-c), and the model enforces $d_{nt} = Load_{nt}$ in (3.27). The first term in the right-hand side of (3.37) represents energy and congestion components of SLMP in the pre-contingency state, while the second and third terms represent energy and congestion components of SLMP in post-contingency states for the generators and non-

radial transmission lines contingencies, respectively. Therefore, the SLMP inherently captures the true value of reserves in the post-contingency state on a nodal basis. The pricing scheme presented here from the ESCUC market model has the advantage that it permits the ISOs to gauge how the market participants should be compensated for providing contingency-based reserve.

The market settlements are compared for three market models, i.e., models in Sections 3.2.1, 3.2.2, and 3.2.3. Fig. 3.1 illustrates the procedure for comparing these market models.

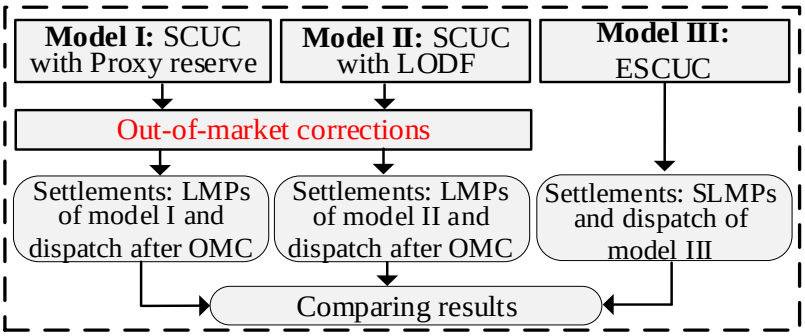

Fig. 3.1. Procedure for Pricing Implications Comparison of Market Models.

3.3.1. Testing & Results of Pricing Implication

CPLEX v12.8 is used to perform all simulations on a computer with an Intel Core i7 CPU @ 2.20 GHz, 16 GB RAM, and 64-bit operating system. A modified 118-bus IEEE test system is used to implement the market auction models, which has 54 generators, 186 lines (177 non-radial), and 91 loads. Set C_g and C_k include N-1 contingencies for all generators and non-radial transmission line elements, respectively. Consequently, there are 232 scenarios modeled in the ESCUC market auction model, including the base-case scenario, 54 generator contingencies, and 177 non-radial transmission line contingencies. The probability of contingencies is calculated from historical failure rates [61]. The

probability of base-case is considered to be 0.946 (i.e., π_{BC}=0.946) in order to make the summation of probabilities over all scenarios equals to 1. The relative MIP gap is set to 0%. The three market auction models, i.e., SCUC with proxy reserve requirements (abbreviated as "SCUC-Prxy"), SCUC with transmission contingency modeled using LODF (abbreviated as "SCUC-LODF"), ESCUC-*expected*, and ESCUC-*base*, are compared in terms of operational cost, incentive compatibility, and market settlements.

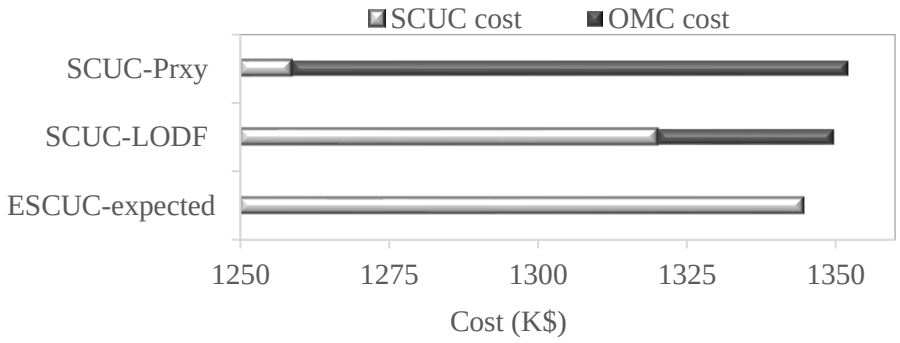

Fig. 3.2. Final Costs Comparison for $N-1$ Reliable Solutions.

Fig. 3.2 compares the final costs for the different market auction models, namely, SCUC-Prxy, SCUC-LODF, and ESCUC-*expected*. This cost includes the SCUC cost and OMC cost. OMC is not performed for ESCUC models as these models explicitly represent contingencies using recourse decision variables and produce an *N*-1 reliable solution. The solution of the ESCUC-expected market auction model has the lowest final cost (benchmark solution) since its scheduled reserve is deliverable in post-contingency states. The SCUC-LODF results in higher SCUC cost compared to the SCUC-Prxy, but it requires less discretionary changes or uneconomic adjustments (OMC actions) to achieve *N*-1 reliability; thus, the SCUC-LODF results in less OMC cost. From the reliability point of view, it can be concluded that the SCUC-LODF provides a solution that is closer to the *N*-1 reliable ESCUC solution. Note that in Fig. 3.2, only the costs of SCUC-Prxy,

SCUC-LODF, and ESCUC-*expected* market action models were compared; however, comprehensive comparisons between different types of costs of the ESCUC-*expected* and ESCUC-*expected* models are presented in Section 3.4.

LMPs of the market models are studied in Fig. 3.3 for hour 22 across the buses. Based on this figure, as the market model moves away from SCUC-Prxy toward capturing a more accurate representation of the contingency events, the prices are increased from bus #67 to bus #109, and also are mostly higher in bus #1-67. The difference between prices is due to the new elements of LMP, i.e., marginal security elements, which represent the value of reserve provision in the modeled contingencies. More specifically, the deterministic model, which utilizes proxy reserve to achieve *N*-1 reliability, does not capture the true value of achieving *N*-1 reliability because the obtained market LMPs do not adequately reflect the value of delivering reserve in the post-contingency state. Accordingly, the LMPs tend to be lower in this model. In this case, the new committed units after OMC may not be fully compensated for providing ancillary services, which can be a reason for the *missing money* issue. This will cause a natural unfairness in market strategy as market participants might not be compensated fairly with this mechanism. On the other hand, the ESCUC-*base* and ESCUC-*expected* market models inherently capture the different values of reserves offered by various entities as they reflect the value of delivering reserve in the post-contingency state on a locational basis, so their SLMPs tend to be higher. This result occurs because markets based on such models explicitly check to see whether the reserve is deliverable for each contingency. Furthermore, the SLMPs comparison between the ESCUC-*base* and ESCUC-*expected* shows that the former model generally has the same SLMPs in bus #1-67 and #109-118,

while it tends to have higher SLMPs from bus #67 to bus #109. *Overall, these analyses confirm that with a more accurate representation of contingencies in the market auction models, the reliability and associated products are priced more accurately.* This would result in fair and accurate market signals for market participants and improve overall market efficiency.

Fig. 3.4 compares the market auction models with respect to market settlements. It can be seen that ESCUC-*base* and ESCUC-*expected* market models have considerably higher generators revenue and load payment compared to SCUC-Prxy and SCUC-LODF; these settlements have their lowest value with the SCUC-Prxy. Furthermore, amongst the ESCUC-*base* and ESCUC-*expected,* the latter has less generators revenue and load payment compared to the former model. The generation rent, which is calculated from subtracting the variable cost of units from their revenues, increases as the models have more explicit and accurate representation of the contingency events. For this settlement, the ESCUC-*base* has the highest value, and the SCUC-Prxy has the lowest value. From these results, it can be said that more accurate modeling of *N*-1 requirement in market models results in increased profit of generators.

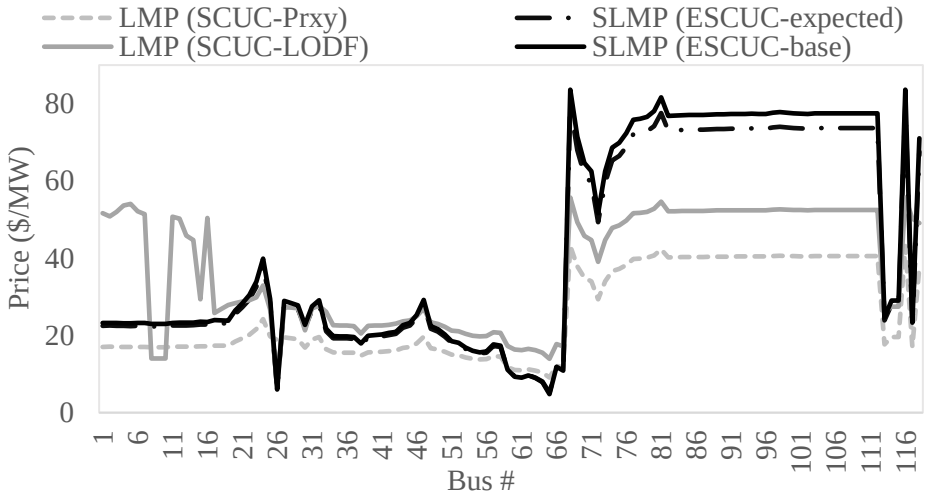

Fig. 3.3. Pricing Comparison of SCUC-Prxy, SCUC-LODF, ESCUC-*expected*, and ESCUC-*base* Market Models.

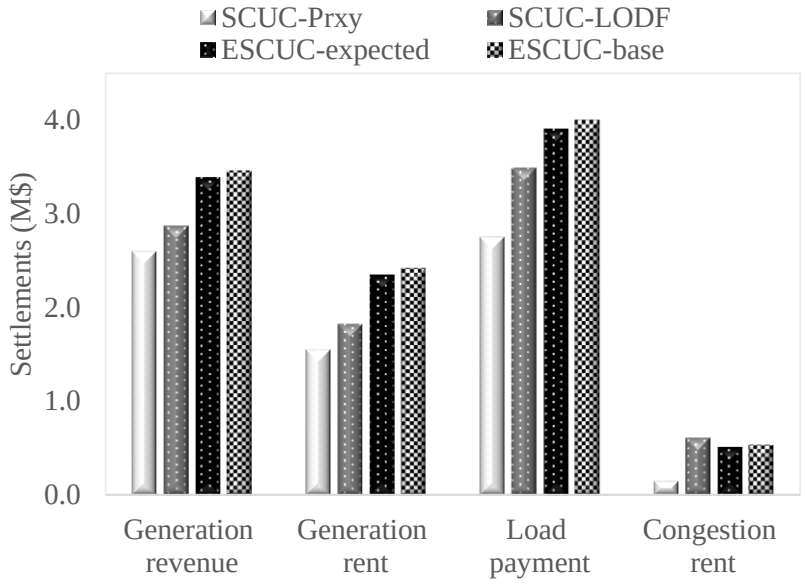

Fig. 3.4. Settlements for Different Market Action Models.

3.4. Objective Function Design and Formulation Evaluation for Stochastic Market Models

As mentioned in Section 3.2, the ESCUC-*expected* model minimizes the expected cost of all scenarios, as presented in (24). However, during emergency conditions in RT, the system operators implement corrective actions, which are aimed to eliminate violations as quickly as possible (not to minimize operation cost) in order to recover from the contingency and to regain *N*-1 reliability. These corrective actions may not necessarily be the lowest cost options. Thus, minimizing post-contingency cost in the DA may result in a solution, which anyways will not be fully implemented. This discrepancy can result in the inefficiency of the stochastic market model with the expected cost minimization objective. Furthermore, minimizing expected cost may result in deviation of the base-case schedule, which has the highest probability of occurrence, from its optimal solution.

In short, such models may generate operational schedules with higher base-case costs with no guarantee of reducing operating costs during contingencies. Additionally, inaccurate estimation of the probability of asset outages can lead to different pricing and market outcomes.

The aforementioned issues create a need for a detailed examination of the objective function design for the stochastic market models. This chapter proposes a framework to identify an effective stochastic market design by comparing two ESCUC models, i.e., ESCUC-*expected* and ESCUC-*base* (presented in Section 3.2.3), from the aforementioned aspects. The detailed analyses are presented in the following sub-sections.

3.4.1. Realized N-1 Final Operating Cost

As discussed, the intention during an emergency condition is not to minimize cost; rather, the goal is to recover from the event as quickly as possible by minimizing violation. In this section, contingency analysis with violation minimization is performed, which mimics the operator's actions in emergency conditions. The realized *N*-1 operating costs for the two ESCUC models are calculated using the dispatch from contingency analysis tool; these costs reflect the corrective generation dispatch actions after the *N*-1 contingencies. Then, the realized *N*-1 costs for the dispatch from two ESCUC models are compared. Fig. 3.5 demonstrates the procedure performed for this analysis.

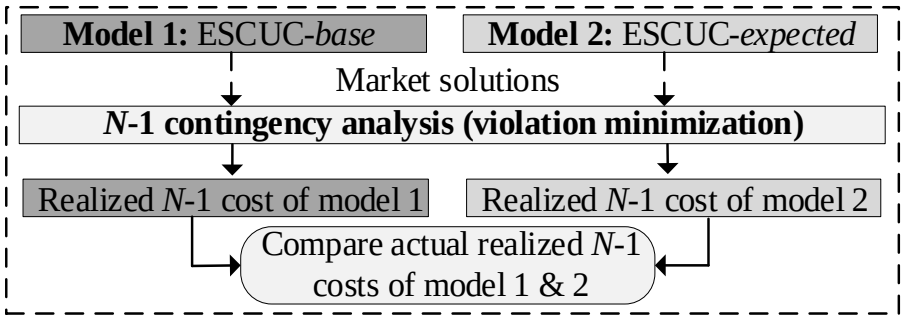

Fig. 3.5. The Procedure of Comparison of Two Models for Actual Realized *N*-1 Costs.

The *N*-1 contingency analysis tool is a linear programming problem that is solved independently at each time interval t for each operating state $c \in C_g, C_k$. The formulation for contingency analysis is given below.

$$minimize \sum_n (LS_n^+ + LS_n^-) \tag{3.38}$$

$$-P_g \leq (\overline{r_g} - \bar{P}_g)\bar{u}_g N1_g, \forall g \tag{3.39}$$

$$P_g \leq (\overline{r_g} + \bar{P}_g)\bar{u}_g N1_g, \forall g \tag{3.40}$$

$$P_g^{min}\bar{u}_g N1_g \leq P_g \leq P_g^{max}\bar{u}_g N1_g, \forall g \tag{3.41}$$

$$P_n^{inj} = \sum_{g \in g(n)} P_g - Load_n + LS_n^+ - LS_n^-, \forall n \tag{3.42}$$

$$\sum_n P_n^{inj} = 0 \tag{3.43}$$

$$-P_k^{max,c} N1_k \leq \sum_n PTDF_{nk}^{ref} P_n^{inj} \leq P_k^{max,c} N1_k, \forall k \tag{3.44}$$

$$LS_n^-, LS_n^+ \geq 0, \forall n \tag{3.45}$$

Positive slack variables, i.e., LS_n^- for load shedding and LS_n^+ for load surplus, indicate the post-contingency security violations. Consequently, the contingency analysis objective (3.38) is to minimize the load shed and the load surplus, when an outage occurs. Constraints (3.39) and (3.40) restrict the deviation of the power generation from the pre-contingency to the post-contingency by the scheduled reserve obtained from the DA

ESCUC models. The generator output limit constraint in the post-contingency state is represented by (3.41). The node balance constraint in the post-contingency state is ensured by (3.42), while (3.43) ensures power balance at the system level. Constraint (3.44) limits the post-contingency transmission line flows to be within the emergency limits for generation and transmission contingencies. In model (3.38)-(3.45), only one $N1_k$ and $N1_g$ is set to zero while the rest of $N1_k$ and $N1_g$ are equal to one.

3.4.2. Impacts of Imprecise Estimation in Probabilities

The second issue that should be investigated when it comes to the design of a stochastic market model is the implications of inaccuracy in the estimation of outages probability. These analyses are also very necessary to be performed as it is difficult to exactly estimate the probability of outages, which itself can lead to different pricing implications and market solutions. In order to realize the impact of this inaccuracy, the procedure shown in Fig. 3.6 is proposed in this chapter.

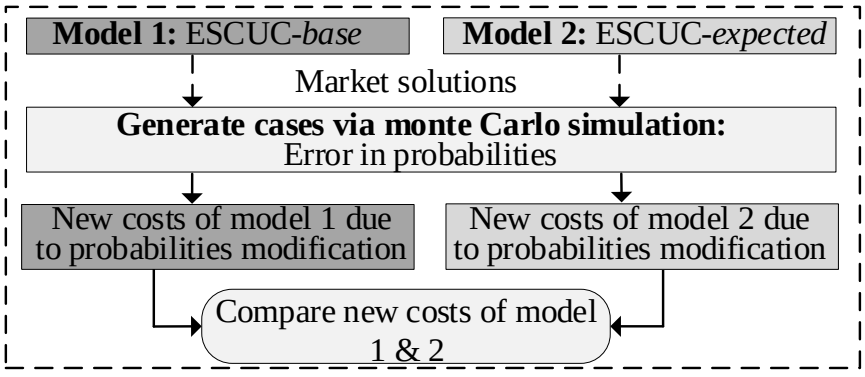

Fig. 3.6. The Procedure of Analysis of Imprecise Probabilities Estimation.

3.4.3. Testing & Results of Objective Function Design

IEEE 118-bus test system that was explained in detail in section 3.3.1 is used to perform the simulations. First, *ESCUC-base* and *ESCUC-expected* models are solved

with relative MIP gap set to 0% to compare their benchmark solutions. The formulations are evaluated based on the following metrics:

- DA base-case cost: this cost is calculated through equation (3.36) based on the DA base-case scenario dispatch and DA commitment decision of ESCUC models.
- Original DA expected cost: this cost is calculated through equation (3.24) based on the DA scenarios' dispatch and DA commitment decision of ESCUC models.
- Original DA scenario cost: this cost includes the expected variable cost of generators for post-contingency scenarios (all scenarios excluding the base-case scenario) calculated based on the DA dispatch of ESCUC models.
- Realized N-1 cost: this cost is the realized operation cost during *N*-1 contingency scenarios (i.e., contingency analysis with violation minimization that mimics the operator's actions in the emergency conditions).

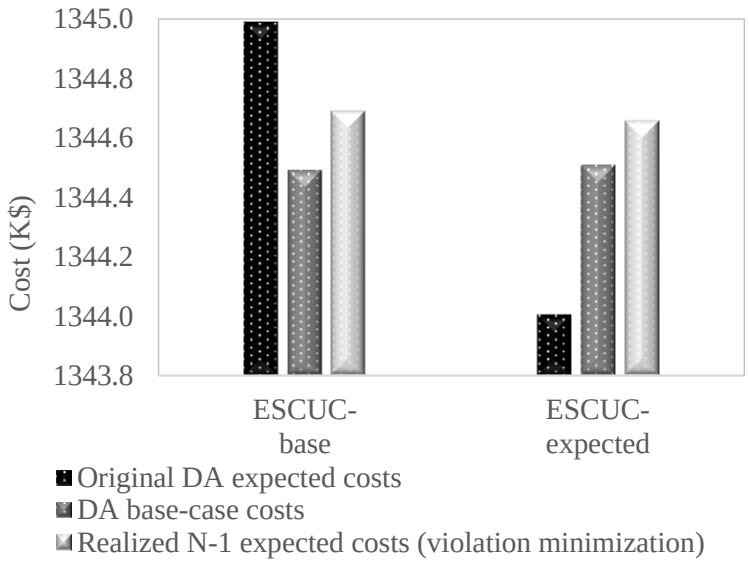

Fig. 3.7. Original DA Expected Costs, DA Base-case Costs, and Realized N-1 Expected Costs Comparison for *N*-1 Reliable Solutions Obtained from ESCUC-*expected* and ESCUC-*base* Models.

Fig. 3.7 compares three different costs, namely, original DA expected costs, DA base-case costs, and realized N-1 expected costs. Since the objective function of the ESCUC-expected is to minimize the costs over all scenarios (as opposed to minimizing only the base-case cost in the ESCUC-base), it is clear that the original DA expected costs of the ESCUC-expected model are lower than the original DA expected costs of ESCUC-base model. Likewise, the DA base-case costs of the ESCUC-expected model are higher than the DA base-case costs of the ESCUC-base model. However, the realized N-1 expected costs of the two models are almost the same (the difference is only 0.002 percent). These results reveal that minimizing post-contingency costs in the ESCUC-expected does not represent operators' actions and may not always result in lower N-1 realized costs in emergency conditions. Similar results are obtained when the original DA scenario costs of the two models are compared as shown in Fig. 3.8. Also, the comparisons on how the market solution of ESCUC-base and ESCUC-expected models can differ from the real-time operational solution during emergency conditions are illustrated in Fig. 3.9 and Fig. 3.10 for the contingency scenarios, namely outage of generator 2 and line 6, respectively.

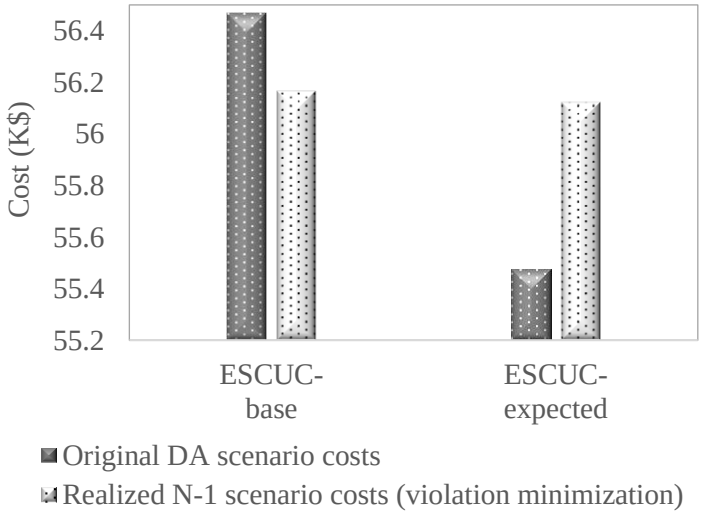

Fig. 3.8. Scenario Cost Comparison for *N*-1 Reliable Solutions Obtained from ESCUC-*expected* and ESCUC-*base* Models.

Moreover, the industry practice of considering a non-zero MIP gap is implemented here to achieve 30 various solutions (all within 1% MIP gap) for the two ESCUC models, for the sake of a comprehensive comparison. By pairing the solutions of two ESCUC models, the total number of pairs is equal to 30×30=900, each of which includes a possible markets outcome from two different models to be compared. Table 3.1 lists the percentage of pairs that the ESCUC-*base* model results in lower costs compared to ESCUC-*expected*. It can be observed that, as expected, the DA base-case costs of ESCUC-*base* is lower in 85 percent of pairs compared to those of the ESCUC-*expected* model. Fig. 3.11 (a) presents the histogram of costs difference calculated from subtracting the DA base-cost cost of ESCUC-*base* from that of ESCUC-*expected*. It can be seen that the density of the pairs cost difference tends to be toward positive values. Moreover, Table 3.1 presents that, as expected, the original DA expected costs of ESCUC-*base* are lower in 30 percent of the pairs (see Fig. 3.11 (b) for histogram illustration of the difference in original DA expected costs). Finally, Table 3.1 shows that in almost 86 percent of pairs, the realized *N*-1 expected costs of the ESCUC-*base* model are less than those of the ESCUC-*expected* model during *N*-1 contingency scenarios. Fig. 3.11 (c) illustrates realized *N*-1 expected costs difference (i.e., $\text{realized}\,\{N-1\}\,\text{costs}_{\text{ESCUC}-expected} - \text{realized}\,\{N-1\}\,\text{costs}_{\text{ESCUC}-base}$) for the 900 pairs.

The summarized results in Table 3.1, as well as Fig. 3.11, confirm that the realized *N*-1 expected costs from the DA dispatch solution of ESCUC-*base* are lower than the realized *N*-1 expected costs of ESCUC-*expected* in most of the pairs regardless of *N*-1 cost minimization in the ESCUC-*expected*. Moreover, the DA base-case costs of the ESCUC-

base are lower than those of the ESCUC-*expected* in most of pairs. As one can see, the ESCUC-*base* performs better in general compared to the ESCUC-*expected* model based on the DA base-case costs and realized *N*-1 final costs.

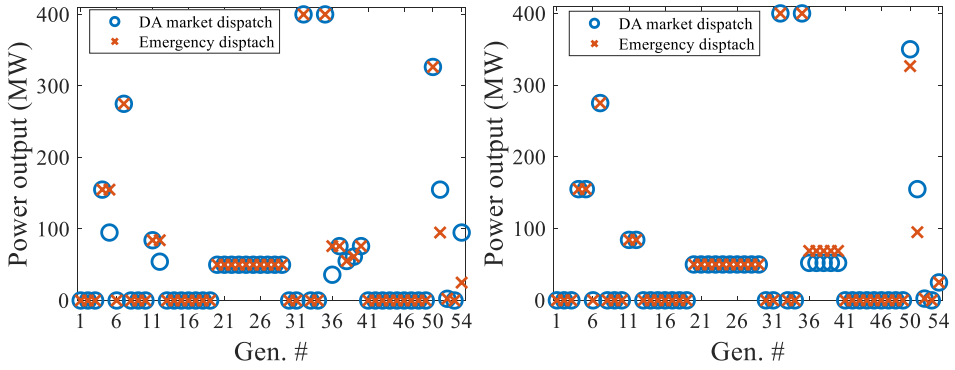

(a) (b)

Fig. 3.9. Comparison of Generators' Dispatch in the DA Market and Emergency Condition for the Contingency Scenario Associated to the Outage of Generator 2: (a) ESCUC-*base* Market Model (b) ESCUC-*expected* Market Model.

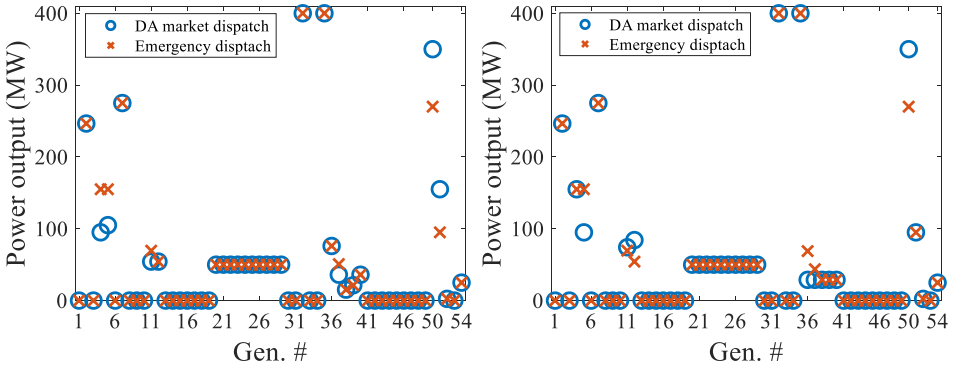

(a) (b)

Fig. 3.10. Comparison of Generators' Dispatch in the DA Market and Emergency Condition for the Contingency Scenario Associated to the Outage of Line 6: (a) ESCUC-*base* Market Model (b) ESCUC-*expected* Market Model.

Table 3.1. Percentage of Pairs with Lower Cost for ESCUC-*base* Model Compared to ESCUC-*expected* Model.

Type of cost	Percentage
DA base-case costs	85%
Original DA expected costs	30%
Realized *N*-1 expected costs (violation minimization)	86%

Moreover, the impact of inaccuracy in the contingency probability estimation is evaluated. It is assumed that there is an error in the estimation of probabilities that follows a Gaussian distribution with zero mean, and the standard deviation of 20% and 40%. For each standard deviation, 2000 cases are generated, each of which includes a set of 231 contingency probabilities (for generator and non-radial transmission line contingencies). Then, the probability of the base case is calculated through the following equation.

$$\pi_{BC,s} = 1 - \sum_{c \in C_k} \pi_{c,s} - \sum_{c \in C_G} \pi_{c,s}, \forall s \quad (3.46)$$

where s is the index of cases, and $\pi_{BC,s}$ and $\pi_{c,s}$ are the probability of base-case scenario and contingency event c in case s. Since the range of probability of base-case scenario is more known for the system operators for a specific electric system, the cases that lead to a base-case probability out of the range 0.948 and 0.944 have been eliminated (perfect estimation has a base-case probability of 0.946). The 2000 cases are applied based on the procedure presented in Fig. 3.6 to each of the 30 solutions of ESCUC-*base* and ESCUC-*expected* models mentioned earlier. Therefore, there are 30×2000=60,000 solutions (costs) for each market model. By pairing the solutions of two different stochastic market models, the total number of pairs is equal to 3,600,000,000, i.e., 60,000×60,000. It is worth mentioning that each pair has two market outcomes, one from the ESCUC-*base* model and one from ESCUC-*expected* that can be compared.

Table 3.2. Effects of Error in the Estimation of Probabilities on the Percentage of Pairs That ESCUC-base Model has Lower Cost Compared to ESCUC-*expected* Model.

	Perfect estimation	20% error in estimation	40% error estimation
% of pairs with lower original DA expected costs	30	36.6	43.0

% of pairs with lower original DA scenario costs	0	7.8	22.2

Table 3.2 presents the impacts of error in the estimation of probabilities on the percentage of the pairs that the ESCUC-*base* model has lower costs (original DA expected costs and scenario costs) compared to the ESCUC-*expected* model. From Table 3.2, it can be seen that the percentage of pairs where ESCUC-*base* model has lower original DA expected cost increases from 30% to 36.6% and 43% as the accuracy in estimation of probabilities moves from being perfect to have 20% and 40% estimation errors, respectively. The percentage of pairs in which the ESCUC-*base* model has lower original DA scenario costs in comparison with the other model increases from 0% for perfect estimation to 7.8% and 22.2% for 20% and 40% error in estimation, respectively. These results demonstrate that after the solutions of two models are affected by the inaccuracy in probabilities estimation, the likelihood that ESCUC-*base* outperforms the other model in having less original DA expected costs and scenario costs increases.

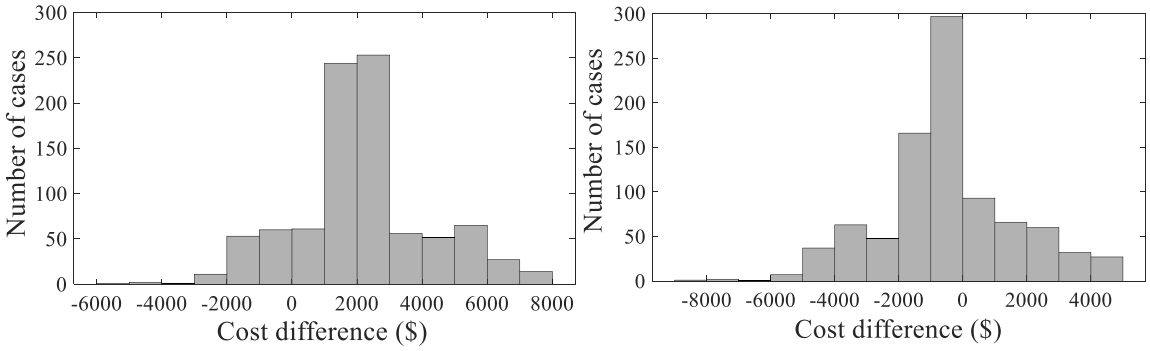

(a) (b)

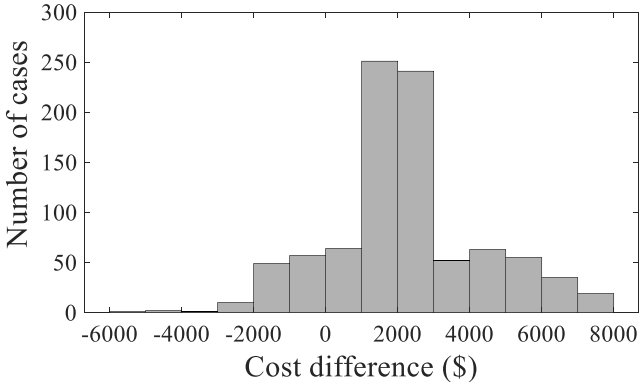

(c)

Fig. 3.11. Histogram of Cost Difference ($cost_{\text{ESCUC}-expected} - cost_{\text{ESCUC}-base}$) of the Pairs: (a) DA Base-case Costs (b) Original DA Expected Costs (c) Realized *N*-1 Expected Costs.

3.5. Conclusion

A comprehensive framework incorporating various procedures was proposed in this chapter to: (i) conduct a fair comparison of pricing and settlements between different market models that ensure different levels of security, and (ii) examine efficient objective formulation for stochastic market design.

To compare various market models: (i) the concept of securitized LMP was developed for the ESCUC model, (ii) an OMC procedure was implemented on the solution of market models with proxy reserve requirement and with LODF to obtain *N*-1 reliable dispatch. The ISO practice of calculating market settlements based on the original market prices and *N*-1 reliable schedule after performing OMC was implemented. Newly committed generators during OMC do not have a direct impact on the value of LMP for their location. At this stage, it is unclear whether this mechanism (a SCUC model following with OMC) enables opportunities for market exploitation. Using this mechanism, the market model is not purely a pool; instead, it is a combination of a pool and pay-as-bid model. This practice is limited and not transparent for all market

participants; therefore, the market participants will not change their bidding strategy accordingly (as they would in a pay-as-bid model). Although this is accepted market manipulation, some participants might receive less than deserved benefits and some might receive more. However, with a more accurate representation of contingencies in the ESCUC compared to SCUC models with approximation on *N*-1 security criteria, *N*-1 grid security requirements are originally captured, thereby, the value of service (contingency-based reserve) provided by generators is reflected in the LMPs to achieve grid security. In other words, if the market SCUC includes the reliability criteria more adequately, prices can better reflect the true marginal cost associated with the provision of reliable electricity. It is worth noting that assessments of the effects of the OMC performed in different market models due to other approximations (e.g., linear approximation of AC power flow, use of cutoffs for PTDFs, voltage security limits, and renewable uncertainties) on the pricing and settlements are interesting directions for future research.

Furthermore, it was shown that the stochastic market design with expected objective function does not give solutions that ensure minimum realized operating costs at *N*-1 contingency states. Instead, the stochastic market design with base-case objective function had better performance compared to the market model with expected objective function in terms of the DA base-case costs and realized *N*-1 costs. Moreover, inaccuracy in estimated probability results in larger differences in the original DA expected costs and scenarios costs of ESCUC-*base* and ESCUC-*expected*, where ESCUC-*base* further outperforms ESCUC-*expected*. It can be concluded that evidently, the stochastic market

design with base-case objective function can be more efficient compared to the stochastic market design with the expected objective function.

Chapter 4.

DAY-AHEAD RESOURCE SCHEDULING WITH ENHANCED FLEXIBLE RAMP PRODUCT: DESIGN AND ANALYSIS

4.1. Introduction

There have been intentions of modeling and procuring FRP in the DA market in order to ensure resource adequacy for meeting the ramping needs in the RT markets. For example, CAISO has started market initiatives to add FRP to its DA market to correctly position and commit resources to address uncertainty and variability in the net load, especially meeting the ramping needs in the FMM, i.e., the next closest market to DA [31] and [32]. Overall, such structural changes, i.e., the inclusion of FRP in DA market formulation, require detailed analyses and design in order to ensure adequate operational flexibility, market efficiency, and pricing.

This chapter first presents the formulation of a DA market model with general FRP constraints. Then, it sheds light on a subtle issue that can potentially happen in the next market processes after the DA market, as a result of procurement of DA ramp capabilities only based on the hourly ramping requirements. Then, a new FRP design is proposed to address this issue. In the proposed formulation, the DA FRP design is modified to accommodate the 15-min net load variability and uncertainty while scheduling hourly FRPs in the DA market. The proposed approach overcomes the concerns raised by CAISO in [9] and [14] regarding the 15-min ramp infeasibility. Furthermore, the DA market models with different FRP designs are developed by incorporating the regulation reserve into the market formulation. Then, coordination among these market products is evaluated to see how they can affect the system operation efficiency in the FMMs against

steep 15-min net load changes. New market-based incentivizing policies are driven for the proposed FRP design in order to properly encourage the ramp-responsive resources that provide the enhanced ramp capability. To effectively evaluate different FRP designs from reliability and market efficiency points of view, a validation methodology is proposed that is similar to the RT unit commitment (RTUC) processes of the CAISO. This validation phase plays a pivotal role in evaluating the performance of DA FRP in the view of how the system ramp capability is improved in RT operation (e.g., FMM); however, this step has been ignored in most of the work in the literature [33]–[36], [48], [49].

The rest of the chapter is organized as follows. Section 4.2 presents model formulations, including the enhanced FRP design. Section 4.3 focuses on the market payment mechanism for the proposed FRP design. Section 4.4 presents the validation phase methodology. Finally, simulation results are discussed in Section 4.5 while Section 4.6 concludes the chapter.

4.2. Model Formulation

The general FRP design within the DA market model is formulated in Section 4.2.1, which is based on [33], [34], [22]. Then, a subtle issue that can potentially happen in the next market processes after the DA market with the shorter granularity or time resolution is discussed in Section 4.2.2. This subtle issue is the motivation behind the proposed DA FRP design presented in Section 4.2.3 to improve the general FRP design from reliability and efficiency points of view. Finally, the DA market model with different FRP designs is developed to include the regulation reserve in Section 4.2.4.

4.2.1. DA Market Model with General FRP Design

DA market model with general FRP design and requirement is presented in (4.1)-(4.22). The objective function (4.1) is to minimize total operating costs (i.e., variable operating costs, no-load costs, startup costs, and shutdown costs):

$$minimize \sum_g \sum_t (c_g^p P_{gt} + c_g^{NL} u_{gt} + c_g^{SU} v_{gt} + c_g^{SD} w_{gt}) \quad (4.1)$$

The set of constraints is shown in (4.2)-(4.22). Minimum up and down time constraints of the generators are enforced by (4.2) and (4.3), while constraints (4.4) and (4.5) ensure hourly ramp rate limits. Constraints (4.6)-(4.9) ensure system-wide and nodal power balance, calculate power flow, and impose transmission line flow limits. Constraints (4.10) and (4.11) model the relationship between the commitment variable, the startup variable, and the shutdown variable. Constrains (4.12)-(4.14) model the binary commitment decision (u_{gt}), the startup (v_{gt}), and shutdown (w_{gt}) decisions, respectively.

$$\sum_{s=t-UT_g+1}^{t} v_{gs} \leq u_{gt}, \forall g, t \in \{UT_g, .., T\} \quad (4.2)$$

$$\sum_{s=t-DT_g+1}^{t} w_{gs} \leq 1 - u_{gt}, \forall g, t \in \{DT_g, .., T\} \quad (4.3)$$

$$P_{gt} - P_{gt-1} \leq R_g^{HR} u_{gt-1} + R_g^{SU} v_{gt}, \forall g, t \geq 2 \quad (\gamma_{gt}^-) \quad (4.4)$$

$$P_{gt-1} - P_{gt} \leq R_g^{HR} u_{gt} + R_g^{SD} w_{gt}, \forall g, t \geq 2 \quad (\gamma_{gt}^+) \quad (4.5)$$

$$\sum_{g \epsilon g(n)} P_{gt} - NL_t = P_{nt}^{inj}, \forall n, t \quad (\delta_{nt}) \quad (4.6)$$

$$\sum_n P_{nt}^{inj} = 0, \forall t \quad (\lambda_t) \quad (4.7)$$

$$\sum_n P_{nt}^{inj} PTDF_{nk} \leq P_k^{max}, \forall k, t \quad (F_{kt}^+) \quad (4.8)$$

$$-P_k^{max} \leq \sum_n P_{nt}^{inj} PTDF_{nk}, \forall k, t \quad (F_{kt}^-) \quad (4.9)$$

$$v_{gt} - w_{gt} = u_{gt} - u_{g,t-1}, \forall g, t \quad (4.10)$$

$$v_{gt} + w_{gt} \leq 1, \forall g, t \quad (4.11)$$

$$0 \leq v_{gt} \leq 1, \forall g, t \tag{4.12}$$

$$0 \leq w_{gt} \leq 1, \forall g, t \tag{4.13}$$

$$u_{gt} \in \{0,1\}, \forall g, t \tag{4.14}$$

Constraints (4.15)-(4.22) are associated with general FRP constraints. The generator output limits, including up and down FRPs, are presented by (4.15) and (4.16). Constraints (4.17) and (4.18) limit the ramp up and down capabilities to the hourly generators' ramp rate, respectively. The hourly FRP requirements are met via (4.19)-(4.20). Finally, the hourly up and down FRP requirements are calculated through (4.21) and (4.22).

$$p_{gt} + ur_{gt} \leq P_g^{max} u_{gt}, \forall g, t \qquad \left(\alpha_{gt}^{+}\right) \tag{4.15}$$

$$p_{gt} - dr_{gt} \geq P_g^{min} u_{gt}, \forall g, t \qquad \left(\alpha_{gt}^{-}\right) \tag{4.16}$$

$$ur_{gt} \leq R_g^{HR} u_{gt}, \forall g, t \qquad \left(\beta_{gt}^{+}\right) \tag{4.17}$$

$$dr_{gt} \leq R_g^{HR} u_{gt}, \forall g, t \qquad \left(\beta_{gt}^{-}\right) \tag{4.18}$$

$$\sum_g ur_{gt} \geq FRup_t, \forall t \qquad (\pi_t^{+}) \tag{4.19}$$

$$\sum_g dr_{gt} \geq FRdown_t, \forall t \qquad (\pi_t^{-}) \tag{4.20}$$

$$FRup_t = \max\{NL_{t+1}^{max} - NL_t, 0\}, \forall t \leq 23 \tag{4.21}$$

$$FRdown_t = \max\left\{NL_t - NL_{t+1}^{min}, 0\right\}, \forall t \leq 23 \tag{4.22}$$

In the above formulation, the dual variable related to each primal constraint is referenced after the primal constraint.

4.2.2. DA Resource Adequacy to Meet RT 15-Min Ramping Needs with General FRP Design

In the market model with the general FRP design presented by (4.1)-(4.22), the FRP formulation is designed in such a way that resultant added ramp capabilities be able to respond to foreseen (variability) and unforeseen (uncertainty) changes in the net load between the hour t and the specified target hour $t + 1$. Although the procured DA FRP is aimed to increase the ramp capabilities to meet the steep ramping needs in the next RT markets [22], such as the FMM (i.e., the next closest RT market process to DA market), this design disregards the magnitude of the intra-hour 15-min net load changes. The FMM seeks to meet the balance between supply and net load in 15-min intervals. The net load changes (including both variability and uncertainty) between the 15-min intervals can potentially experience a steeper slope, which happens in a shorter time than the hourly net load variations – see case I and case II in Fig. 4.1. The CAISO also raises this issue in [31], [32], where it is mentioned that even with a perfect 15-min forecast (no uncertainty or unforeseen changes), the DA market may produce a schedule that cannot meet a single 15-min ramping need due to the DA hourly scheduling granularity. In other words, the DA hourly schedule in some cases may not even be able to accommodate the steep 15-min net load variability or foreseen changes, putting the 15-min net load uncertainty aside [32]. Indeed, uncertainty can worsen such situations. As previously mentioned, this inability to follow the 15-min net load changes can lead to 15-min ramp infeasibilities [32], which potentially can (i) jeopardize the system reliability and (ii) cause price spikes that create market inefficiency in the long run [28], [37].

Thus, (1a)-(1w) may not ensure adequate procurement of up and down DA ramp capabilities to cover potential steep net load changes in FMM. In the next section, a new approach is proposed to address this issue.

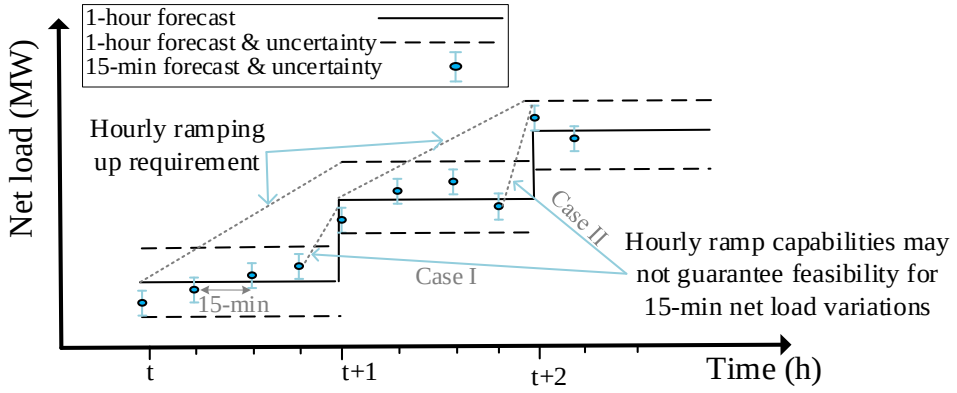

Fig. 4.1. Hourly FRP Versus 15-Min Variability and Uncertainty.

4.2.3. Feasibility of Hourly DA FRP Awards Against Intra-hour 15-Min Variability And Uncertainty

In this chapter, the DA ramping requirements are quantified more accurately so as to potentially capture (i) the hourly net load changes and (ii) 15-min net load changes in FMM. The hourly ramping requirements have already been included in the DA market model through (4.1)-(4.22). For preemptively securing the DA ramp capability awards against the variability and uncertainty in the 15-min granularity, the proposed FRP design incorporates a set of effective constraints, related to the 15-minute ramping requirements, to the general FRP design. The goals of the additional constraints are to:

- Quantify the DA FRP requirements more adaptively regarding the RT 15-min net load changes to improve reliability and efficiency in the next market processes (especially FMM) without adding too much complexity to the existing DA FRP design.
- Enable more consistency between DA and RT scheduling frameworks.

The 15-min ramping requirements should accommodate: (i) foreseen variability in the 15-min net load and (ii) unexpected net load variations between two successive time intervals considering a desired confidence level. For intra-hour 15-min ramp up, the requirements are formulated via (4.23)-(4.26).

$$FRup_{t,0min}^{ih} = max\{NL_{t,15min}^{ih,max} - NL_{t,0min}^{ih}, 0\}, \forall t \quad (4.23)$$

$$FRup_{t,15min}^{ih} = max\{NL_{t,30min}^{ih,max} - NL_{t,15min}^{ih}, 0\}, \forall t \quad (4.24)$$

$$FRup_{t,30min}^{ih} = max\{NL_{t,45min}^{ih,max} - NL_{t,30min}^{ih}, 0\}, \forall t \quad (4.25)$$

$$FRup_{t,45min}^{ih} = max\{NL_{t+1,0min}^{ih,max} - NL_{t,45min}^{ih}, 0\}, \forall t \quad (4.26)$$

(4.21)-(4.25) represent 15-min ramping up requirements for each two successive 15-min intervals of hour t. (4.26) shows the ramping up requirement associated with the last 15-min interval of hour t and the first 15-min interval of hour $t+1$. The enhanced formulation uses auxiliary variables, i.e., ur_{gt}^{ih}, for intra-hour ramping schedules from resources. The summation of these auxiliary variables should satisfy all intra-hour 15-min ramping requirements as shown in (4.27).

$$\sum_{\forall g} ur_{gt}^{ih} \geq \max\left(FRup_{t,0min}^{ih}, FRup_{t,15min}^{ih}, FRup_{t,30min}^{ih}, FRup_{t,45min}^{ih}\right), \forall t \quad \left(\pi_t^{ih,+}\right) \quad (4.27)$$

where $ur_{g,t}^{ih}$ is limited to 15-min ramp rate.

$$ur_{g,t}^{ih} \leq R_g^{15} u_{g,t}, \forall g, t \quad \left(\beta_{gt}^{ih,+}\right) \quad (4.28)$$

Finally, in order to ensure sufficiency of DA FRP to accommodate 15-min variability and uncertainty, constraint (4.29) is included. This constraint identifies that the DA FRP of each ramp-responsive resource should be greater than its corresponding intra-hour ramping schedule.

$$ur_{g,t}^{ih} \leq ur_{g,t}, \forall g, t \qquad \left(\omega_{gt}^{+}\right) \qquad (4.29)$$

A similar formulation can be proposed for the enhanced DA downward FRP design, which is presented in (4.30)-(4.36):

$$FRdown_{t,0min}^{ih} = max\left\{NL_{t,0min}^{ih} - NL_{t,15min}^{ih,min}, 0\right\}, \forall t \qquad (4.30)$$

$$FRdown_{t,15min}^{ih} = max\left\{NL_{t,15min}^{ih} - NL_{t,30min}^{ih,min}, 0\right\}, \forall t \qquad (4.31)$$

$$FRdown_{t,30min}^{ih} = max\left\{NL_{t,30min}^{ih} - NL_{t,45min}^{ih,min}, 0\right\}, \forall t \qquad (4.32)$$

$$FRdown_{t,45min}^{ih} = max\left\{NL_{t,45min}^{ih} - NL_{t+1,0min}^{ih,min}, 0\right\}, \forall t \qquad (4.33)$$

$$\sum_{\forall g} dr_{gt}^{ih} \geq max\left(FRdown_{t,0min}^{ih}, FRdown_{t,15min}^{ih}, FRdown_{t,30min}^{ih}, FRdown_{t,45min}^{ih}\right), \forall t$$

$$\left(\pi_{t}^{ih,-}\right) \qquad (4.34)$$

$$dr_{g,t}^{ih} \leq R_{g}^{15} u_{g,t}, \forall g, t \qquad \left(\beta_{gt}^{ih,-}\right) \qquad (4.35)$$

$$dr_{g,t}^{ih} \leq dr_{g,t}, \forall g, t \qquad \left(\omega_{gt}^{-}\right) \qquad (4.36)$$

The proposed DA market model with the enhanced FRP requirements is shown in (4.37)-(4.38).

$$minimize \sum_{g} \sum_{t} (c_{g}^{p} P_{gt} + c_{g}^{NL} u_{gt} + c_{g}^{SU} v_{gt} + c_{g}^{SD} w_{gt}) \qquad (4.37)$$

subject to:

(4.2)-(4.22) and (4.23)-(4.36) (4.38)

One of the advantages of the proposed DA market model with enhanced FRP design presented by (4.34)-(4.38) is that it does not need to change the DA scheduling framework from hourly granularity to 15-min granularity. This notion is in accordance with the industry practice as the 15-min scheduling granularity for the DA market model has been ceased due to the concerns of complexities caused by quadrupling the number of binary variables [22], [32]. To achieve the goal of capturing 15-min ramping needs in DA

and maintaining the hourly commitment and dispatch, the hourly net load forecasts for 24 time intervals are used in the power balance equation (4.6) while hourly ramp rate constraints are enforced through (4.4)-(4.5). Also, 15-min net load forecasts and uncertainties, i.e., four time intervals within each hour, are used in the 15-min FRP requirement constraints (i.e., (4.23)-(4.29) for 15-min ramping up need and (4.30)-(4.36) for 15-min ramping down need). Finally, the DA FRP of each generator is identified such that it satisfies the intra-hour 15-min ramping response of the generators (i.e., (4.29) for DA up FRP and (4.36) for DA down FRP). For the sake of clarity, Fig. 4.2 illustrates the granularity of DA dispatch and commitment along with the hourly and 15-min ramping up requirements. It is pertinent to note that the 15-min ramping up requirement shown in Fig. 4.2 is associated with the last 15-min interval of hour t and the first 15-min interval of hour $t + 1$.

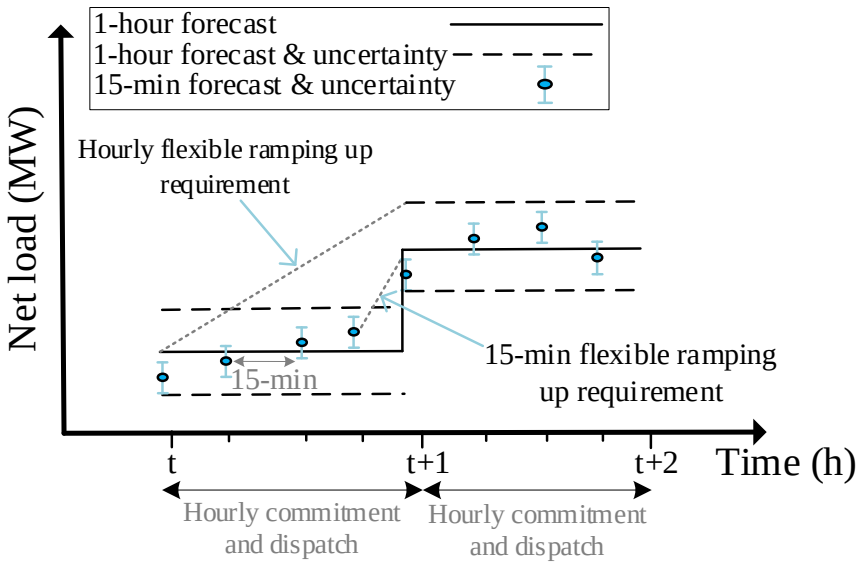

Fig. 4.2. 15-min Ramping Requirements Incorporated in DA FRP Design.

4.2.4. DA Market Model with FRP Designs and Other Ancillary Services

In this section, a DA market model with simultaneous consideration of both FRP and regulation reserve is analyzed. The regulation reserve is used for load following with a different deployment process than FRP, e.g., duration of net load uncertainty coverage. More explanation regarding the difference between FRP and regulation reserve is provided in Section 1.3. Both the proposed FRP and the general FRP requirements are analyzed in the section. Since the contingency-based reserve has a different purpose and deployment process as mentioned in Section 1.3, it has not been considered here. The constraint related to the regulation reserve can be written by (4.39)-(4.42) [98].

$$0 \leq r_{gt}^{u} \leq R_{g}^{10} u_{gt}, \forall g, t \tag{4.39}$$

$$0 \leq r_{gt}^{d} \leq R_{g}^{10} u_{gt}, \forall g, t \tag{4.40}$$

$$\sum_{g} r_{gt}^{u} \geq \eta\% \sum_{n} Load_{nt}, \forall t \tag{4.41}$$

$$\sum_{g} r_{gt}^{d} \geq \eta\% \sum_{n} Load_{nt}, \forall t \tag{4.42}$$

In the above formulation, the constraints (4.39) and (4.40) limit the up and down regulation reserves to the 10-min ramp rate of the generators, while constraints (4.41) and (4.42) model the requirements for up and down regulation reserves, respectively.

4.2.4.1. DA Market Model with General FRP Design and Regulation Reserve

The DA market model, which co-optimizes energy, ramp capability product (based on the general FRP design), and the regulation reserve, is presented by (4.43)-(4.48).

$$minimize \sum_{g} \sum_{t} (c_{g}^{p} P_{gt} + c_{g}^{NL} u_{gt} + c_{g}^{SU} v_{gt} + c_{g}^{SD} w_{gt}) \tag{4.43}$$

subject to:

$$p_{gt} + ur_{gt} + r_{gt}^{u} \leq P_{g}^{max} u_{gt}, \forall g, t \tag{4.44}$$

$$p_{gt} - dr_{gt} - r_{gt}^{d} \geq P_{g}^{min} u_{gt}, \forall g, t \quad (4.45)$$

$$0 \leq ur_{gt} + r_{gt}^{u} \leq R_{g}^{HR} u_{gt}, \forall g, t \quad (4.46)$$

$$0 \leq dr_{gt} + r_{gt}^{d} \leq R_{g}^{HR} u_{gt}, \forall g, t \quad (4.47)$$

(4.2)-(4.14), (4.17)-(4.22), and (4.39)-(4.42) (4.48)

The power generation range of generators that includes the regulation reserve and the FRP is defined through (4.44) and (4.45). The summation of regulation reserve and FRP should not exceed the generator ramp rate as presented by (4.46) and (4.47) [75].

4.2.4.2. DA Market Model with Proposed FRP Design and Regulation Reserve

The DA market model, which co-optimizes energy, ramp capability product (based on the proposed FRP design), and regulation reserve, is given in (4.49)-(4.54).

$$minimize \sum_{g} \sum_{t} (c_{g}^{p} P_{gt} + c_{g}^{NL} u_{gt} + c_{g}^{SU} v_{gt} + c_{g}^{SD} w_{gt}) \quad (4.49)$$

subject to:

$$p_{gt} + ur_{gt} + r_{gt}^{u} \leq P_{g}^{max} u_{gt}, \forall g, t \quad (4.50)$$

$$p_{gt} - dr_{gt} - r_{gt}^{d} \geq P_{g}^{min} u_{gt}, \forall g, t \quad (4.51)$$

$$0 \leq ur_{gt} + r_{gt}^{u} \leq R_{g}^{HR} u_{gt}, \forall g, t \quad (4.52)$$

$$0 \leq dr_{gt} + r_{gt}^{d} \leq R_{g}^{HR} u_{gt}, \forall g, t \quad (4.53)$$

(4.2)-(4.14), (4.17)-(4.22), (4.23)-(4.36), and (4.39)-(4.42) (4.54)

The power generation range of generators that includes the regulation reserve and the FRP is presented through (4.50) and (4.51). The summation of regulation reserve and FRP should not exceed the generator ramp rate as presented by (4.52) and (4.53) [75].

4.3. Market Payment Mechanism for the Proposed FRP Design

Generally, the generators do not give bids for ramping products. Instead, the shadow price (dual variable) of the ramping requirements is employed to calculate the payment for FRP awards [28], [29], [72]. For the general FRP design, these market payments in terms of lost opportunity cost, to compensate generators for making the up and down ramp capabilities available, are given through (4.55) and (4.56), respectively [28].

$$OC_g^{Rup} = \sum_t \left(\pi_t^+ ur_{g,t}\right), \forall g \tag{4.55}$$

$$OC_g^{Rdown} = \sum_t \left(\pi_t^- dr_{g,t}\right), \forall g \tag{4.56}$$

It can be proved that these market payments are composed of a capacity component and a ramping component [72]. With the new FRP design for the DA market model, (4.37)-(4.38), a new market payment mechanism is essential for ramp-responsive resources that provide the enhanced ramp capability product to properly incentivize them to follow the ISO signal. To do so, after deriving the primal-dual formulation of the DA market model (4.37)-(4.38) and performing the complementary slackness (CS) conditions, equation (4c) is obtained. Detailed derivation processes of primal-dual formulation and CS conditions are presented in Appendix B.

$$\pi_t^+ ur_{g,t} + \pi_t^{ih,+} ur_{g,t}^{ih} = \alpha_{gt}^+ ur_{g,t} + \beta_{gt}^+ ur_{g,t} + \beta_{gt}^{ih,+} ur_{g,t}^{ih}, \forall g, t \tag{4.57}$$

In (4.57), right-hand side terms, i.e., $\alpha_{gt}^+ ur_{g,t}$, $\beta_{gt}^+ ur_{g,t}$, and $\beta_{gt}^{ih,+} ur_{g,t}^{ih}$, are respectively associated with the opportunity cost for the generator in terms of withholding some portion of its capacity and ramp capabilities. Based on the equation (4.57), the left-hand side, i.e., $\pi_t^+ ur_{g,t} + \pi_t^{ih,+} ur_{g,t}^{ih}$, is the flexible ramp-up payment of generator g at time interval t for procuring enhanced upward FRP. Hence, a generator that is ramp up

qualified should be compensated based on $OC_g^{Rup,new}$ for its up FRP provision for the entire scheduling horizon.

$$OC_g^{Rup,new} = \sum_t \left(\pi_t^{+} ur_{g,t} + \pi_t^{ih,+} ur_{g,t}^{ih}\right), \forall g \quad (4.58)$$

Similarly, it can be derived that the ramp down qualified generator for procuring down DA FRP should be compensated based on $OC_g^{Rdown,new}$ for the entire scheduling horizon.

$$OC_g^{Rdown,new} = \sum_t \left(\pi_t^{-} dr_{g,t} + \pi_t^{ih,-} dr_{g,t}^{ih}\right), \forall g \quad (4.59)$$

It can be seen that the new FRP market payment (4.58) for providing upward ramp capability awards includes one more additional term, i.e., $\pi_t^{ih,+} ur_{g,t}^{ih}$, compared to the general FRP market payment presented in (4.55). This additional term is for valuing the additional ramp capability procured by the resource to capture the 15-min variability and uncertainty in the FMM. Therefore, in the case that a resource is dispatched out of merit because of providing intra-hour 15-min ramp capability, (4.55) would not be enough to compensate generators; therefore, the new FRP market payment based on (4.58) is necessary for the recourses with the upward FRP awards. A similar comparison applies between the new (4.59) and general (4.56) FRP market payments for resources with downward FRP awards.

4.4. Validation Methodology

An RT validation methodology is needed to compare the performance of the proposed FRP design and the general FRP design. Some of the previous work have implemented RT economic dispatch performed every 5-minute as the validation methodology while ignoring the other market processes, i.e., the FMM, that happens between the DA market and RT economic dispatch market. The FMM is the first market that (i) makes the

preliminary modifications to the posted DA market solutions for meeting RT net load, and (ii) experiences the impacts of DA market reformulations and enhancements. Hence, it can be a good candidate to evaluate the performance of the DA market decisions from the flexibility, economic and reliability points of view. This chapter creates an RT validation methodology, which mimics the FMM of CAISO. This methodology is used to conduct comprehensive reliability and economic comparisons of the proposed method with the general FRP model under 15-min net load scenarios. The flowchart of the proposed simulation procedure is presented in Fig. 4.3.

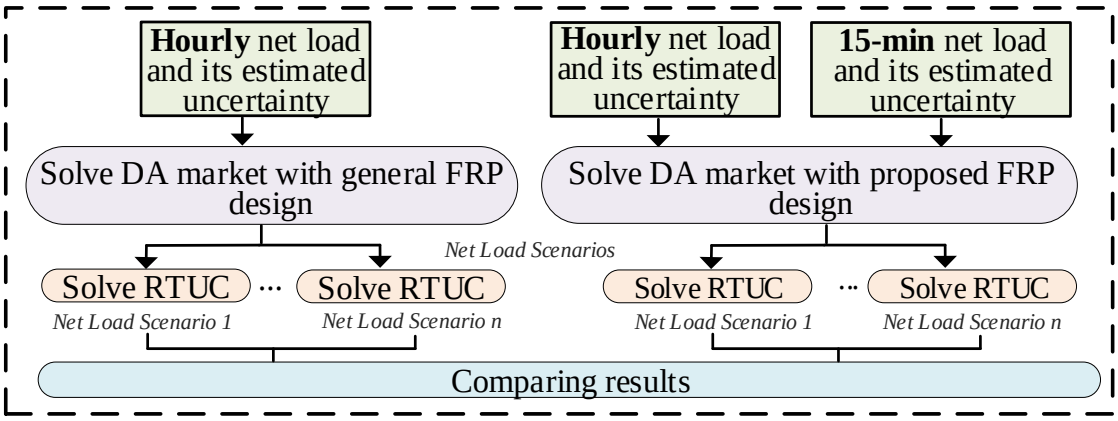

Fig. 4.3. Flowchart of the Proposed Simulation Procedure.

4.4.1. FMM of CAISO [99]

The FMM of CAISO includes four RTUC runs for each trading hour. RTUC is a market process for committing fast-start (FS) units at 15-minute intervals, which is performed on a rolling-forward basis. The four RTUC processes, i.e., RTUC#1, RTUC#2, RTUC#3, and RTUC#4, include time horizons of 60-105 minutes spanning from the previous trading hour and the current trading hour. The binding interval is the second interval of the RTUC run horizon, and the rest are advisory intervals.

4.4.2. Proposed Validation Phase

For the sake of simplicity in the proposed validation methodology, without loss of generality, all the four RTUC runs are combined into a one-process RTUC run for each trading hour. The one-process RTUC run has the same number of intervals as RTUC#1 (i.e., seven 15-min intervals) and is performed in the same time schedule as RTUC#1 is performed. It approximately starts 7.5 minutes prior to the first trading hour for $T-45$ minutes to $T+60$ minutes, where T is the top of the trading hour as shown in Fig. 4.4, and it continues on a rolling-forward basis for the next trading hours. Since each original RTUC process has one binding interval, the one-process RTUC simulation would have four successive binding intervals out of 7 intervals. It is pertinent to note that the binding intervals of trading hour T that are also a part of intervals of the next trading hour $T+1$, are used and kept the same (dispatch and commitment) in one-process RTUC run of trading hour $T+1$.

After performing all one-process RTUC runs, the final schedule for the 96 intervals of a day is achieved by putting together all the binding intervals. Furthermore, in each one-process RTUC run, power balance violations are allowed to occur if there are insufficient ramp capabilities to follow the sudden net load changes.

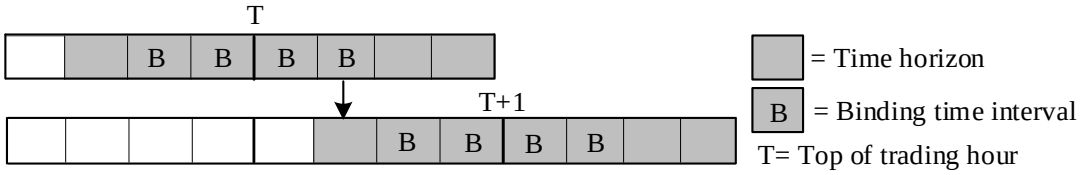

Fig. 4.4. One-process RTUC Run in the Validation Phase.

4.4.3. Data Transferring from DA Market to FMMs

In the proposed validation methodology, the DA market solutions are transferred and embedded into the FMMs for running the multiple one-process RTUC problems. The commitments obtained from the DA market model are kept fixed for long-start units in the FMMS. Furthermore, the dispatch modification of the committed units in the DA market model is limited to their 15-min ramp rate in the first interval of the RTUC process so as to not deviate much from DA market dispatch decisions. Furthermore, FS units can be further committed to following the realized net load if the ramping shortage occurs.

4.5. Numerical Studies and Discussion

A 118-bus IEEE test system is employed for testing the proposed framework. It is pertinent to note that the DA market models presented in Section 4.2 are formulated as MILP models, which can be solved with the MILP solvers. In this chapter, CPLEX v12.8 is utilized to solve the MILP models on a computer with an Intel Core i7 CPU @ 2.20 GHz, 16 GB RAM, and a 64-bit operating system.

4.5.1. System Data and Assumptions

The 118-bus IEEE test system has 54 generators, 186 lines, and 91 loads [100]. The hourly and 15-min net load profiles were adopted from the real data of CAISO [101]. It is pertinent to note that since the net load is the difference between load and renewable power generation, it contains information related to renewable power generation, including variability and uncertainty of renewable resources. The relative mixed-integer programming gap is set to be 0.2% [102]. First, the simulation results are performed for

the first test day, i.e., February 4, 2020; Fig. 4.5 shows the load, net load, and renewable power generations associated with this first test day. The uncertainty in the net load of CAISO is mainly introduced by renewable resources, especially solar and wind [101]. The error of the hourly net load forecast is assumed to have a Gaussian distribution with zero mean and ~5% standard deviation. Also, 95% confidence level, i.e., 1.96 standard deviations, is considered for hourly ramping requirements, i.e., (1v) and (1w). Based on the total probability theory [67] and [103], the relationship between the standard deviation of error of hourly and 15-min net load can be quantified, i.e., $\sigma_{hourly} = 2\sigma_{15-min}$. By using this formula, the 15-min ramping requirements formulated by (4.23)-(4.26) and (4.30)-(4.33) can be calculated. The confidence level for 15-min ramping requirements is also 95%.

In the validation methodology, 18 gas and oil generators, which have a maximum capacity of up to 50 MW, are considered as the FS units. The violation is allowed to occur if the available ramp capabilities are not enough to follow the realized net load. The penalty price is in terms of the value of lost load (VOLL), which is chosen as $10000/MWh. Additionally, 500 different 15-min net load scenarios are generated based on the 15-min net load uncertainty for this validation phase.

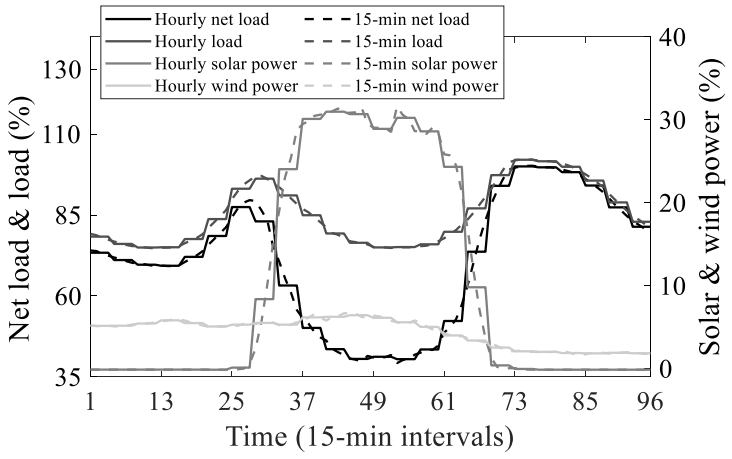

Fig. 4.5. Netload, Load, Solar Power Generation, and Wind Power Generation Profiles in the First Day.

4.5.2. Proposed FRP Design Versus General FRP Design

Fig. 4.6 compares the increased number of 15-min commitments of FS units against the total violation for the net load test scenarios in FMMs obtained from the validation phase. The increased number of FS units 15-min commitments represents the increase in the total commitment of FS units from DA market to RT market for the total of 96-time intervals. Furthermore, Table 4.1 presents the number of scenarios where the proposed approach outperforms the general approach from economic and reliability metrics. According to Fig. 4.6 and Table 4.1, it can be seen that for almost all the scenarios, the proposed approach provides Pareto optimal solutions (with respect to the increased number of 15-min commitments of FS units and the violation) compared to the general approach, wherein less violation and increased commitment number occur in the FMMs. The reason is that the proposed approach preemptively takes into account the impacts of 15-min net load variability and uncertainty on the DA FRP decisions. Please note that a lower number for commitment increase is an indication of less discrepancy between the

DA and RT markets, which potentially can lead to the reduction of the necessity for expensive adjustments in the RT market processes. These results show the efficiency of the proposed FRP design in quantifying more adaptive FRP requirements in the DA market with respect to the RT condition. Owing to discounting the impacts of the nodal FRP deployment on the physical network limitations (e.g., congestion) in the DA market model, the proposed approach is not expected to fully remove the additional need for commitment of FS units in the FMM. That is why in Fig. 4.6, the FS units are still required to be turned on to follow the net load. Future work should investigate how to address the deliverability issue associated with the post-deployment of FRP in the RT markets. Fig. 4.7 compares the real-time operating costs of FMMs (excluding the violation cost with VOLL) against the total violation for the corresponding FRP designs over the net load test scenarios. In Fig. 4.7, in order to assess the performance of the proposed approach under different bids of FS units in RT, the results are presented not only for the FMMs in which the FS units have the same bids as their bids in the DA market but also for the FMMs with FS units having increased bid (by 15% of the DA bids). It is worth mentioning that if the operating costs include the violation cost (similar to what is usually done in the literature [40], [67], [68], [78]), the comparisons between the operating costs of different models may be subjective as the results are sensitive to the choice of VOLL. In this chapter, the real-time operating costs are compared through different approaches so that the comparisons can be more objectively conducted. These approaches include: (i) performing sensitivity analysis and (ii) removing the cost associated with violations and VOLL from the operating costs while comparing the violation as another metric. Based on Fig. 4.7 and Table 4.1, it can be observed that the

proposed approach is effectively capable of reducing the violation while resulting in lower or comparable real-time operating costs (excluding the violation cost with VOLL) to those of the general approach. In other words, considerably less load shedding has been observed for the proposed approach (proposed approach has less or equal violation in 98.4% of scenarios), while in 62.4% and 69.2% of scenarios, the obtained real-time operating costs (excluding the violation cost with VOLL) of the proposed approach are lower than those of the general approach for the original and the increased bids, respectively. These results prove the enhanced performance of the proposed FRP design for improving the RT market efficiency from the economic and reliability aspects for different bids in the RT market.

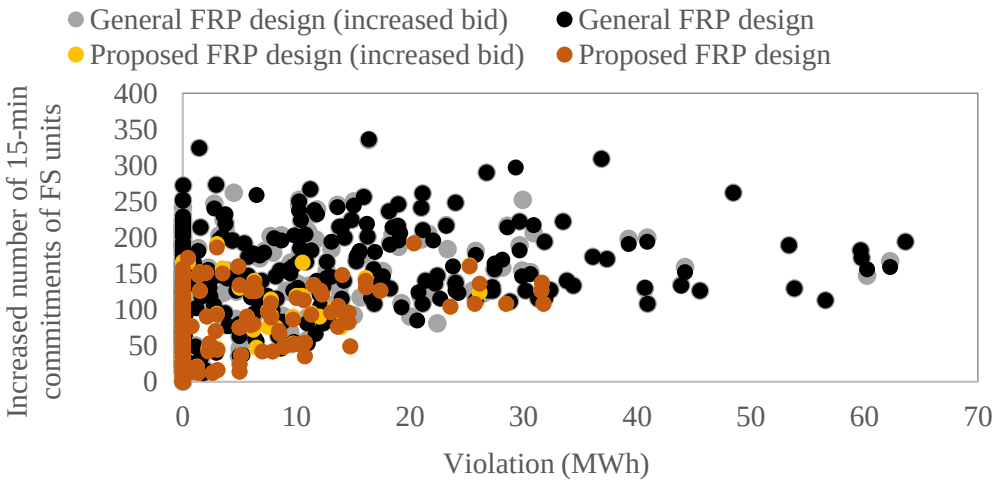

Fig. 4.6. Increased Number of 15-min Commitment of the FS Units Versus Violation in RT Operation (First Test Day).

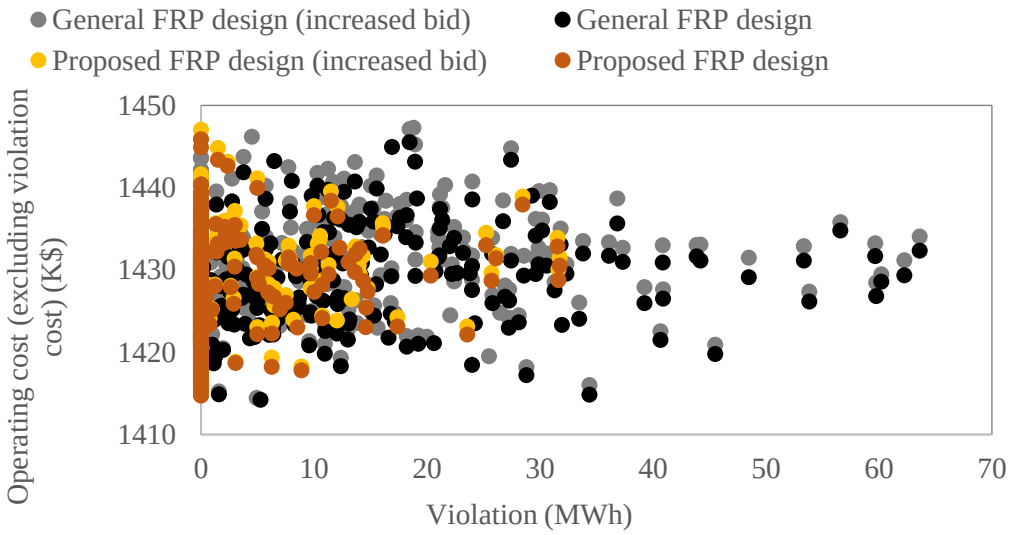

Fig. 4.7. RTUC Operating Cost Versus Violation in RT Operation (First Test Day).

Table 4.2 lists the operating costs of DA markets and FMMs for both the FRP designs. Although the proposed approach results in higher DA operating costs in comparison to the other model (only 0.3% increase), it has much fewer expensive adjustments in the FMMs and has less real-time operating costs in the FMMs. It is evident from these results that the DA operating cost has not been relatively changed with respect to the corresponding average real-time operating costs for the proposed approach, while a huge difference can be seen for the other approach. The average real-time operating cost of the general approach over all of the scenarios in the FMM with original bids is equal to $ 1692k, which is considerably higher than that of the proposed method, i.e., $ 1483k. On the other hand, the standard deviation of real-time operating costs of the proposed approach is effectively less than that of the general approach, which demonstrates the robustness of the proposed approach performance in response to the different realized net load scenarios. Finally, from evaluating the results for the increased bid of FS units in

Table 4.2, it can be seen that the performance of the proposed approach is consistent with the results of the non-increased bid explained above.

Table 4.1. Number of Scenarios with Improvement Over all Time Intervals in RT Operation (Total Number of Scenarios = 500)

Metric	
# Scenarios with total violation improvement*	492
# Scenarios with reduction in total commitment of FS units	478
# Scenarios with cost (excluding violation cost) improvement	312

*Scenarios with same or less violation

Table 4.2. Comparison of Operating Costs for DA Market and FMMs (First Day)

Approach	General FRP design	Proposed FRP design	General FRP design (with increased bid of FS units in FMMs)	Proposed FRP design (with increased bid of FS units in FMMs)
DA operating cost (K$)	1420	1424	1420	1424
Real-time operating costs in FMMs				
Ave (K$)	1692	1483	1693	1483
Standard deviation (K$)	478	184	478	183
Max (K$)	3977	2701	3979	2702

In Table 4.3, five statistical measures are utilized to assess and compare the reliability extent in the FMMs that can be resulted from implementing two approaches. The results confirm that the proposed approach outperforms the general approach with respect to all violation statistical measures because the proposed FRP design considers the 15-min net load changes on the dispatch and commitment of the DA market to attain adequate responsiveness from the flexible resources in RT (resource adequacy). Note that effectively decreasing the max violation is mainly useful when the ISO is interested in decreasing worst-case violation.

Table 4.3. Comparison of Violation in RT 15-min Operation (First Day)

Metric	General FRP design	Proposed FRP design
Average [violation] (MWh)	6.6	1.4
Standard deviation [violation] (MWh)	11.9	4.6
Σ violation (MWh)	3298.8	702.3
# Scenarios with violation	204	73
Max violation (MWh)	63.6	31.8

Table 4.4. Comparison of the Increased Number of 15-min Commitments of FS Units in RT Operation (First Day)

Metric	General FRP design	Proposed FRP design
Ave [Increased commitment of FS units]	125	44
Σ increased commitment of FS units	62278	22083
# Scenarios with increased commitment of FS units	498	377
Max increased commitment of FS units	336	192

The metrics presented in Table 4.4 compare the 15-min commitments number of FS units that are turned on in the FMMs to follow the 15-min net load changes, in addition to the FS units that were previously committed from the DA market. Four metrics, which are indicative of the discrepancy between DA and RT operations, are presented in this table. It can be observed that the proposed model effectively reduces the need for the expensive FS units to be additionally committed in the RT market by turning on cheaper flexible units that are available in the DA market.

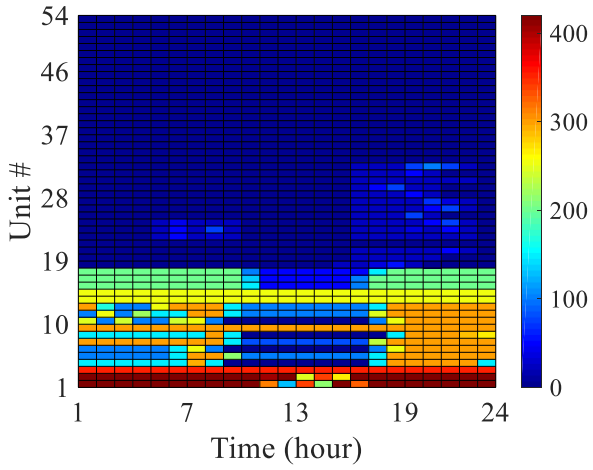

(a)

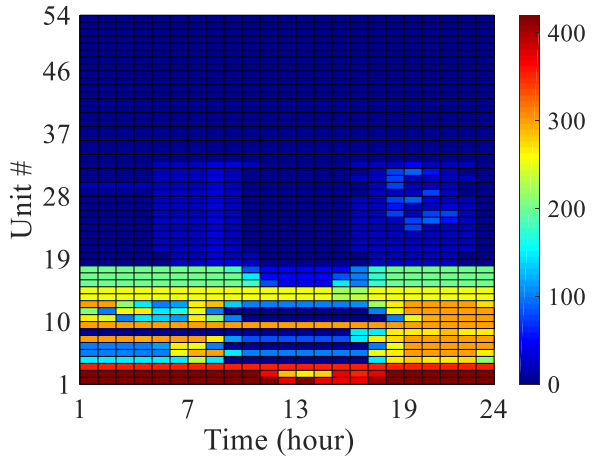

(b)

Fig. 4.8. DA Generation Scheduling Comparison: (a) General FRP Design, (b) Proposed FRP Design.

Fig. 4.8 illustrates the DA generation scheduling for the general and proposed approaches, wherein the number of units is indicative of the sorted units based on their maximum power capacity (unit with number 1 has the highest capacity and the one with number 54 has the lowest capacity). As it can be seen, with the general approach, generation units 1-17 (that have a maximum capacity of 200-420 MW) are mainly responsible for meeting the net load. However, with the proposed approach, in the hours

with high ramping needs (e.g., 5-10 and 18-22), generation units 18-32 (with a maximum capacity of 100 MW) are committed and dispatched more compared to generation units scheduling in the general approach. This increases the ramp capability adequacy for following the realized net load in the FMMs. Consequently, in these hours, generation units 1-17 relatively participate less in meeting the net load, creating more headroom for upward ramping needs.

4.5.3. Market Implications of Modeling FRP in DA

Table 4.5 summarizes DA energy revenue, FRP up revenue, and FRP down revenue for each approach. The DA FRP procurement aids in ensuring the DA resource adequacy to meet the net load changes in RT, which potentially leads to increase of the energy revenue in DA models with FRP requirements in comparison to the DA model without FRP requirements. Furthermore, it is evident that, as quantification of the DA FRP requirements becomes more accurate, the revenue of the generators for providing the ramp capabilities increases. Table 4.6 presents the DA market settlement results for the different approaches. According to Table 4.6, the DA model with general FRP design has the highest generation revenue and generation rent, while the lowest value for these market settlements belongs to the DA model without FRP design. It is pertinent to note that the generation revenue is the result of summation over the energy revenue and FRP up and down revenues. Additionally, the lowest and highest congestion rents belong to the DA model without FRP and the DA model with general FRP design, respectively. Finally, in terms of load payment, the DA model with general FRP design has the highest value, and the DA model without FRP design has the lowest value. From the locational marginal prices (LMPs) stand view in the FMMs, in all scenarios and intervals, the

general approach has 453 cases with price spikes, while the proposed approach has only 169 cases with price spikes. Table 4.7 shows the distribution of these cases. It is clear that the proposed approach is able to considerably reduce the frequency of price spikes in the FMMs, which potentially can prevent market inefficiency.

Table 4.5. DA Market Revenues Comparison

Approach	Energy revenue (k$)	FRP up revenue (k$)	FRP down revenue (k$)
DA market without FRP	1622.8	0	0
DA market with general FRP design	1644.7	5.6	0
DA market with proposed FRP design	1627.1	11.2	2.9

Table 4.6. DA Market Settlements Comparison

Approach	Generation revenue (k$)	Load payment (k$)	Generation rent (k$)	Congestion rent (k$)
DA market without FRP	1622.8	1622.8	220.7	0.0
DA market with general FRP	1650.3	1645.4	245.3	0.7
DA market with proposed FRP	1641.2	1627.5	233.4	0.3

Table 4.7. Distribution of Price Spikes Among Cases in RT Market

Approach	Number of cases
General approach only with price spike	320
Proposed approach only with price spike	36
Both approaches simultaneously have price spike	133

4.5.4. Sensitivity Analyses

Figures 4.9 and 4.10 illustrate the results of sensitivity analyses of the reliability and economic metrics with respect to VOLL and the percentage of DA net load uncertainty for the proposed FRP design in comparison to the general FRP design. It is pertinent to note that various percentages of DA net load uncertainty, i.e., net load forecast error, impact the analysis of this chapter and validation of the proposed method in twofold: (i)

changing the general and proposed DA FRP requirements, (ii) changing the generated scenarios in the validation methodology. The goal of sensitivity analysis with respect to the DA net load uncertainty is to evaluate how the proposed FRP design improves system response to different net load uncertainties; such analysis is important as it clarifies how proper modifications in operational approaches can enhance ramp responsiveness in the system and reduce the need to invest in additional flexible but expensive resources, e.g., power plants or energy storage resources. Based on Figures 4.9 and 4.10, the results show the robustness of the proposed approach as the percentage of improvements of all metrics remains considerable.

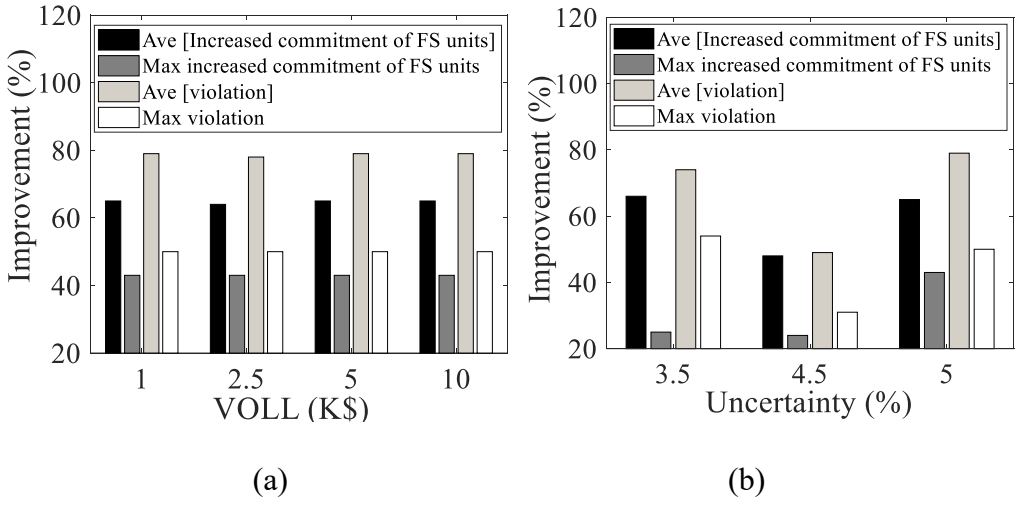

Fig. 4.9. Sensitivity Analyses of Violation and Increased FS 15-min Commitment with Respect to: a) VOLL, and b) the Percentage of Uncertainty.

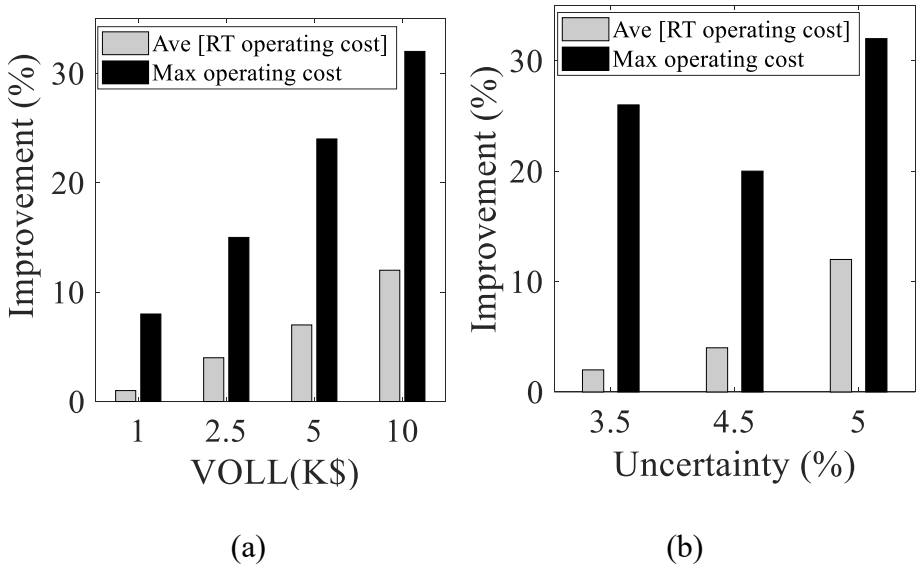

Fig. 4.10. Sensitivity Analyses of RT Operating Costs with Respect to: a) VOLL, and b) Percentage of Uncertainty.

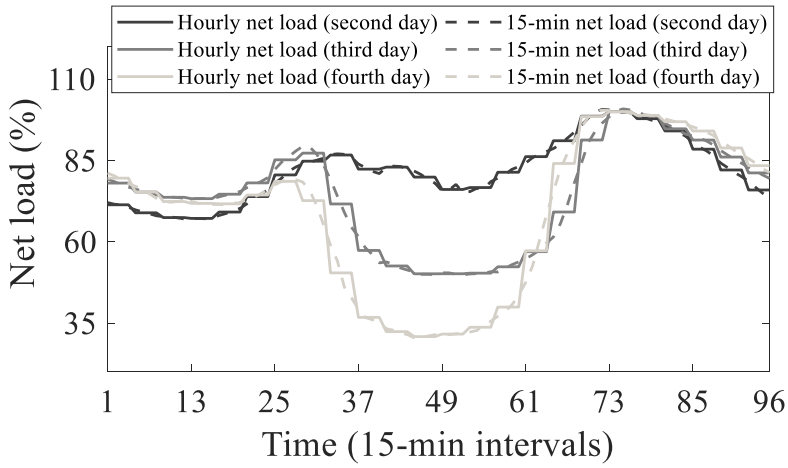

Fig. 4.11. Hourly Net Load Versus 15-min Net Load for the Second, Third, and Fourth Test Days.

4.5.5. Coordination of FRP with the Regulation Reserve in DA Market

Three different cases that represent different DA market model structures are solved in order to evaluate the coordination among ramp capability products (based on different FRP designs) and regulation reserve; the model formulation for this section is provided in

Section 4.2.4. These cases are listed in Table 4.8. The regulation reserve requirement ranges, i.e., $\eta\%$ in (3c) and (3d), between one to five percent of the total demand [104]. Here, two regulation reserve requirements are chosen to perform the analyses, i.e., 3 percent (average of the maximum and minimum regulation reserve requirements) and 5 percent (maximum regulation reserve requirement); associated results are shown in Tables 4.9 and 4.10, respectively (please note the net load scenarios used here for the validation phase are the same as the ones used in Section 4.5.2 for the first test day). As shown in Table 4.9, when the DA market structure only includes the regulation reserve (i.e., case 1), the average RT operating costs, average violation, and average increased number of the 15-min commitment of FS units in FMMs are higher than those of cases 2 and 3 that simultaneously coordinate ramp capability product (based on different FRP designs) and regulations reserve. The proposed model (i.e., case 3) has the best performance among different cases from reliability and economic points of view. Furthermore, as it can be seen in Table 4.10, increasing the regulation reserve requirement to its maximum value would not solve the problem of ramping shortage in the next market process after DA, i.e., FMMs, due to steep net load changes in RT 15-min markets.

Table 4.8. Characteristic of Different Cases for Evaluation the Coordination Among Different Products in DA Market

Product	Case 1	Case 2	Case 3
Regulation reserve product	×	×	×
Ramp capability product (based on the general FRP design)		×	
Ramp capability product (based on the proposed FRP design)			×

Table 4.9. Results for DA Market and FMMs (Regulation Reserve Requirement = 3%)

Approach	Case 1	Case 2	Case 3
DA operating cost (K$)	1417	1420	1425
Real-time operating costs in FMMs			
Average (K$)	1744	1697	1480
Max (K$)	4201	4331	2701
Violation comparison in RT 15-min operation			
Average [violation] (MWh)	8.0	6.8	1.3
# Scenarios with violation	209	196	67
Increased number of 15-min commitments of FS units in RT operation			
Ave [Increased commitment of FS units]	143	78	21
# Scenarios with increased commitment of FS units	492	446	225

4.5.6. DA FRP Design Performance Against Different Test Days

In order to evaluate the robustness of the proposed approach, it is also assessed on the net load of CAISO from three additional test days, each of which includes different level of ramping needs (see Fig. 4.11). These days include January 20, 2020 (i.e., second day), October 18, 2020 (i.e., third day), January 1, 2021 (i.e., fourth day). Tables 4.11, 4.12, and 4.13 summarize the corresponding results across 15-min net load scenarios for these days. Consistent with the first test day results, the proposed model outperforms the general approach by improving the reliability of the system while also reducing the final operating costs in FMMs.

Table 4.10. Results for DA Market and FMMs (Regulation Reserve Requirement = 5%)

Approach	Case 1	Case 2	Case 3
DA operating cost (K$)	1419	1425	1427
Real-time operating costs in FMMs			
Average (K$)	1719	1636	1480
Max (K$)	3947	3819	2701
Violation comparison in RT 15-min operation			
Average [violation] (MWh)	7.4	5.2	1.3
# Scenarios with violation	211	173	66
Increased number of 15-min commitments of FS units in RT operation			
Ave [Increased commitment of FS units]	84	51	18
# Scenarios with increased commitment of FS units	447	375	190

Table 4.11. Results for DA Market and FMMs (Second Test Day)

Approach	General FRP design	Proposed FRP design
DA operating cost (K$)	1647.8	1649.3
Real-time operating costs in FMMs		
Average (K$)	1731.8	1665.5
Standard deviation (K$)	224.8	84.5
Max (K$)	3093.7	2661.0
Violation comparison in RT 15-min operation		
Average [violation] (MWh)	2.0	0.4
Standard deviation [violation] (MWh)	5.6	2.1
Σ violation (MWh)	980.7	177.8
# Scenarios with violation	90	27
Max violation (MWh)	36.0	25.0
Increased number of 15-min commitments of FS units in RT operation		
Ave [Increased commitment of FS units]	91	33
Σ increased commitment of FS units	45590	16634
# Scenarios with increased commitment of FS units	489	386
Max increased commitment of FS units	269	146

Table 4.12. Results for DA Market and FMMs (Third Test Day)

Approach	General FRP design	Proposed FRP design
DA operating cost (K$)	1477.7	1480.0
Real-time operating costs in FMMs		
Average (K$)	1594.4	1529.4
Standard deviation (K$)	251.1	167.0
Max (K$)	2953.6	2829.8
Violation comparison in RT 15-min operation		
Average [violation] (MWh)	2.7	1.2
Standard deviation [violation] (MWh)	6.2	4.1
Σ violation (MWh)	1354.1	590.3
# Scenarios with violation	140	66
Max violation (MWh)	36.6	33.4
Increased number of 15-min commitments of FS units in RT operation		
Ave [Increased commitment of FS units]	150	54
Σ increased commitment of FS units	74973	27030
# Scenarios with increased commitment of FS units	496	407
Max increased commitment of FS units	374	358

4.6. Conclusion

The high penetration of renewable resources is imposing new challenges (e.g., potential ramp capability shortage) to modern power systems by intensifying the uncertainty and variability in the system net load. The ramp capability shortage not only can jeopardize reliability but also can cause inefficiencies in the RT markets. Energy markets are evolving to overcome such challenges by implementing new ancillary service products called FRP. There have been proposals to implement the FRP into the DA markets, e.g., the DA market of CAISO, in order to ensure resource adequacy to respond to net load variability and uncertainty in the next market processes such as the FMM and the RT economic dispatch. The DA formulation with FRP proposed by existing work is

based on the hourly ramping requirements with the aim to enhance ramp capabilities in the shorter scheduling granularity, e.g., 15 min. However, it ignores the impacts of steep 15-min net load changes while scheduling DA FRP awards. To address this challenge, this chapter proposes a novel DA FRP design to preposition and commit the ramp-responsive resources to better respond to the RT 15-min ramping needs. The proposed DA FRP formulation is designed in such a way that (i) the hourly net load variability and uncertainty are taken into account, and (ii) impacts of the 15-min net load variability and uncertainty are captured in the awarded DA FRP. The proposed model is more adaptive to the RT 15-min condition through enhancing the quantity allocation of FRP by making effective market changes compared to the general FRP design. The proposed FRP design leads to less expected final operating cost in the FMMs, higher reliability as the power system gets close to RT operation, less discrepancy between DA and FMMs decisions, and less number of price spikes in the FMMs. Furthermore, corresponding incentive policies were derived based on the duality theory for the proposed FRP design, and then a comprehensive evaluation of the DA market implications of new reformulation was presented and discussed.

The focus of this chapter is to improve DA operational scheduling models to enhance flexibility procurement and ramp-responsiveness from available resources. The future research direction can include: (i) incorporating other flexible resources including energy storage systems and adjustable loads in the proposed DA FRP scheduling framework, and (ii) extending the proposed FRP design to the RTUC problem with 15-min granularity to capture 5-min variability and uncertainty in the RT economic dispatch.

Table 4.13. Results for DA Market and FMMs (Fourth Test Day)

Approach	General FRP design	Proposed FRP design
DA operating cost (K$)	1377.3	1383.4
Real-time operating costs in FMMs		
Average (K$)	1634.2	1450.1
Standard deviation (K$)	461.5	221.9
Max (K$)	4512.0	2990.6
Violation comparison in RT 15-min operation		
Average [violation] (MWh)	6.3	1.6
Standard deviation [violation] (MWh)	11.5	5.5
Σ violation (MWh)	3139.5	821.9
# Scenarios with violation	204	65
Max violation (MWh)	77.9	39.8
Increased number of 15-min commitments of FS units in RT operation		
Ave [Increased commitment of FS units]	88	36
Σ increased commitment of FS units	44009	18123
# Scenarios with increased commitment of FS units	490	413
Max increased commitment of FS units	314	368

Chapter 5.

A DATA-DRIVEN POLICY FOR ADDRESSING DEPLOYABILITY ISSUE OF REAL-TIME FRPS: RESOURCES QUALIFICATION AND DELIVERABILITY

5.1. Introduction

In general, a basic way to manage uncertainty caused by renewable resources in net load in the power system operations is to procure the ancillary services (e.g., reserves, and ramp capability products) in the deterministic models [29], [105]–[108]. In other words, the ISOs add constraints to the existing market models to procure ancillary services so that the system can respond to the deviations of net load and generation from desired dispatch points (DDP). Since the FRP design proposed by the industry is based on proxy system-wide or zonal requirements, there is no guarantee that FRPs, which are procured by the market, will be deployable without violating transmission line limits. The reason can simply be associated with the fact that the bus-level deliverability for the post-deployment of FRPs within transmission limits is disregarded when deciding on the FRP awards.

More advanced techniques to deal with the uncertainty imposed on the power system include, but are not limited to, (i) stochastic programming, wherein the uncertainties are explicitly represented and simultaneously solved in the model [109]–[111] and (ii) robust optimization, which mitigates worst-case consequences [42], [112]–[115]. The ISOs in the U.S. do not utilize stochastic programming and robust optimization for the generation scheduling since the former has extensive computational requirements, and the latter is often very conservative and still computationally challenging for large-scale UC models [43].

In this chapter, to address the deployability issue of FRPs, a computationally tractable data-driven policy is proposed for FRPs awarded in FMMs, which improves upon the existing industry models. The key idea is to allocate the FRPs to the resources that can effectively deploy their ramping capabilities in the corresponding locations when needed without violating transmission line limits. To do so, the proposed approach uses data-mining algorithms to specify ramping response factor sets for generation resources that have higher responsiveness given a set of ramping deployment events. Furthermore, the impacts of the FRPs post-deployment on the transmission line flows are considered so that the ramp capabilities are allocated to more likely deployable locations. Finally, the performance of the enhanced FMM market model, modified to include the proposed FRP design, is compared against the FMM market model with proxy FRP design through an out-of-sample validation methodology. This validation methodology mimics RT unit commitment (RTUC) of CAISO's FMM.

The rest of the chapter is organized as follows. Section 5.2 presents the different market processes structures, and Section 5.3 gives FMMs formulation based on the general FRP design. Section 5.4 focuses on the proposed FRP design including the data-mining algorithm and the proposed data-driven policy for the FMM FRP design. The out-of-sample validation phase is elaborated in Section 5.5. Finally, simulation results are presented and analyzed in Section 5.6 while Section 5.7 shows the conclusions of the chapter.

5.2. Structure of Market Processes

The focus of this work is on improving the FRP design in the FMMs. However, to get more realistic results and follow the practice in most ISOs, the DA and FMM are run

consecutively. The DA market, which is based on the DA structure of most ISOs, schedules the energy product to meet the netload while assigning contingency-based reserve and regulation reserve to the generation resources.

After the DA market is solved, the DA market decisions are utilized in the FMMs. The commitment decisions of the must-run (MR) generation resources in the FMMs are fixed based on the DA commitment decisions while short-start and fast-start (FS) units can further be committed to satisfy the realized netload for meeting ramping needs. Please note that power balance violation can happen in both markets with consideration of the value of lost load (VOLL) if there are insufficient ramping flexibilities to follow the netload changes.

The FMM structure in this work is based on the FMM structure of CAISO. CAISO performs four RTUC processes i.e., RTUC#1, RTUC#2, RTUC#3, and RTUC#4, for each trading hour in the CAISO's FMM, spanning from 60 minutes (or 4 intervals) to 105 minutes (or seven intervals) [99]. These RTUC processes are run based on a rolling-forward basis, wherein the second 15-min time interval is binding and the rest are advisory time intervals [99]. This work slightly modifies this FMM structure and performs only a one-process RTUC for each trading hour in the FMM that includes 7 intervals with 4 binning intervals, as depicted in Fig. 5.1.

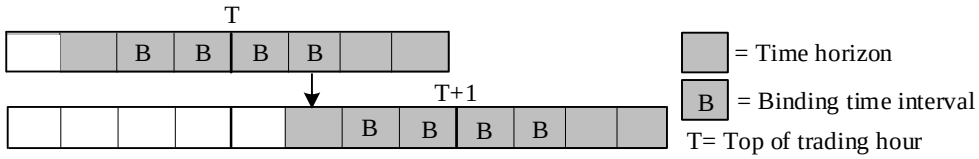

Fig. 5.1. One-process RTUC Run in the FMMs [116].

5.3. FMM Formulation with General FRP Design (Proxy Policy)

The general FMM market model with proxy FRP requirement is given in (5.1)-(5.27). The objective function minimizes total operating costs (i.e., linearized variable operating costs and fixed costs that includes no-load costs, startup costs, and shutdown costs) as follows.

$$minimize \sum_g \sum_t (\underline{F_g} u_{gt} + \sum_{b=1}^{B} P_{gtb} B_{gb} + c_g^{SU} v_{gt} + c_g^{SD} w_{gt} + c_g^{UR} ur_{gt} + c_g^{DR} dr_{gt}) \quad (5.1)$$

The objective function is subject to generation resource's operational constraints, transmission network constraints, and general FRP constraints presented through (5.2)-(5.27). Constraints (5.2) and (5.3) links DA and FMM commitment decision variables of the MR and FS generation resources, respectively. Minimum up time and down time constraints of the generation resources are modeled by (5.4) and (5.5). The power output of generation resources and the limit on each power generation block are given by (5.6) and (5.7). Constraints (5.8) and (5.9) enforce 15-min ramp rate limits. Constraint (5.10) ensures nodal balance at each bus, while constraint (5.11) guarantees the system-wide energy balance between total loads and generation resources throughout the system. Constraint (5.12) enforces the transmission line limits. Finally, constraints (5.13)-(5.17) are associated with modeling the commitment variables, the startup variables, and the shutdown variables of the generation resources.

$$u_{gt} = \overline{u_{gt}^h}, \forall g \in G^M, t \quad (5.2)$$

$$u_{gt} \geq \overline{u_{gt}^h}, \forall g \in G^F, t \quad (5.3)$$

$$\sum_{s=t-UT_g+1}^{t} v_{gs} \leq u_{gt}, \forall g \in G^F, t \in \{UT_g, \cdots, T\} \quad (5.4)$$

$$\sum_{s=t-DT_g+1}^{t} w_{gs} \leq 1 - u_{gt}, \forall g \in G^F, t \in \{DT_g, \cdots, T\} \quad (5.5)$$

$$P_{gt} = P_g^{min} u_{gt} + \sum_{b=1}^{B} P_{gtb}, \forall g, t \quad (5.6)$$

$$0 \leq P_{gtb} \leq P_{gb}^{max} u_{gt}, \forall g, t, b \quad (5.7)$$

$$P_{gt} - P_{gt-1} \leq R_g^{15} u_{gt-1} + R_g^{SU} v_{gt}, \forall g, t \geq 2 \quad (5.8)$$

$$P_{gt-1} - P_{gt} \leq R_g^{15} u_{gt} + R_g^{SD} w_{gt}, \forall g, t \geq 2 \quad (5.9)$$

$$\sum_{g \epsilon g(n)} P_{gt} + \sum_{i \epsilon i(n)} P_{it}^{solar} - Load_{nt}^{nodal} = P_{nt}^{inj}, \forall n, t \quad (5.10)$$

$$\sum_n P_{nt}^{inj} = 0, \forall t \quad (5.11)$$

$$-P_k^{max} \leq \sum_n P_{nt}^{inj} PTDF_{nk} \leq P_k^{max}, \forall k, t \quad (5.12)$$

$$v_{gt} - w_{gt} = u_{gt} - u_{g,t-1}, \forall g, t \quad (5.13)$$

$$v_{gt} + w_{gt} \leq 1, \forall g, t \quad (5.14)$$

$$0 \leq v_{gt} \leq 1, \forall g, t \quad (5.15)$$

$$0 \leq w_{gt} \leq 1, \forall g, t \quad (5.16)$$

$$u_{gt} \in \{0,1\}, \forall g, t \quad (5.17)$$

Constraints (5.18)-(5.29) represent the FMM FRP design based on the proxy policy. The power capacity constraints including energy power output with consideration of upward and downward FRP awards are given by (5.18) and (5.19). Constraints (5.20)-(5.23) model the limitation on the upward and downward ramp capabilities considering the commitment status of generation resources. The proxy up and down ramping requirements are calculated by (5.24) and (5.25) and are met through (5.26) and (5.27), respectively.

$$p_{gt} + ur_{gt} \leq P_g^{max} u_{gt} + P_g^{max} v_{gt+1}, \forall g, t \in T \quad (5.18)$$

$$p_{gt} - dr_{gt} \geq P_g^{min} u_{gt} - R_g^{SD} w_{gt+1}, \forall g, t \in T \quad (5.19)$$

$$ur_{gt} \leq R_g^{15} u_{gt} + R_g^{SU} v_{gt+1}, \forall g, t \in \{1, \cdots, T-1\} \quad (5.20)$$

$$dr_{gt} \leq R_g^{15} u_{gt+1} + R_g^{SD} w_{gt+1}, \forall g, t \in \{1, \cdots, T-1\} \quad (5.21)$$

$$ur_{gt} \leq P_g^{max} u_{gt+1}, \forall g, t \in \{1, \cdots, T-1\} \quad (5.22)$$

$$dr_{gt} \leq P_g^{max} u_{gt}, \forall g, t \in \{1, \cdots, T-1\} \quad (5.23)$$

$$FRu_t = \max\left[Load_{t+1}^{f,max} - \sum_i P_{it+1}^{solar,min} - \left(Load_t^f - \sum_i P_{it}^{solar}\right), 0\right], \forall t \in \{1, \cdots, T-1\} \quad (5.24)$$

$$FRdown_t = \max[Load_t^f - \sum_i P_{it}^{solar} - \left(Load_{t+1}^{f,min} - P_{it+1}^{solar,max}\right), 0], \forall t \in \{1, \cdots, T-1\} \quad (5.25)$$

$$\sum_g ur_{gt} \geq FRup_t, \forall t \in \{1, \cdots, T-1\} \quad (5.26)$$

$$\sum_g dr_{gt} \geq FRdown_t, \forall t \in \{1, \cdots, T-1\} \quad (5.27)$$

It is pertinent to note that FMM FRP constraints (5.18)-(5.23) take into consideration the effects of the commitment status on FRP awards in the FMM framework. The FRP design in some prior work is only valid when generation resources are committed in both time intervals t and $t+1$ [33]–[36], [116]. However, this FRP design cannot properly represent ramping capability from the generation resources that are committed only during one of the time intervals t and t+1. For example, if a generation resource is committed at time interval t and is not committed at time interval $t+1$, it should only be allowed to provide the downward FRP up to its shutdown ramp rate. Also, when a generation resource is not committed at time interval t and is committed at time $t+1$, it should only provide the upward FRP up to its startup ramp rate. The FMM FRP constraints (5.18)-(5.23) represent the mathematical formulation of these situations for

the generation resources that their commitment status varies between two successive time intervals. These formulations can also be extended to the DA framework.

Finally, the dispatch changes of generation resources should be within the FRP awards as presented by (5.28)-(5.29). These constraints are very important as the FRP awards cover both foreseen (variability) and unforeseen (uncertainty) netload changes; therefore, if a generation resource changes its power generation for covering variability, the associated FRP award should be able to cover it [117].

$$p_{gt+1} - p_{gt} \leq ur_{gt}, \forall g, t \in \{1, \cdots, T-1\} \quad (5.28)$$

$$p_{gt} - p_{gt+1} \leq dr_{gt}, \forall g, t \in \{1, \cdots, T-1\} \quad (5.29)$$

5.4. Proposed FRP Design (Data-driven Policy)

As mentioned earlier, to cope with the deployability issue of FRPs, it is necessary to assign FRP awards to qualified resources that are not located behind transmission bottlenecks. In this chapter, a new framework is proposed to pave the way for achieving the above goal. The proposed framework (i) predicts ramping responses of generation resources in RT to a given set of deployment ramping events, (ii) assigns deployable FRP awards to qualified resources, and enforces the transmission line constraints for post-deployment of FRP awards. In the following, Sections 5.4.1 and 5.4.2 talk about how to predict the ramping response of generation resources (for generating ramping response factor sets in this chapter), and Section 5.4.3 presents the proposed data-driven policy for the FMM FRP design considering these ramping response factor sets.

5.4.1. Data Generation for the Data-Mining Algorithm

In this section, the process for generating data for the data-mining algorithm explained in the next section is elaborated. To get the data, first different load and solar power generation scenarios using the corresponding forecast value and forecast error are generated through Monte Carlo simulation. Then, FMM presented by (5.30)-(5.32) is solved for each scenario w to see how the generators respond to different netload changes.

$$minimize \sum_g \sum_t (\underline{F_g} u_{gt} + \sum_{b=1}^{B} P_{gtb} B_{gb} + c_g^{SU} v_{gt} + c_g^{SD} w_{gt} + c_g^{UR} ur_{gt} + c_g^{DR} dr_{gt}) \quad (5.30)$$

subject to:

(5.2)-(5.9) and (5.11)-(5.17) (5.31)

$$\sum_{g \epsilon g(n)} P_{gt} + \sum_{i \epsilon i(n)} P_{itw}^{solar} - Load_{ntw} = P_{nt}^{inj}, \forall n, t \quad (5.32)$$

Please note that the FRP constraints are not incorporated in the FMM formulation (5.30)-(5.32) to loosely analyze how different generation resources increase and decrease their output power generation to follow the realized netload changes. Please note that after solving the above FMM formulation, for each scenario w at each time interval t, we can obtain the following recorded data (i) dispatch change of each generator due to ramp capability provision, (ii) net-load, load, nodal solar generations, net-load change, load change, nodal solar generation changes. These data can be used in the data-mining algorithm explained in the next section.

Please note that this stage, i.e., running FMMs based on the Monte Carlo simulation, can also be replaced with available historical data.

5.4.2. Data-Mining Algorithm for Obtaining Ramping Response Factor Sets

The goal here is to assess the deployability of ramping responses for various generation resources and to allocate FRP effectively in the right location. The data-mining algorithm can be utilized to create a function that predicts ramping response of a generation resource to a given ramping event. To do so, a run of FMM in the data acquisition stage, under each scenario that contains corresponding power solar generations and load, provides an instance for the data-mining algorithm. Each instance includes (i) target value that is the per-unit dispatch change of a generator, i.e., $\frac{P_{gt+1}-P_{gt}}{R_g^{15}}$, and (ii) the features that are net-load, load, nodal solar power generations, net-load change, load change, and nodal solar power generation changes. The data mining algorithm should be performed for each time interval t and each generation resource $g \in G^M$. In this chapter, the ramping response of MR generation resources is only predicted as the FS generation resources are constantly committed and decommitted to follow the realized netload. The ramping response of generation resources may be influenced by previous and next time intervals in the FMM due to its multi-period dispatch characteristic and intertemporal constraints. Therefore, the features explained above are extended to include net-load, load, nodal solar power generations, net-load change, load change, nodal solar power generation changes of next and previous 3 intervals in addition to interval t (i.e., 7 intervals in total, including time interval t). So, the total number of features would be $7 \times (4 + 2 \times I)$.

The machine learning algorithm utilized in this chapter is a neural network (NN) regression function. Please note that both data acquisition and performing the NNs are offline processes that happen before running the actual FMM in RT. Then, the generation

resources that are qualified to respond to a set of deployment scenarios can be identified through the concept of the ramping response factor set, which are target values of different NNs regression functions. Finally, these factor sets can be utilized to improve the FRP decision in FMMs as explained in the next section.

5.4.3. FMM Formulation with Data-Driven FRP Design and Ramping Response Factor Sets

This section presents the FMM formulation incorporating the ramping response factor sets and the proposed data-driven FRP design. First, after obtaining the NN functions from the offline process, close to running the RT FMMs, a set of possible deployment scenarios can be generated based on RT conditions, which include corresponding power solar generations and load values. Please note that these deployment scenarios can be the most probable scenarios that can happen for the load and solar power generations as we get close to RT operation. Then, these scenarios can be fed to the NNs function already obtained from the offline process to obtain the ramping response factor sets ζ_{gts}.

Second, the proposed data-driven FRP design is extended based on the existing FRP formulation (5.18)-(5.29), wherein qualified generation resources, capable of deploying FRP awards with respect to the deployable scenario set S, satisfy the system-wide FRP requirements firstly while simultaneously the transmission line flow limits are enforced for post-deployment of ramping capabilities.

For each time interval t, the deployment scenarios can be divided into two *upward* and *downward* deployment scenarios based on the value of ΔNL_{ts} defined by (5.33).

$$\Delta NL_{ts} = Load_{t+1s}^{f,dep} - Load_{t}^{f} + \sum_i P_{it+1s}^{solar,dep} - \sum_i P_{it}^{solar},\ s,t \in \{1,\cdots,T-1\} \quad (5.33)$$

If ΔL_{ts} is greater than zero for time interval t, then scenario s is considered as upward deployment scenarios with the positive ramping requirement at time interval t, otherwise, it is downward deployment scenarios at time interval t. Constraints (5.34)-(5.37) present the proposed data-driven policy for upward FRP, wherein $\Delta NL_{ts} > 0$ for time interval t and deployment scenario s. The enhanced formulation utilizes positive auxiliary variables, i.e., ur^{a}_{gts}, to represent the upward ramping response of generation resources at the deployment scenarios. Constraint (5.34) assigns ramp capabilities to the qualified generation resources by using the ramping response set factors ζ^{fru}_{gts}. The upward FRP award is set to be greater than all the upward auxiliary variables through (5.35). Also, summation over the auxiliary variables should meet the ramping requirement of the deployment scenario, i.e., ΔL_{ts}, by (5.36). Finally, constraint (5.37) models transmission line constraint for upward FRP post-deployment for the ramping scenarios. In constraint (3e), the first term is the pre-activation flow of transmission line, the second term is the change in the flow due to the upward FRP activation, the third term is related to the change in flow due to solar generation change, and finally, the fourth term is associated to the change in flow due to load change.

$$ur^{a}_{gts} \geq \zeta_{gts} R^{15}_{g}, g \in G^{M}, s, t \in \{1, \cdots, T-1\} \tag{5.34}$$

$$ur^{a}_{gts} \leq ur_{gt}, g, s, t \in \{1, \cdots, T-1\} \tag{5.35}$$

$$\sum_{g \in G} ur^{a}_{gts} \geq \Delta NL_{ts}, \forall s, t \in \{1, \cdots, T-1\} \tag{5.36}$$

$$-P^{max}_{k} \leq \sum_{n} P^{inj}_{nt}\, PTDF_{nk} + \sum_{g} ur^{a}_{gts}\, PTDF_{n(g)k} + \sum_{i}\left(P^{solar,dep}_{it+1s} - P^{solar}_{it}\right) PTDF_{n(i)k} - \sum_{n}\left(Load^{nodal,dep}_{nt+1s} - Load^{nodal}_{nt}\right) PTDF_{nk} \leq P^{max}_{k}, k, s, t \in \{1, \cdots, T-1\} \tag{5.37}$$

The symmetric formulation can be presented for the enhanced data-driven policy for downward FRP, which is given in (5.38)-(5.41).

$$dr^{a}_{gts} \geq -\zeta_{gts} R^{15}_{g}, g \in G^{M}, s, t \in \{1, \cdots, T-1\} \quad (5.38)$$

$$dr^{a}_{gts} \leq dr_{gt}, g, s, t \in \{1, \cdots, T-1\} \quad (5.39)$$

$$\sum_{g \in G} dr^{a}_{gts} \geq -\Delta NL_{ts}, \forall s, t \in \{1, \cdots, T-1\} \quad (5.40)$$

$$-P^{max}_{k} \leq \sum_{n} P^{inj}_{nt} PTDF_{nk} - \sum_{g} dr^{a}_{gts} PTDF_{n(g)k} + \sum_{i}\left(P^{solar,dep}_{it+1s} - P^{solar}_{it}\right) PTDF_{n(i)k} - \sum_{n}\left(Load^{nodal,dep}_{nt+1s} - Load^{nodal}_{nt}\right) PTDF_{nk} \leq P^{max}_{k}, k, s, t \in \{1, \cdots, T-1\} \quad (5.41)$$

The proposed FMM with the enhanced data-driven FRP policy is given in (5.42)-(5.43).

$$minimize \sum_{g} \sum_{t} (\underline{F_g} u_{gt} + \sum_{b=1}^{B} P_{gtb} B_{gb} + c^{SU}_{g} v_{gt} + c^{SD}_{g} w_{gt} + c^{UR}_{g} ur_{gt} + c^{DR}_{g} dr_{gt}) \quad (5.42)$$

subject to:
(5.2)-(5.29) and (5.34)-(5.41) (5.43)

Please note that the transmission constraints presented by (5.37) and (5.41) add $T \times K \times S$ constraints to the FMM formulation. However, most of these FRPs post-deployment transmission line constraints can be superfluous and do not set up the feasibility space of the FMM problem. In this chapter, an iterative procedure is presented to avoid the computational burden of the proposed approach by considering only binding FRPs post-deployment transmission line constraints, wherein the minimum set of these constraints, that limits the feasible region, are set up. More specifically, the transmission line flow cuts associated with the FRPs post-deployment, added to the FMM problem using the iterative procedure (similar to branch and cut procedure), serve as umbrella

constraints for all the transmission line constraints for FRPs post-deployment. To do so, first, the FMM problem (5.42)-(5.43) is solved without considering constraints (5.37) and (5.41). Then, transmission line flows for the post-deployment of FRPs are calculated through equations (5.44) and (5.45). If calculated flows are out of the limit of the transmission lines, the corresponding transmission line constraints for post-deployment of FRPs are added to the FMM problem, and this process continues till no other line can be found to be problematic during post-deployment of FRPs.

$$\overline{f_{kst}^{dep,ur}} = \sum_n P_{nt}^{inj} PTDF_{nk} + \sum_g ur_{gts}^{a} PTDF_{n(g)k} + \sum_i \left(P_{it+1s}^{solar,dep} - P_{it}^{solar}\right) PTDF_{n(i)k} - \sum_n \left(Load_{nt+1s}^{nodal,dep} - Load_{nt}^{nodal}\right) PTDF_{nk}, k, s, t \in \{1, \cdots, T-1\} \tag{5.44}$$

$$\overline{f_{kst}^{dep,dr}} = \sum_n P_{nt}^{inj} PTDF_{nk} - \sum_g dr_{gts}^{a} PTDF_{n(g)k} + \sum_i \left(P_{it+1s}^{solar,dep} - P_{it}^{solar}\right) PTDF_{n(i)k} - \sum_n \left(Load_{nt+1s}^{nodal,dep} - Load_{nt}^{nodal}\right) PTDF_{nk}, k, s, t \in \{1, \cdots, T-1\} \tag{5.45}$$

5.5. Out-of-Sample Validation Phase

To compare the effectiveness of different FRP policies from reliability and economic aspects, it is essential to have a proper validation phase that mimics the RT operation. In this chapter, an out-of-sample validation phase is presented based on the FMM of CAISO, which includes out-of-sample 15-min netload scenarios. While running the FMMs under the out-of-sample scenarios, dispatch change of MR generation resources between two successive time intervals is limited by their corresponding upward and downward FRP awards as given in (5.46) and (5.47), respectively.

$$P_{gt} - P_{gt-1} \leq \overline{ur_{gt}} u_{gt-1} + R_g^{SU} v_{gt}, \forall g, t \geq 2 \tag{5.46}$$

$$P_{gt-1} - P_{gt} \leq \overline{dr_{gt}} u_{gt} + R_g^{SD} w_{gt}, \forall g, t \geq 2 \quad (5.47)$$

It is pertinent to note that, if there is insufficient system ramping capability to follow the netload changes, power balance violation can happen in the validation phase with consideration of VOLL and the FS generation resources can still be committed. These additional adjustments and commitments can be translated into the ad-hoc and out-of-merit operator actions which can be potentially expensive for procuring additional ramp capabilities to meet changes in the netload. The reason can simply be associated with the fact that operators do not constantly adjust these ad-hoc actions to make a trade-off between the additional ramp needed and the RT operating costs.

Fig. 5.2 illustrates the flowchart of the proposed algorithm to address the deployability issue of FRP in RT operation, wherein, for the proposed approach, an offline process is performed before running the enhanced FMM formulation with the data-driven FRP policy. The data-driven policy generates ramping response factor sets to assign FMM FRP awards to qualified generation resources in the right location with respect to the transmission line limits for post-deployment of FRPs.

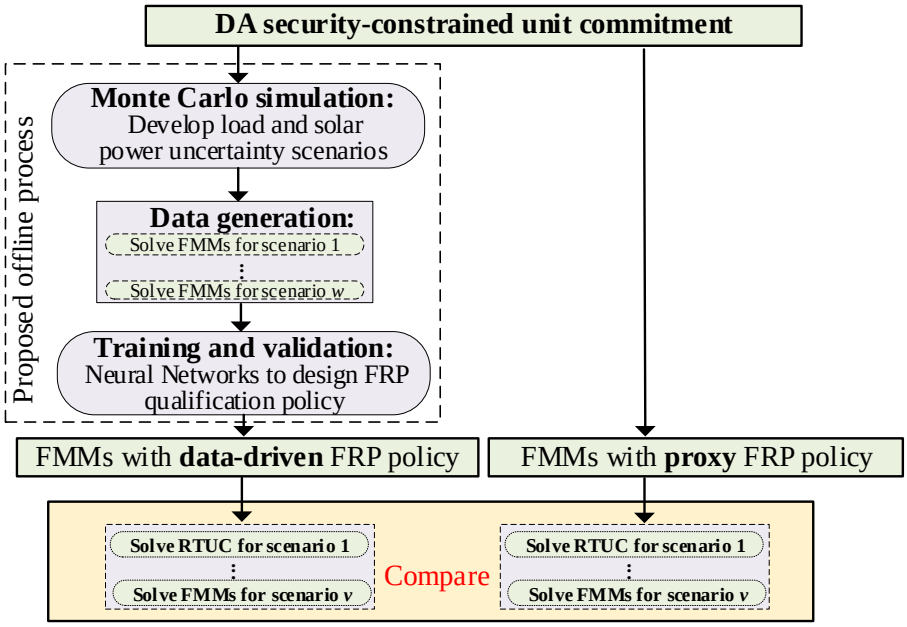

Fig. 5.2. Comparison of the Proxy and Data-driven Policies for FMM FRP Design.

5.6. Numerical studies and discussion

A modified IEEE 118-bus system is utilized for performing simulation analyses. CPLEX v12.8 is utilized to solve the different DA and RT market model processes on a computer with an Intel Core i7 CPU @ 2.20 GHz, 16 GB RAM, and 64-bit operating system.

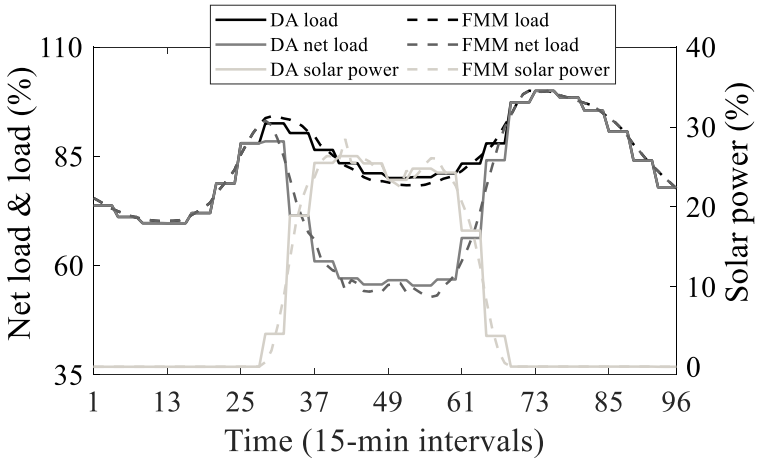

Fig. 5.3. Hourly and 15-min Load, Netload, and Solar Power Profiles for Test Day One.

5.6.1. Assumptions and System Data

The modified 118-bus IEEE test system has 51 generation resources, 3 solar power generations (located at buses 25, 55, and 89 with 20 %, 20 %, and 60 % share of total solar power generation, respectively), 91 loads, and 186 transmission lines [100]. In this chapter, only solar power generation is included in the simulation due to the high ramping needs it imposes on the electric system, but the proposed model can be easily be extended to include any variable renewable resource. Hourly and 15-min load and solar power generation profiles of two days, i.e., January 15, 2020, and September 2, 2021, were chosen from the CAIOS's real data [101]. The uncertainty of hourly load and solar power generation for the DA model is considered to be ~5%, based on which, the associated FMM uncertainty can be calculated through the total probability theory [67] and [103], i.e., $\sigma_{hourly} = 2\sigma_{15-min}$. Also, 1.96 standard deviations that is equivalent to 95% confidence level is considered for system-wide FRP requirement calculation. Power balance violation can occur in different market processes in the case of insufficient ramp capability at the cost of 10000 $/MW. In the FMMs, 21 generation resource with the maximum capacity of 50 MW are considered as FS units, i.e., G^F. The NN functions were trained through the Python v.3.7 with Scikit-learn library. 5000 scenarios were generated in the data-generations phase, 75% and 25% of which were respectively used as training and testing datasets. The NN functions have 3 hidden layers with 100, 100, and 25 neurons. The number of features of NNs with three bulk solar power generation units is $7 \times (4 + 2 \times 3) = 70$.

5.6.2. Simulation Results

For the first test day, profiles of which are shown in Fig. 5.3, Fig. 5.4 gives comparisons of the total number of FS units commitment reduction against the total violation improvement in the validation phase for the out-of-sample load and solar power generations scenarios. As Fig. 5.4 illustrates, most of the results of the out-of-sample scenarios are located in the first quadrants of the coordinate plane, in which the data-driven policy is effectively capable of lowering the total violation and the total number of FS units commitment in RT compared to the proxy policy. The reason for this improvement is that the data-driven policy preemptively assigns the FRP awards to the ramp-qualified units that are capable of delivering their products with respect to the transmission line limits. It is pertinent to note that a lower need for committing FS units indicates that there is less necessity for ad-hoc or out-of-merit expensive adjustments after FMMs by ISOs. This goal also is being perused by the CAISO through the FRP nodal delivery test [44]. These results show the performance of the data-driven policy for the FMM FRP design in awarding the FRPs to the generation resources and locations that can be dispatched for following the realized load and solar power generation changes.

Table 5.1 lists the number of out-of-sample scenarios in which the data-driven policy outperforms the proxy policy with respect to the economy, need for ad-hoc corrections, and reliability metrics. Based on this table, it can be seen that the proposed FRP design leads to 100%, 68% and 97.4% of out-of-sample scenarios have less real-time operating costs (the violation cost with VOLL is removed), total violation, and commitment of FS units, respectively. Comparisons with respect to the real-time operating costs, while the

violation cost with VOLL is excluded, are important for avoiding subjective analyses as the results are sensitive to the value of VOLL.

Table 5.1. Number of Out-of-sample Scenarios with Improvement in RT Operation, Total Number=500, First Test Day

Metric	
# Scenarios with RT cost (excluding violation cost) improvement	500
# Scenarios with reduction in number of total commitments of FS units	487
# Scenarios with total violation improvement	340

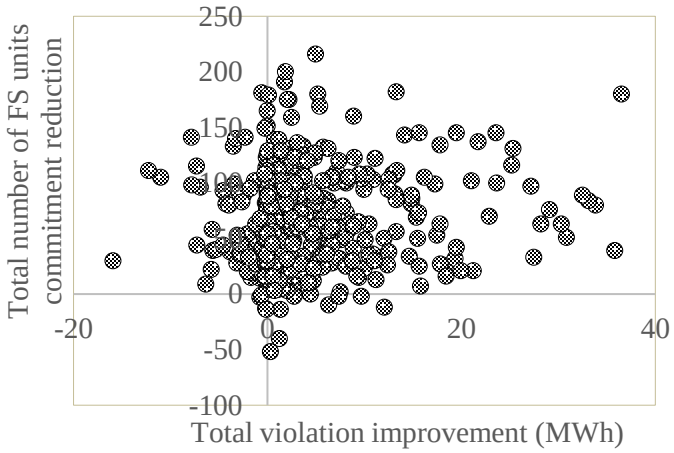

Fig. 5.4. Total Violation Improvement Versus the Total Number of FS Units Commitment Reduction for the Proposed Policy Compared to the Proxy Policy (First Test Day).

In this chapter, to be more objective, two metrics, i.e., the real-time operating costs excluding the violation cost and the total violations are compared simultaneously. To do so, three reliability statistical measures are presented in Table 5.2 to compare and evaluate the security extent in the RT operation due to implementing two proxy and data-driven approaches. Also, Fig. 5.5 illustrates improvements of the RT operating costs excluding the violation cost for each 15-min time interval in RT operation. For each time interval, the points on the top and bottom respectively represent the first and third quartiles of improvement while the height of the bar shows the median average

improvement. The results given in Table 5.2 show that the data-driven policy outperforms the proxy policy with respect to reliability statistical measures. It is pertinent to note that reducing maximum violation is important when the operator is concerned with the worst-case violation. Also, it can be seen in Fig. 5.5, the proposed approach leads to RT operating cost (excluding violation cost) improvement in almost all the time intervals through enhancing the FRP decisions. In other words, based on Table 5.2 and Fig. 5.5, while more load is met by the data-driven policy, the RT operating costs (not including the violation cost) of the data-driven policy are lower than those of the proxy policy.

Table 5.2. Comparison of Metrics Associated with Total Violation in RT Operation (First Day)

Metric	Proxy policy	Proposed policy
Average [Total violation] (MWh)	28	24
Σ Total violation (MWh)	13852	12023
Max Total violation (MWh)	140	107

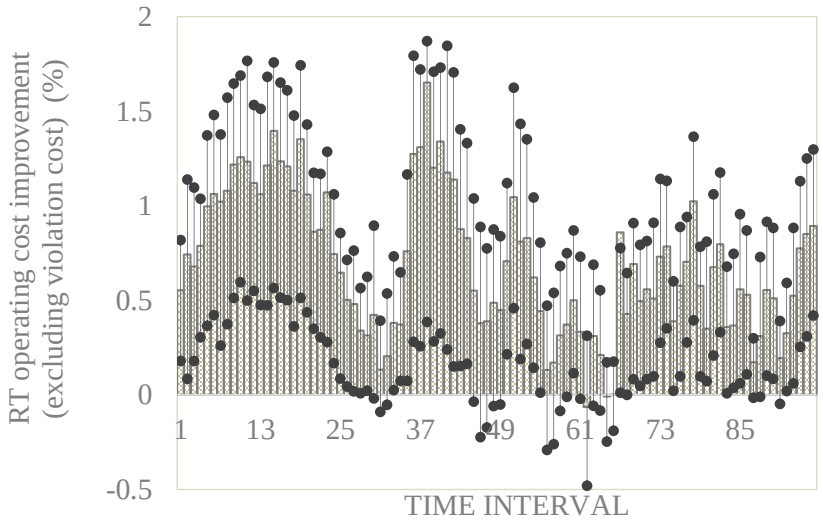

Fig. 5.5. Total Violation Improvement Versus the Total Number of FS Units Commitment Reduction for the Proposed Policy Compared to the Proxy Policy.

The FMM and RT operating costs are tabulated in Table 5.3 for proxy and data-driven policies. The data-driven policy leads to greater FMM operating costs (about 0.35%

increase) in contrast to the other policy; however, it results in much less ad-hoc expensive adjustments in the RT operation by having less RT operating cost. The average RT operating cost of the proxy policy over all of the out-of-sample scenarios equals $ 2313k, which is significantly greater than the one associated with the data-driven policy that is $ 2159k. The metrics associated with the number of total commitments of FS units are presented in Table 5.4. These additional commitments can be translated into the ad-hoc and out-of-merit operator actions, which is likely a high-cost procedure for procuring additional ramp capabilities to meet changes in the netload. The reason can simply be associated with the fact that operators do not constantly tune these ad-hoc actions to make a trade-off between the additional ramp needed and the RT operating costs. According to Table 5.4, it can be observed that the data-driven policy efficiently lowers the necessity of committing additional expensive FS units.

Table 5.3. Comparison of Metrics Associated with Operating Costs for FMMs and RT Operation (First Day)

Metric	Proxy policy	Data-driven policy
FMM operating costs (K$)	1171	1175
RT operating costs		
Ave (K$)	2313	2159
Max (K$)	6805	5500

Table 5.4. Comparison of Metrics Associated with the Number of Total Commitments of FS Units in RT Operation (First Day)

Metric	Proxy policy	Data-driven policy
Σ Number of total commitments of FS units	198803	166163
Ave [Number of total commitments of FS units]	398	332
Max Number of total commitments of FS units	747	666

Solving each FMM that includes 7 intervals for each trading hour takes around 1.05 seconds for the proxy policy to be solved while solving the one for the data-driven policy takes 5.6 seconds. Also, the NN functions need around ~6-25 seconds to be trained.

Please note that since the NN functions are independent, multiple machines can be used to train them in parallel. To further evaluate the performance of the proposed data-driven policy, one additional test day (i.e., September 2, 2021) was chosen from CAISO's data profiles, as illustrated in Fig. 5.6. The associated results over the out-of-sample scenarios are given in Tables 5.5 and 5.6 and Fig. 5.7. Based on these results, it can be observed that the proposed data-driven policy outperforms the proxy policy from economic, need for additional ad-hoc actions, and reliability points of view.

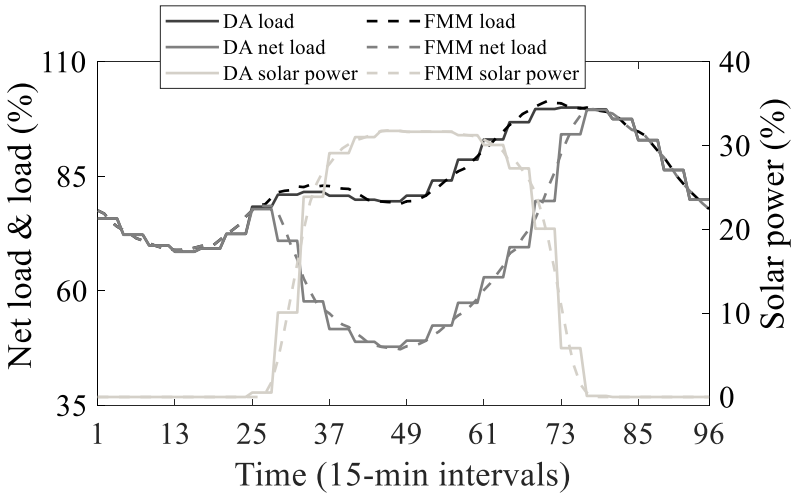

Fig. 5.6. Hourly and 15-min Load, Netload, and Solar Power Profiles for the Second Test Day.

Table 5.5. Number of Out-of-sample Scenarios with Improvement in RT Operation, Total Number=500, Second Test Day

Metric	
# Scenarios with RT cost (excluding violation cost) improvement	498
# Scenarios with reduction in number of total commitments of FS units	347
# Scenarios with total violation improvement	488

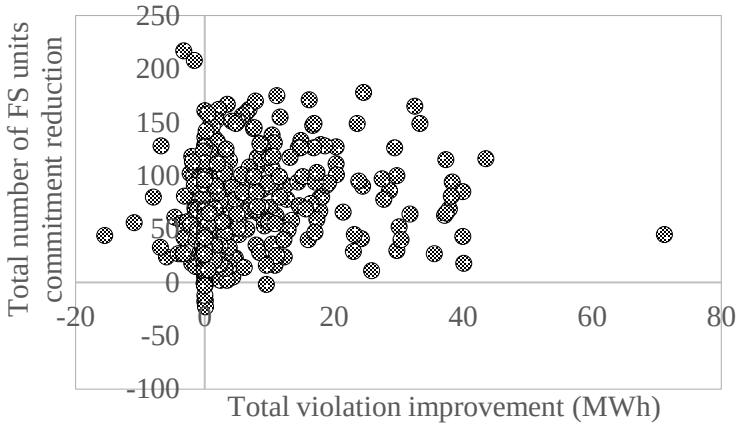

Fig. 5.7. Total Violation Improvement Versus the Total Number of FS Units Commitment Reduction for the Proposed Policy Compared to the Proxy Policy (Second Test Day).

Table 5.6. Results for FMMs and RT Operation (Second Test Day)

Metric	Proxy policy	Data-driven policy
FMM operating costs (K$)	1092.0	1094.7
RT operating costs		
Ave (K$)	1876	1689
Max (K$)	5160	4146
Total violation in RT operation		
Average [Total violation] (MWh)	19	14
Σ Total violation (MWh)	9476	7216
Max Total violation (MWh)	101	76
Number of total commitments of FS units in RT operation		
Σ Number of total commitments of FS units	172923	140386
Ave [Number of total commitments of FS units]	346	281
Max Number of total commitments of FS units	830	703

5.7. Conclusion

The general FRP design implemented in most ISOs utilizes a proxy ramping requirement for coping with the ramp capability shortage caused by high variability and uncertainty in the netload. However, these requirements do not consider the influence of the transmission line limits during making decisions on FRP awards. This ignorance can cause a major problem, as also stated by CAISO [26], since the deployability of

generation resources FRP awards are dependent not only on its operational limits but also on the ability of the resource to deliver this product in RT operation with respect to the transmission network limits. Therefore, the ISO should carefully consider which generation resources are qualified for awarding the FRPs while considering the limitation of transmission networks during the decision-making on FRP. In this chapter, the concept of data-driven FRP policy is introduced and proposed in order to improve the deployability of the FRP awards. To this end, first, by utilizing the NN algorithm, the generation resources ramping response to a set of deployment scenarios are predicted. Then, the system-wide ramping requirement is firstly met with these eligible resources, and at the same time, the transmission line limits are enforced for post-deployment of FRP awards. To evaluate the performance of different FRP policies, an out-of-sample validation phase is presented which mimics the RT operation of the CAISO's market and provides valuable insights about the ad-hoc actions needed to increase the ramp capability to follow the realized netload. The obtained results, based on the load and solar power generation profiles of CAISO, show that the enhanced FMM FRP design improves the deployability of FRPs with minimal disruption to existing RT market models. The proposed data-driven policy for FRP designs lead to (i) less RT operating costs, (ii) less potential violation in RT operation, (iii) less need for expensive committing FS units in RT operations and less need for ad-hoc corrections.

Chapter 6.

QUALIFICATION AND DISQUALIFICATION OF AGGREGATORS ENERGY AND ANCILLARY SERVICE AWARDS IN WHOLESALE MARKETS

6.1. Introduction

In this chapter, first, a distribution system operator and ISO coordination framework (architecture I in this report) is presented, wherein the DER aggregators directly participate in the wholesale market. In architecture I, the ISOs do not consider the DS limits while making decisions on the aggregators awards. It is pertinent to note that the distribution system operator role in this chapter is primarily for the safe and reliable operation of the DS network rather than dispatching the aggregators and DERs.

Then, a proposed distribution system operator and ISO coordination framework (architecture II in this report) is presented. In this architecture, the ISO schedules the aggregators in the wholesale market by considering the DS OSTN hosting capacity. The DS OSTN hosting capacity, i.e., maximum nodal DERs aggregation penetration considering safe and reliable DS network operation, can be used as a measure to qualify and disqualify different services provided by aggregators before running the wholesale market. Architecture II utilizes the statistical information obtained using different distribution system conditions and data-mining algorithms (offline analyses) to predict the hosting capacity of the DS before the DA wholesale market. Then, the ISO can assign the awards to the aggregators based on the predicted DS OSTN hosting capacity in the DA wholesale market.

Finally, a validation phase is proposed to compare the performance of architectures I and II. The validation phase, which mimics the DS condition during an uncertain event,

utilizes an unbalanced ACOPF based on current and voltage (IVACOPF) formulation. Also, the Volt-VAr support provided by distributed photovoltaics (PV) smart inverters is leveraged to increase the DS flexibility to improve the deployability of the aggregators promised awards in the DS. The Q-V curve of Volt-VAr controllers of distributed PVs is based on the IEEE 1547-2018 standard [118] and formulated as proposed mixed-integer linear constraints using the Big-M method. The primary contributions of this work are as follows:

- to propose an offline stage before the DA wholesale market to predict the DS hosting to a given DS condition. Then, a new coordination framework is proposed for the ISO and distributions utility based on this hosting capacity to award services to aggregators without posing any major risk to the DS. To this end, the concept of the maximum qualified aggregation capacity is proposed to determine the level of qualification and disqualification of the total services provided by aggregators. Then, using the maximum qualified aggregation capacity (translatable into the DS OSTN hosting capacity), the wholesale market can award any combination of services to an aggregator located in the relevant DS region as long as the total amount falls within the limit stated by this function.
- to propose the mixed-integer linear programming model of Volt-VAr droop controller of the distributed PV smart inverters inside a detailed unbalanced ACOPF based on current and voltage (IVACOPF) formulation [47].
- to develop a validation phase that represents transmission and distribution management during uncertain events. The validation phase mimics the ISOs dispatch instructions to aggregators during transmission-level uncertain events. It also includes

the IVACOPF with the objective function of minimizing voltage and thermal limits violation while avoiding the aggregators curtailment.

- to consider and assess the effects of Volt-VAr support from distributed PV units on the DS OSTN hosting capacity, and mitigating the voltage and thermal violations caused by aggregators meeting their obligations to ISOs during transmission-level uncertain events.

6.2. Architecture I: General Aggregator Participation Framework in the Wholesale Market

As mentioned earlier, in general architecture I, ISO manage the wholesale market without visibility over DS limitations, as shown in Fig. 6.1. Thus, the DS limitations and hosting capacity are not considered during wholesale market decision-making.

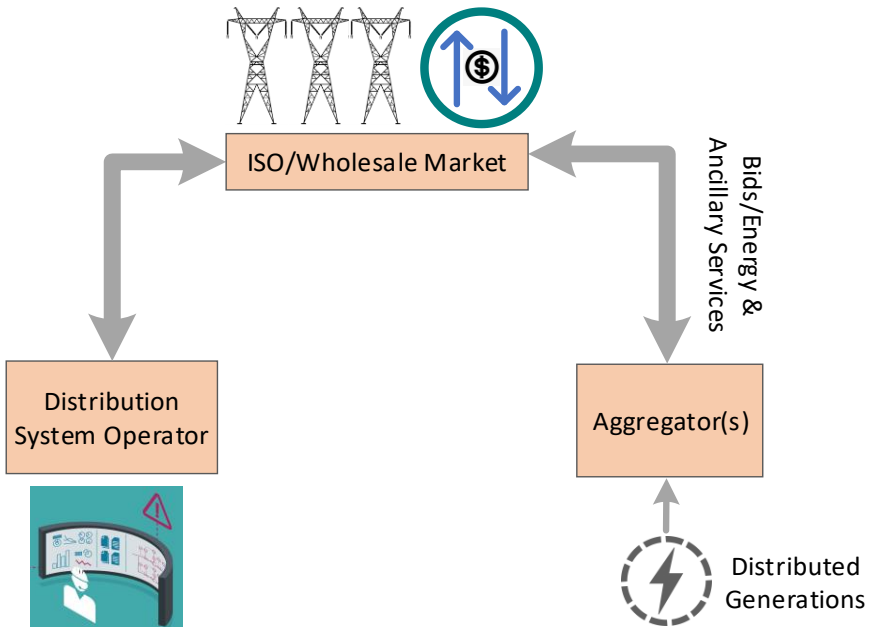

Fig. 6.1. Aggregator Participation in the Wholesale Market Based on Architecture I.

The DA wholesale market model formulation based on architecture I is presented in (6.1)-(6.26), wherein the aggregators bid their maximum available market capacity without considering the effects of DS limitations. The objective function of the DA wholesale market model, i.e., (6.1), is to minimize the total operating costs of the generators and the aggregators.

$$minimize \sum_g \sum_t (\underline{F_g} u_{gt} + \sum_{b=1}^{B} P_{gtb} B_{gb} + c_g^{SU} v_{gt} + c_g^{SD} w_{gt} + c_g^{Res} r_{gt}) +$$

$$\sum_a \sum_t (c_a^A P_{at}^A + c_a^{Res,A} r_{at}^A) \quad (6.1)$$

The objective function is subject to the operational constraints of the generators and the aggregators and the transmission network constraints. The generators minimum up and down time constraints are modeled by (6.2) and (6.3). The relationship of generators power generation with power generation block, used for linearizing cost curve, is given by (6.4) and (6.5). Constraints (6.6) and (6.7) enforce the hourly ramp rate limits for the generators, while generators power generation, including the associated reserve award, is limited through (6.8) and (6.9). The generators reserve award is limited to the 10-minute generators ramp rate through (6.10). Finally, the commitment variables, the startup variables, and the shutdown variables of the generators are modeled through (6.11)-(6.13).

$$\sum_{s=t-UT_g+1}^{t} v_{gs} \leq u_{gt}, t \in \{UT_g, \cdots, T\} \quad (6.2)$$

$$\sum_{s=t-DT_g+1}^{t} w_{gs} \leq 1 - u_{gt}, t \in \{DT_g, \cdots, T\} \quad (6.3)$$

$$P_{gt} = P_g^{min} u_{gt} + \sum_{b=1}^{B} P_{gtb}, \forall g, t \quad (6.4)$$

$$0 \leq P_{gtb} \leq P_{gb}^{max} u_{gt}, \forall g, t, b \quad (6.5)$$

$$P_{gt} - P_{gt-1} \leq R_g^{HR} u_{gt-1} + R_g^{SU} v_{gt}, \forall g, t \geq 2 \quad (6.6)$$

$$P_{gt-1} - P_{gt} \leq R_g^{HR} u_{gt} + R_g^{SD} w_{gt}, \forall g, t \geq 2 \quad (6.7)$$

$$P_{gt} + r_{gt} \leq P_g^{max} u_{gt}, \forall g, t \quad (6.8)$$

$$P_{gt} - r_{gt} \geq P_g^{min} u_{gt}, \forall g, t \quad (6.9)$$

$$0 \leq r_{gt} \leq R_g^{10} u_{gt}, \forall g, t \quad (6.10)$$

$$v_{gt} - w_{gt} = u_{gt} - u_{g,t-1}, \forall g, t \quad (6.11)$$

$$v_{gt} + w_{gt} \leq 1, \forall g, t \quad (6.12)$$

$$u_{gt}, v_{gt}, w_{gt} \in \{0,1\}, \forall g, t \quad (6.13)$$

Constraints (6.14) and (6.15) model the aggregators hourly ramp rate limits, while power generation of aggregators, including the associated reserve award, is limited through (6.16) and (6.17). The reserve award of aggregators is enforced to not exceed the 10-minute aggregators ramp rate through (6.18). Finally, the aggregators commitment, startup, and shutdown variables are modeled through (6.19)-(6.21).

$$P_{at}^A - P_{at-1}^A \leq R_a^{HR} u_{at-1} + R_a^{SU} v_{at}, \forall a, t \geq 2 \quad (6.14)$$

$$P_{at-1}^A - P_{at}^A \leq R_a^{HR} u_{at} + R_g^{SD} w_{at}, \forall a, t \geq 2 \quad (6.15)$$

$$P_{at}^A + r_{at}^A \leq P_{a,t}^{max} u_{at}, \forall a, t \quad (6.16)$$

$$P_{at}^A - r_{at}^A \geq P_{a,t}^{min} u_{at}, \forall a, t \quad (6.17)$$

$$0 \leq r_{at}^A \leq R_a^{10} u_{at}, \forall a, t \quad (6.18)$$

$$v_{at}^A - w_{at}^A = u_{at}^A - u_{at-1}^A, \forall a, t \quad (6.19)$$

$$v_{at}^A + w_{at}^A \leq 1, \forall a, t \quad (6.20)$$

$$u_{at}^A, v_{at}^A, w_{at}^A \in \{0,1\}, \forall a, t \quad (6.21)$$

In constraint (6.16), $P_{a,t}^{max}$ is the available maximum capacity, which represents the maximum total of the services (i.e., energy, reserve, regulation) related to an aggregator

active power in the wholesale market. The available maximum capacity could be time-varying if the aggregator manages different types of DERs (e.g., solar generation, dispatchable distributed generation, and energy storage system), the availability of which could change during different time intervals. More specifically, this availability is dependent on various factors such as solar irradiance or different state of charge of battery systems, etc. Thus, the available maximum capacity is always lower than or equal to the installed maximum capacity as shown in Fig. 6.2.

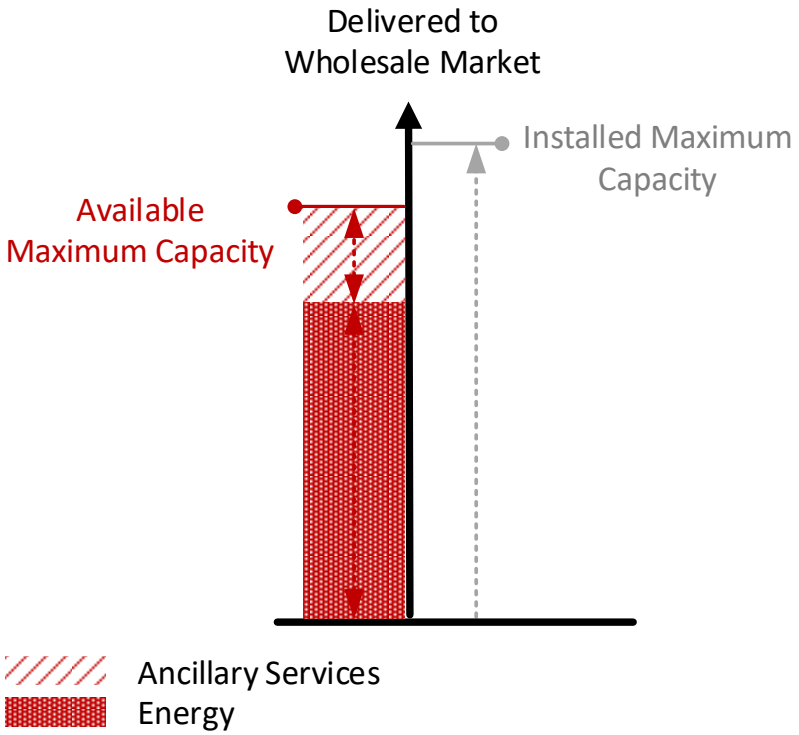

Fig. 6.2. Aggregators Installed Maximum Capacity Versus Available Maximum Capacity.

Constraint (6.22) ensures nodal power balance. Constraint (6.23) ensures the system-wide energy balance in the wholesale market throughout the system. Transmission line flow limits are imposed by (6.24). The total system reserve is enforced at each interval to

be larger than a percentage of demand through (6.25). Also, the system must withstand the loss of any single bulk power generation as represented through equation (6.26).

$$\sum_{g\epsilon g(n)} P_{gt} + \sum_{a\epsilon a(n)} P_{at}^{A} - Load_{nt} = P_{nt}^{inj}, \forall n, t \quad (6.22)$$

$$\sum_{n} P_{nt}^{inj} = 0, \forall t \quad (6.23)$$

$$-P_{k}^{max} \leq \sum_{n} P_{nt}^{inj} PTDF_{nk} \leq P_{k}^{max}, \forall k, t \quad (6.24)$$

$$\sum_{g} r_{gt} + \sum_{a} r_{at}^{A} \geq \eta\% \sum_{n} Load_{nt}, \forall t \quad (6.25)$$

$$\sum_{j} r_{jt} + \sum_{j} r_{jt}^{A} \geq P_{g0t} + r_{gt}, \forall g, t \quad (6.26)$$

It is pertinent to note that the aggregators awards deployment, during the realization of a transmission-level uncertain event, can cause voltage violations and line thermal overloads in the DS. The reason is associated with the fact that the aggregators participate in the transmission-level wholesale market and locate at the DS while the DS OSTN hosting capacity effects have not been considered in the above DA wholesale market clearing.

6.3. Validation Phase: Evaluation of DS Operational Limits During Transmission-Level Uncertain Events

A validation phase is essential to show the effectiveness of market solutions obtained based on the different distribution system operator and ISO coordination frameworks. During a transmission-level uncertain event, e.g., contingencies, ramping events, and netload uncertainty, the ISOs perform different analyses to determine new desired dispatch point (DDP) based on the resources promised energy and ancillary services awards. Then, these DDP signals are sent to the resources, including aggregators, to be met. Suppose the DS limitation was not considered while deciding on the aggregators

awards in the wholesale market. In that case, the distribution system operator might experience DS operational limits during transmission-level uncertain events. To mitigate the DS violation while avoiding the curtailment of the aggregators promised awards to the ISO, the flexibility of the DS, e.g., Volt-Var controllers, can also be employed. In the following subsection, a validation phase is proposed based on an unbalanced IVACOPF formulation that incorporates Volt-VAr support from PV units smart inverters to determine the DS operational limits caused by responding aggregators to the ISO dispatch signals. The general picture of transmission and distribution management during transmission-level uncertain events is shown in Fig. 6.3.

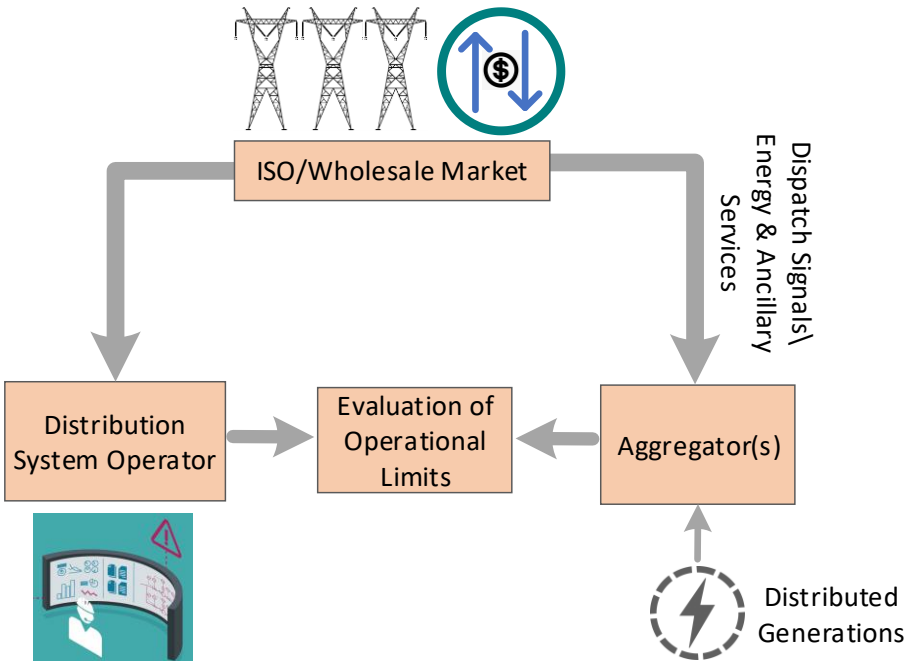

Fig. 6.3. Transmission and Distribution Management During Uncertain Events.

6.3.1. ISO Signals to Aggregators During Transmission-Level Uncertain Events

As mentioned in the previous section, the ISO sends dispatch signals to each aggregator based on a particular transmission-level uncertain event and the aggregators

energy and ancillary services awards from the wholesale market. In this chapter, the products offered by aggregators to the wholesale market are energy (i.e., P_{at}^{A}) and reserve (i.e., r_{at}^{A}) products. For the sake of simplicity in the validation phase, without loss of generality, to mimic the ISOs dispatch signals for aggregators in response to uncertain scenario s at time t, a random output power is generated in the range $\overline{P_a^A} \in [P_{at}^{A} - r_{at}^{A}, P_{at}^{A} + r_{at}^{A}]$. Thus, $\overline{P_a^A}$ represents the requested ISO DDP from the aggregator a during a particular uncertain scenario and time interval.

6.3.2. Evaluation of DS Operational Limits: IVACOPF with PV Units Volt-Var Support Model

This section presents the IVACOPF problem [47] to evaluate DS operational limits during transmission-level uncertain events, incorporating the proposed formulation for accurately modeling the Volt-VAr controller of smart PV inverters. The IVACOPF formulation models DSs details, including line losses and untransposed distribution lines with mutual admittances and mutual impedances [119].

The objective function is to evaluate DS operational limits in an unbalanced DS that minimizes total DS violation (including voltage and thermal line limit).

$$\min_{\substack{V_{ni}^{r,x}, V_{ni}^{im,x}, I_{ni}^{r,x}, I_{ni}^{im,x}, I_{l}^{r,x}, \\ I_{l}^{im,x}, P_{e,x}^{PV}, P_{f,x}^{PVV}, \\ Q_{f,x}^{PVV}, Q_{kc,x}^{C}, V_{ni}^{x}}} \begin{Bmatrix} \sum_{ni\in\mathcal{P}} \sum_{x\in\phi} V_{ni}^{x,+} + V_{ni}^{x,-} \\ \sum_{l\in\mathcal{K}} \sum_{x\in\phi} I_{l}^{x,+} \end{Bmatrix} \tag{6.27}$$

The objective function in (6.27) is subject to constraints given in (6.28)-(6.44) and (6.46)-(6.56). In an unbalanced DS, the current in phase x depends not only on the voltages of phase x, but also on the current and voltage of other phases due to the mutual

impedances and admittances. This current can be defined as (6.28) and (6.29) in a rectangular coordinate.

$$I_l^{r,x} = \left(R_l^{x,x}\right)^{-1}\left[V_{ni}^{r,x} - V_{nj}^{r,x} - \sum_{m\in\phi,m\neq x} R_l^{x,m}\, I_l^{r,m} - \frac{1}{2}\sum_{m\in\phi} R_l^{x,m}\left(\sum_{n\in\phi} y_l^{m,n}\, V_{ni}^{im,n}\right) + \sum_{m\in\phi} X_l^{x,m}\left(I_l^{im,m} - \frac{1}{2}\sum_{n\in\phi} y_l^{m,n}\, V_{ni}^{r,n}\right)\right], \forall\, x \in \phi, l \in \mathcal{K} \quad (6.28)$$

$$I_l^{im,x} = \left(R_l^{x,x}\right)^{-1}\left[V_{ni}^{im,x} - V_{nj}^{im,x} - \sum_{m\in\phi,m\neq x} R_l^{x,m} I_l^{im,m} + \frac{1}{2}\sum_{m\in\phi} R_l^{x,m}\left(\sum_{n\in\phi} y_l^{m,n}\, V_{ni}^{r,n}\right) - \sum_{m\in\phi} X_l^{x,m}\left(I_l^{r,m} + \frac{1}{2}\sum_{n\in\phi} y_l^{m,n}\, V_{ni}^{im,n}\right)\right], \forall\, x \in \phi, l \in \mathcal{K} \quad (6.29)$$

It is worth noting that (6.28) and (6.29) are linear constraints. In a rectangular coordinate, the injected current in each DS bus at each phase is modeled by (6.30) and (6.31).

$$I_{ni}^{r,x} = \sum_{l\epsilon\hbar(ni)} I_l^{r,x}\,, \forall\, x \in \phi, ni \in \mathcal{P} \quad (6.30)$$

$$I_{ni}^{im,x} = \sum_{l\epsilon\hbar(ni)} I_l^{im,x}\,, \forall\, x \in \phi, ni \in \mathcal{P} \quad (6.31)$$

The active and reactive power balance constraints in an unbalanced DS for each bus phase are given in (6.32) and (6.33), respectively.

$$\sum_{\forall sb\epsilon sb(ni)} P_{sb,x}^{B} + \sum_{\forall a\epsilon a(ni)} \overline{P_{a,x}^{A}} + \sum_{\forall f\epsilon f1(ni)} P_{f,x}^{PVV} + \sum_{\forall e\epsilon f2(ni)} P_{e,x}^{PV} - \sum_{\forall d\epsilon d(ni)} D_{d,x}^{P} = P_{ni,x} = V_{ni}^{r,x} I_{ni}^{r,x} + V_{ni}^{im,x} I_{ni}^{im,x}, \forall\, x \in \phi, ni \in \mathcal{P} \quad (6.32)$$

$$\sum_{\forall sb\epsilon sb(ni)} Q_{sb,x}^{B} + \sum_{\forall f\epsilon f1(ni)} Q_{f,x}^{PVV} + \sum_{kc\forall kc(ni)} Q_{kc,x}^{C} = Q_{ni,x} = V_{ni}^{im,x} I_{ni}^{r,x} - V_{ni}^{r,x} I_{ni}^{im,x} \forall\, x \in \phi, ni \in \mathcal{P} \quad (6.33)$$

Since constraints (6.32) and (6.33) are nonconvex and nonlinear, in the IVACOPF, they are reformulated as linear constraints (6.34) and (6.35) around ($V_{ni}^{r,x(it)}$, $V_{ni}^{im,x^{(it)}}$) and ($I_{ni}^{r,x(it)}$, $I_{ni}^{im,x^{(it)}}$) by first-order approximation of Taylor series.

$$P_{ni,x} = V_{ni}^{r,x(it)} I_{ni}^{r,x} + V_{ni}^{im,x^{(it)}} I_{ni}^{im,x} + I_{ni}^{r,x(it)} V_{ni}^{r,x} + I_{ni}^{im,x^{(it)}} V_{ni}^{im,x} - V_{ni}^{r,x(it)} I_{ni}^{r,x(it)} - V_{ni}^{im,x^{(it)}} I_{ni}^{im,x^{(it)}}, \forall\, x \in \phi, ni \in \mathcal{P} \quad (6.34)$$

$$Q_{ni,x} = V_{ni}^{im,x^{(it)}} I_{ni}^{r,x} - V_{ni}^{r,x(it)} I_{ni}^{im,x} + I_{ni}^{r,x(it)} V_{ni}^{im,x} - I_{ni}^{im,x^{(it)}} V_{ni}^{r,x} - V_{ni}^{im,x^{(it)}} I_{ni}^{r,x(it)} + V_{ni}^{r,x(it)} I_{ni}^{im,x^{(it)}}, \forall\, x \in \phi, ni \in \mathcal{P} \quad (6.35)$$

The IVACOPF is an iterative model, wherein the parameters of the Taylor series, i.e., $V_{ni}^{r,x(it)}, V_{ni}^{im,x^{(it)}}, I_{ni}^{r,x(it)}, I_{ni}^{im,x^{(it)}}$, in each iteration, are updated based on the results of the previous iteration.

The voltage magnitude in each bus phase can be formulated as (6.36), which is a nonlinear equation. The Taylor series is utilized to linearize this equation to (6.37). Please note that in (6.37), orders greater than one is disregarded.

$$V_{ni}^{x} = \sqrt{V_{ni}^{r,x^2} + V_{ni}^{im,x^2}}, \forall\, x \in \phi, ni \in \mathcal{P} \quad (6.36)$$

$$V_{ni}^{x} = \frac{V_{ni}^{r,x(it)}}{\sqrt{V_{ni}^{r,x(it)^2} + V_{ni}^{im,x(it)^2}}} V_{ni}^{r,x} + \frac{V_{ni}^{im,x^{(it)}}}{\sqrt{V_{ni}^{r,x(it)^2} + V_{ni}^{im,x(it)^2}}} V_{ni}^{im,x}, \forall\, x \in \phi, ni \in \mathcal{P} \quad (6.37)$$

Each bus phase voltage magnitude limits, including associated voltage violation variables, are modeled through (6.38). Also, the thermal line limit, including the associated thermal line violation variable for each line phase, is presented by (6.39).

$$-V_{ni}^{x,-} + 0.95 \leq V_{ni}^{x} \leq 1.05 + V_{ni}^{x,+}, \forall\, x \in \phi, ni \in \mathcal{P} \quad (6.38)$$

$$I_{l}^{r,x^2} + I_{l}^{im,x^2} \leq (I_{l}^{max,x} + I_{l}^{x,+})^2, \forall\, x \in \phi, l \in \mathcal{K} \quad (6.39)$$

Also, capacitors bank units reactive power generation is limited by (6.40) in DS.

$$Q_{kc,x}^{C} \leq Q_{kc,x}^{C,max}, \forall\, x \in \phi, kc \in \mathcal{C} \quad (6.40)$$

Two types of PV units are modeled in the IVACOPF problem: PV units with and without Volt-VAr controller. The former, i.e., without Volt-VAr controller, only can generate the available active power, which is modeled through (6.41).

$$P_{e,x}^{PV} = P_{e,x}^{PV,av}, \forall\, x \in \phi, e \in F2 \tag{6.41}$$

On the other hand, the PV unit with a Volt-VAr controller can generate both the active and reactive powers, restricted through its apparent power rating by (6.42), and it can provide Volt-VAr support in the DS system. Also, the active power generation of such PV units is limited by their available active power (6.43). In contrast, their reactive power generation is restricted by their apparent power rating as presented (6.44), respectively.

$$Q_{f,x}^{PVV\,2} + P_{f,x}^{PVV\,2} \leq S_{i,x}^{PVV\,2}, \forall\, x \in \phi, f \in F1 \tag{6.42}$$

$$P_{f,x}^{PVV} \leq P_{f,x}^{PVV,av}, \forall\, x \in \phi, f \in F1 \tag{6.43}$$

$$-S_{f,x}^{PVV} \leq Q_{f,x}^{PVV} \leq S_{f,x}^{PVV}, \forall\, x \in \phi, f \in F1 \tag{6.44}$$

As mentioned earlier, participation of aggregators in the wholesale market and providing services to the transmission system without considering the DS OSTN hosting capacity may cause voltage and thermal line capacity challenges in the DS. The PV units with Volt-VAr controllers can mitigate these challenges by injecting/absorbing the reactive power in the DS system. Most of the work in the literature model this Volt-VAr support based on only constraints (6.42)-(6.44), which may lead to unrealistic results due to ignoring the inverter Volt-VAr droop controller model. In this work, the Volt-VAr support from PV units is modeled based on the IEEE 1547-2018 standard [118], which represents a more accurate Q-V curve of Volt-VAr controllers of distributed PV units, as shown in Fig. 6.4.

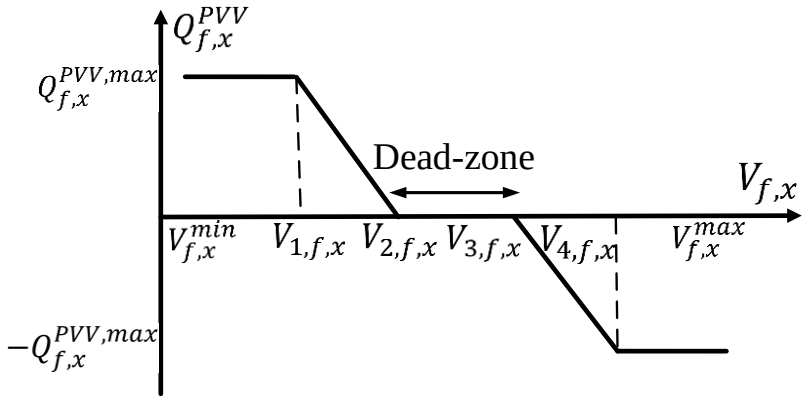

Fig. 6.4. Q-V Characteristic of a PV Smart Inverter with Volt-VAr Controller [118].

The Q-V curve shown in Fig. 6.3 can be represented by equation (6.45). In this equation, $V_{1,f,x}$,$V_{2,f,x}$, $V_{3,f,x}$, and $V_{4,f,x}$ are the Q-V curve set points for a PV unit smart inverter. This Q-V curve defines five different operating zones.

$$Q_{f,x}^{PVV} = \begin{cases} Q_{f,x}^{PVV,max} & V_{f,x}^{min} \le V_{f,x} < V_{1,f,x} \\ \frac{Q_{f,x}^{PVV,max}}{V_{2,f,x}-V_{1,f,x}}\left(V_{2,f,x} - V_{f,x}\right) & V_{1,f,x} \le V_{f,x} < V_{2,f,x} \\ 0 & V_{2,f,x} \le V_{f,x} < V_{3,f,x} \\ \frac{Q_{f,x}^{PVV,max}}{V_{3,f,x}-V_{4,f,x}}\left(V_{f,x} - V_{3,f,x}\right) & V_{3,f,x} \le V_{f,x} < V_{4,f,x} \\ -Q_{f,x}^{PVV,max} & V_{4,f,x} \le V_{f,x} < V_{f,x}^{max} \end{cases} \quad (6.45)$$

Equation (6.45) is an if-then function, wherein the reactive power generation of the smart inverter is determined based on voltage magnitude at the corresponding PV unit bus phase, i.e., $V_{f,x}$. In this work, this equation is converted into a proposed mixed-integer linear programming formulation using the Big-M method. Each operation zone of the Q-V curve of Fig. 6.3 is represented by the corresponding binary variable as mathematically given below.

$$V_{f,x} \le V_{1,f,x} + Mz_{1,f,x} \quad (6.46)$$

$$-Mz_{1,f,x} \le Q_{f,x}^{PVV} - Q_{f,x}^{PVV,max} \le Mz_{1,f,x} \quad (6.47)$$

$$-Mz_{2,f,x} + V_{1,f,x} \leq V_{f,x} \leq V_{2,f,x} + Mz_{2,f,x} \tag{6.48}$$

$$-Mz_{2,f,x} \leq Q_{f,x}^{PVV} - \frac{Q_{f,x}^{PVV,max}}{V_{2,f,x} - V_{1,f,x}}\left(V_{2,f,x} - V_{f,x}\right) \leq Mz_{2,f,x} \tag{6.49}$$

$$-Mz_{3,f,x} + V_{2,f,x} \leq V_{f,x} \leq V_{3,f,x} + Mz_{3,f,x} \tag{6.50}$$

$$-Mz_{3,f,x} \leq Q_{f,x}^{PVV} \leq Mz_{3,f,x} \tag{6.51}$$

$$-Mz_{4,f,x} + V_{3,f,x} \leq V_{f,x} \leq V_{4,f,x} + Mz_{4,f,x} \tag{6.52}$$

$$-Mz_{4,f,x} \leq Q_{f,x}^{PVV} - \frac{Q_{f,x}^{PVV,max}}{V_{3,f,x} - V_{4,f,x}}\left(V_{f,x} - V_{3,f,x}\right) \leq Mz_{4,f,x} \tag{6.53}$$

$$-Mz_{5,f,x} + V_{4,f,x} \leq V_{f,x} \tag{6.54}$$

$$-Mz_{5,f,x} \leq Q_{f,x}^{PVV} + Q_{f,x}^{PVV,max} \leq Mz_{5,f,x} \tag{6.55}$$

$$z_{1,f,x} + z_{2,f,x} + z_{3,f,x} + z_{4,f,x} + z_{5,f,x} \leq 4 \tag{6.56}$$

In the above formulation, constraints (6.46)-(6.47), (6.48)-(6.49), (6.50)-(6.51), (6.52)-(6.53), and (6.54)-(6.55) are associated with operating zones from one to five, respectively. Finally, the relationship between different binary variables of zones, i.e., $z_{1,f,x}$, $z_{2,f,x}$, $z_{3,f,x}$, $z_{4,f,x}$, $z_{5,f,x}$, is given in (6.56).

It is worth noting that the IVACOPF problem presented above with the proposed modeling of Volt-VAr controller of smart PV inverters is a mixed-integer quadratically constrained program (MIQCP). This problem is solved independently at each time interval t for each uncertain scenario s using commercial solver GUROBI.

6.4. Architecture II: Proposed Aggregator Participation Framework in the Wholesale Market

In this architecture, the ISOs manage the wholesale market with visibility over the DS OSTN hosting capacity. Before running the wholesale market, the ISO coordinates with

the distribution system operator to get the level of qualification and disqualification for different services provided by aggregators, as shown in Fig. 6.5. To this end, the hosting capacity (i.e., maximum per-feeder DER penetration considering safe and reliable DS network operation [79]) is predicated using data-mining algorithms based on the statistical information obtained using different DS conditions. Then, the ISO can use this predicted hosting capacity to award an appropriate amount of products to the aggregators in a competitive environment.

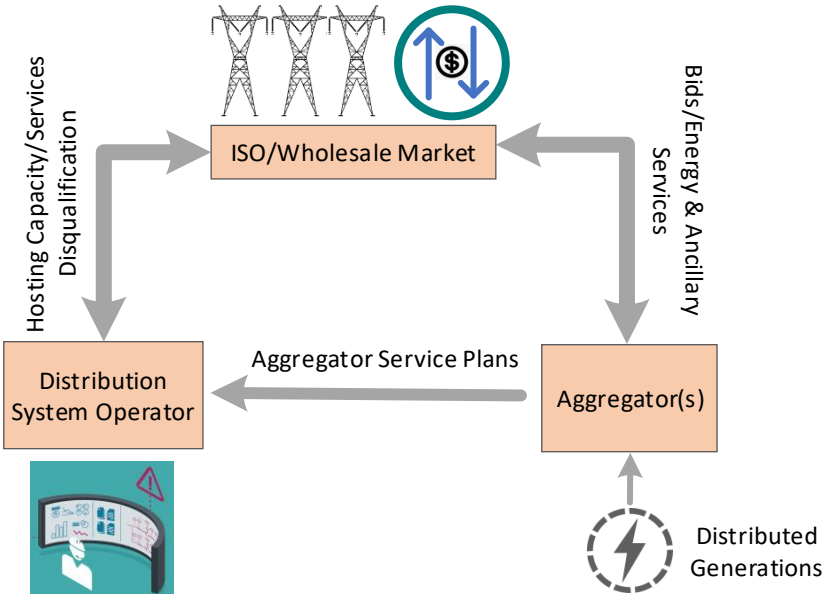

Fig. 6.5. Aggregator Participation in the Wholesale Market Based on Architecture II.

6.4.1. Data Generation for Ata-Mining Algorithm

To obtain the data for the data-mining algorithm, different DS load scenarios using the corresponding forecast value and forecast error are generated through Monte Carlo simulation. Then, the IVACOPF problem with the objective function of maximizing the instantaneous penetration (i.e., active power generation) of the aggregations within their maximum available capacity is solved for each scenario. It is worth noting that

maximizing the availability of the DERs aggregation under the reliable and safe operation of the DS was also persuaded in FERC order No. 2222 [45]. With these analyses, we can see how much of the aggregators maximum available capacity is qualified to participate in the wholesale market under different DS conditions. In other words, the obtained maximized active power generation can determine the level of qualification and disqualification of the total capacity of the services provided by aggregators.

$$\max_{\substack{V_{ni}^{r,x}, V_{ni}^{im,x}, I_{ni}^{r,x}, I_{ni}^{im,x}, I_{l}^{r,x}, \\ I_{l}^{im,x}, P_{e,x}^{PV}, P_{f,x}^{PVV}, \\ Q_{f,x}^{PVV}, Q_{kc,x}^{C}, V_{ni}^{x}, P_{a,x}^{A}}} \left\{ \sum_{a \in A} \sum_{x \in \phi} P_{a,x}^{A} \right\} \tag{6.57}$$

subject to:

(6.28)-(6.31), (6.34)-(6.35), (6.37)-(6.44), and (6.46)-(6.56) (6.58)

$$P_{a,x}^{A} \leq P_{a,x}^{max} \tag{6.59}$$

The optimization model (6.57)-(6.59) includes the dynamic effect of the Volt-VAr support from the PV units on the DS OSTN hosting capacity and is solved for each scenario and time interval before solving the DA wholesale market. Finally, each scenario run includes (i) the maximum qualified capacity of an aggregator and (ii) different loading conditions in the DS, which can be used in the data-mining stage. Please note that the maximum qualified capacity of aggregators incorporates nodal and per-feeder information of aggregators (depending on their location in the DS network).

6.4.2. Data-Mining Stage: Obtaining Aggregators Maximum Qualified Capacity (DS OSTN hosting capacity)

In this section, neural network (NN) regression is utilized to create functions that predict the maximum qualified capacity of the aggregators, i.e., $P_{a,t}^{max,qualified}$, to a given

DS conidiation under the reliable and safe DS operation. Each scenario from section 6.4.1, i.e., data-acquisition stage, represents an instance that includes (i) target value that is the maximum qualified capacity of an aggregator and (ii) the features that are loads summation at each phase at each feeder. So, the total number of features would be $3 \times (number\ of\ feeders)$. The NN function creation is performed for each time interval t and aggregator $a \in A$. Please note that data acquisition and performing the NNs are offline processes before running the DA wholesale market.

6.4.3. DA Wholesale Market Model Considering Predicted DS OSTN hosting capacity

This section presents the DA wholesale market, which assigns the total services (i.e., energy and reserve) to an aggregator based on its maximum qualified capacity, i.e., $P_{a,t}^{max,qualified}$. The maximum qualified capacity is the target values of different NNs regression functions. After obtaining the NN functions from the offline process, the maximum qualified capacity can be easily predicted based on the most-updated DS information and condition close to running the DA wholesale market. Therefore, there is no need to perform different DS analyses close to solving DA wholesale market for determining DS OSTN hosting capacity, which could be potentially very time-consuming.

Please note that the maximum qualified capacity is calculated using these functions with this understanding: the wholesale market can award any combination of services to an aggregator located in the relevant DS region as long as the total amount falls within the limit stated by this function. It is worth mentioning that the qualified maximum

capacity is always lower than or equal to the available maximum capacity, as shown in Fig. 6.6.

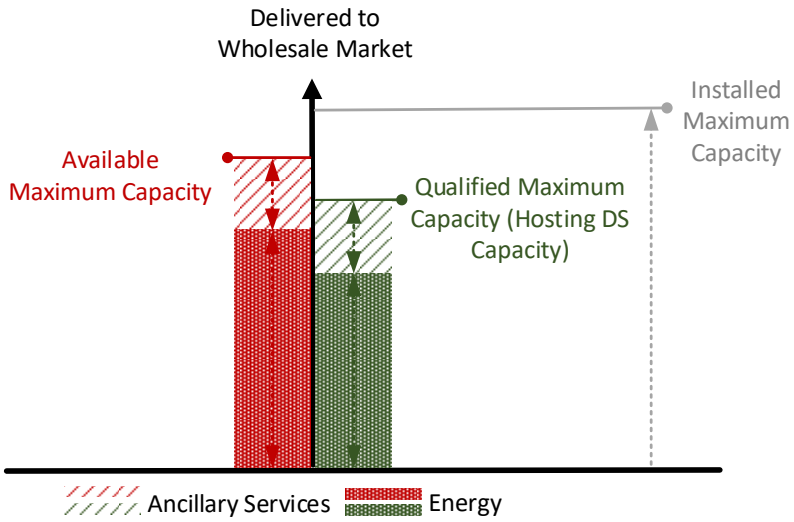

Fig. 6.6. Aggregators Installed Maximum Capacity, Available Maximum Capacity, and Maximum Qualified Capacity (Considering DS OSTN Hosting Capacity).

Finally, the DA wholesale market model considering predicted qualified maximum capacity representing the DS OSTN hosting capacity is given below.

$$minimize \sum_g \sum_t (\underline{F_g} u_{gt} + \sum_{b=1}^{B} P_{gtb} B_{gb} + c_g^{SU} v_{gt} + c_g^{SD} w_{gt} + c_g^{Res} r_{gt}) +$$

$$\sum_a \sum_t (c_a^A P_{at}^A + c_a^{Res,A} r_{at}^A) \quad (6.60)$$

subject to:

(6.2)-(6.26) (6.61)

$$P_{at}^A + r_{at}^A \leq P_{a,t}^{max,qualified} u_{at}, \forall a, t \quad (6.62)$$

Flowchart of the proposed framework is presented in Fig. 6.7.

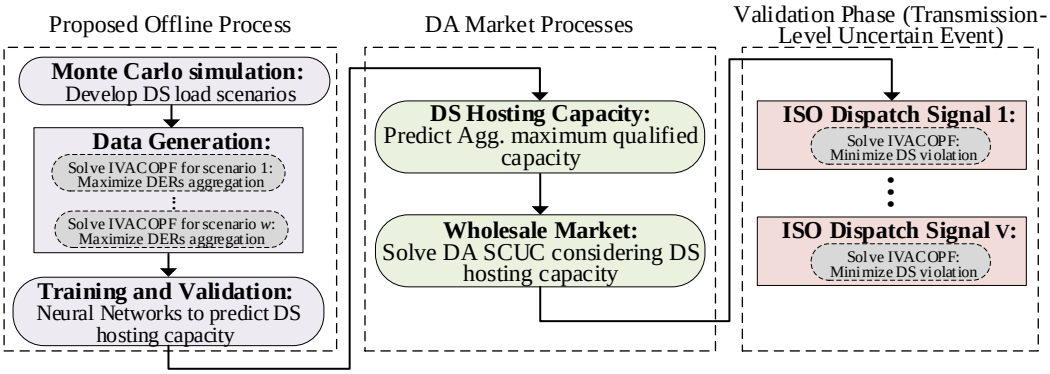

Fig. 6.7. Flowchart of the Proposed Framework.

6.5. Numerical Studies and Discussion

An IEEE 118-bus system [100] and 240-bus distribution test system [120] are used to perform simulation analyses of the DA wholesale market and the DS. DOcplex and Pyomo Python modeling libraries were used to solve the DA wholesale market model and IVACOPF model on a computer with an Intel Core i7 CPU @ 2.20 GHz, 16 GB RAM, and 64-bit operating system. In addition, the NN functions for determining the qualified capacity of aggregators were trained through Python v.2.7 with the Scikit-learn library.

6.5.1. Assumptions and System Data

The 118-bus IEEE test system has 91 loads, 54 generators, and 186 lines [100]. The DS substation is assumed to be connected to bus # 71 of the 118-bus IEEE test system. Fifteen aggregators with 0.25, 0.5, 1, 1.5 MW maximum capacity (see Table 6.1) and a maximum total of 8.25 MW were added to the 240-bus distribution test system. Seven of these aggregators manage and own different types of DERs (solar generation, dispatchable distributed generation, energy storage); therefore, they have time-varying available maximum aggregation capacity. The rest eight aggregators have a non-time-varying available maximum capacity. The aggregators bids were randomly generated in

the range of the generators minimum and average wholesale market bids. Also, fifteen PV units were added to the DS system based on the data from a local utility in Arizona. For these PV units, the hourly solar generation profile of CAIOS's actual data, February 10, 2022, was chosen [101]. Also, the number of iterations for the IVACOPF is 2. The relative MIP gap is set at 0.2%. For the data-mining stage associated with architecture II, 1000 DS load scenarios were generated, 80% and 20% of which were used as training and testing datasets. The NN models have three hidden layers with 100, 100, and 25 neurons.

Table 6.1. Aggregators Characteristics.

Agg. #	Bus #	Phase #	Maximum installed capacity (MW)
1	1004	3	0.5
2	1008	3	0.5
3	1009	3	0.5
4	1013	3	0.25
5	1016	3	1
6	2010	2	1.5
7	2015	2	0.25
8	2036	2	0.25
9	2038	2	0.5
10	2048	2	0.25
11	3038	1	1.5
12	3079	1	0.5
13	3107	1	0.25
14	3132	1	0.25
15	3135	1	0.25

6.5.2. Study 1

This study aims to evaluate (i) the capability of the PV units Volt-VAr support installed in DS to mitigate the DS limits while avoiding the curtailment of the aggregators

promised awards to the ISOs, and (ii) the accuracy of the Taylor series approximations used in the IVACOPF. It is pertinent to note that only the general aggregator participation model in the wholesale market, i.e., architecture I, is implemented in this study. The ISO signals requested from the aggregators are only energy awards accepted in the DA wholesale market; therefore, the IVACOPF is only solved for one 24-hours. This study considers two PV models, PV models 1 and 2. In the "PV model 1", all PV units have smart inverters and provide Volt-VAr support, while in the "PV model 2", none of the PV units have smart inverters and do not provide Volt-VAr support.

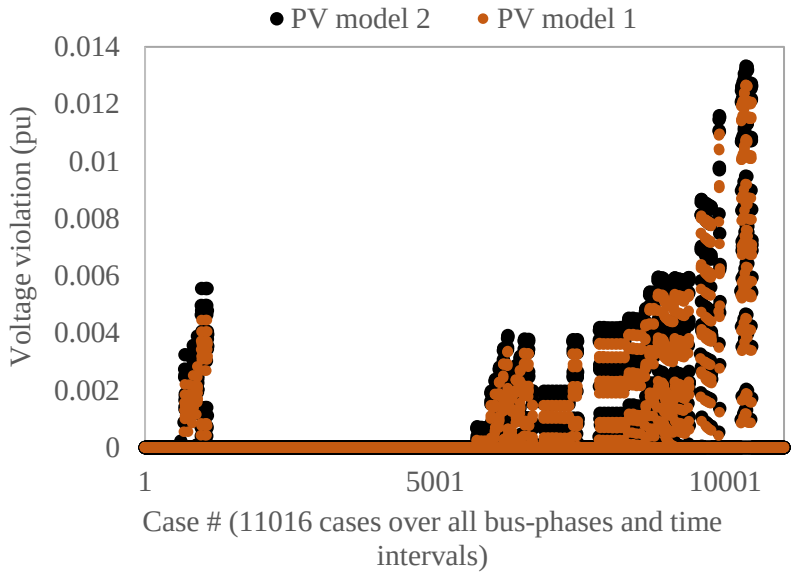

Fig. 6.8. Voltage Violation in DS with and without Having PV Units Volt-VAr Controllers, Architecture I.

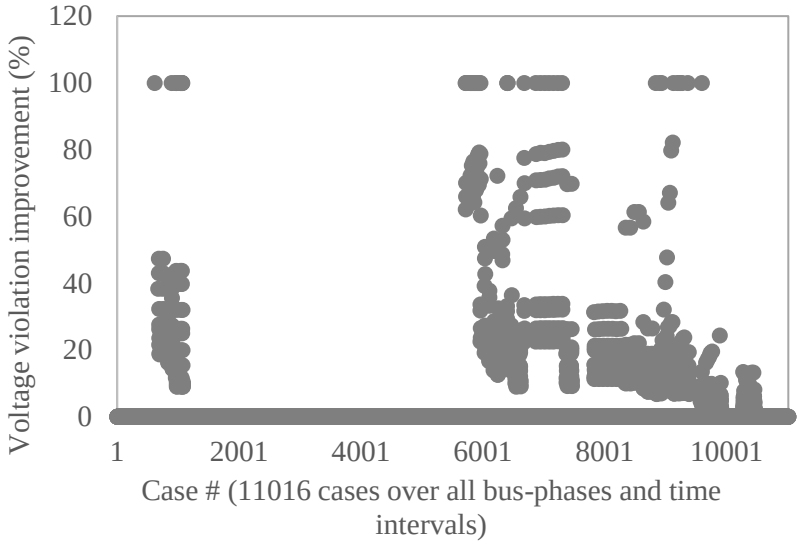

Fig. 6.9. Voltage Violation Improvement in DS with PV Units Having Volt-VAr Controllers, Architecture I.

Fig. 6.8 illustrates the voltage violation comparison across different bus phases, and the 24-hour time horizon with and without considering Volt-VAr support from PV units. The total number of cases is 11016, which is obtained through multiplying the number of bus phases, i.e., 459, by the number of time intervals, i.e., 24. As can be seen, proper management of the Volt-VAr support in the DS can reduce the voltage issue associated with the aggregators meeting the ISOs dispatch signals after the DA wholesale market. The reason is that the Q-V curve of Volt-VAr controllers of distributed PVs was precisely modeled in the IVACOPF to optimally mitigate the DS voltage issues by using bi-directional utility-interactive inverters and their capability in injecting/absorbing reactive power into DS. In Fig 6.8, 11010 or ~100% of all cases have the same or less voltage violation with PV model 1. Although the Volt-VAr support from PV units mitigates the voltage violation, it cannot remove the voltage issue entirely. Also, Fig. 6.9 presents corresponding voltage violation improvement for the 11016 cases due to having Volt-VAr

support from PV units, i.e., PV model 1. It is pertinent to note that there was no current thermal violation for this case study.

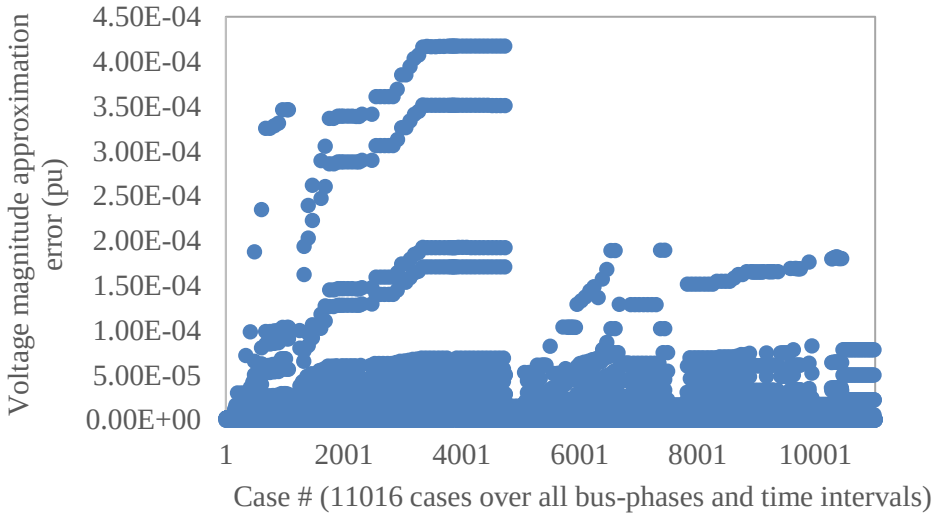

(a)

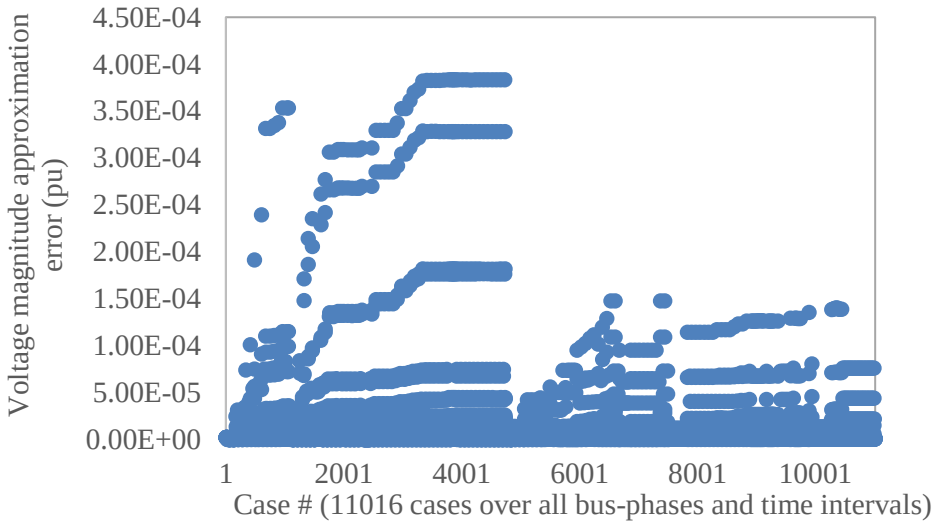

(b)

Fig. 6.10. Voltage Magnitude Approximation Error in IVACOPF Model: (a) Architecture I with PV Model 2, and (b) Architecture I with PV Model 1.

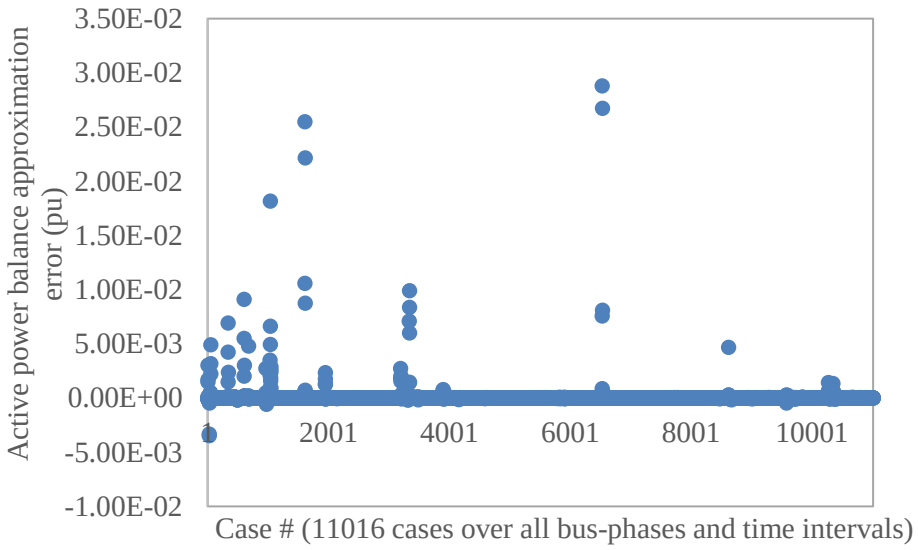

(a)

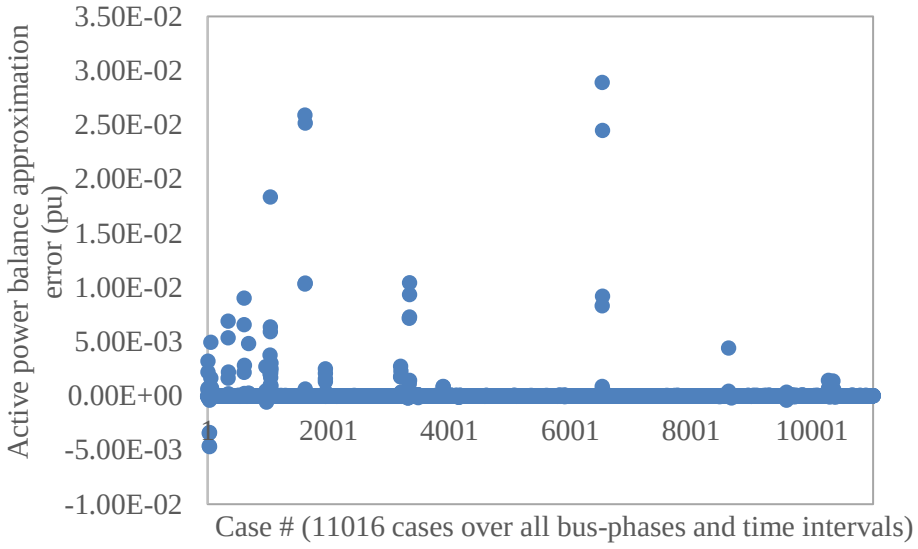

(b)

Fig. 6.11. Active Power Balance Approximation Error in IVACOPF Model: (a) Architecture I with PV Model 2, and (b) Architecture I with PV Model 1.

Fig. 6.10 shows the voltage magnitude approximation errors in the IVACOPF model. This error is obtained by substituting the obtained values of $V_{ni}^{r,x}$, $V_{ni}^{im,x}$, $V_{ni}^{r,x(it)}$, and $V_{ni}^{im,x(it)}$ from the last iteration of the IVACOPF problem in equations (6.36) and (6.37), and subtracting the resulting values. Based on the presented errors in Fig. 6.10, the

maximum voltage magnitude approximation error is less than 4.5E-04, which shows the precision of the IVACOPF model for solving optimal power flow in the unbalanced DS in the presence of PV units with and without Volt-VAr support capability. Furthermore, Fig. 6.11 illustrates the active power balance approximation error in the IVACOPF model, wherein the error is almost zero in most bus phases over different time intervals.

Table 6.2. Total Bus-phase DS Voltage Violation over All Time Intervals, Architecture I (pu).

PV Pen. %	PV model 1	PV model 2	Improvement of PV model 1 to model 2 (%)
15	3.69	4.15	12.61
30	3.48	4.42	26.78
45	3.29	4.70	42.83

Table 6.3. Maximum of Total Bus-phase DS Voltage Violation Among all Time Intervals, Architecture I (pu).

PV Pen. %	PV model 1	PV model 2	Improvement of PV model 1 to model 2 (%)
15	0.37	0.41	12.70
30	0.35	0.44	26.65
45	0.34	0.48	41.68

Sensitivity analyses with respect to the penetration of the PV units in the DS system were performed, and associated results are given in Table 6.2, wherein the reported voltage violation is the summation across bus phases and time intervals. The 15% is the PV penetration based on the original data from a local utility in Arizona. From this table, it can be seen that with more penetration of PV units, the flexibility of the DS system can be increased in managing voltage issues caused by aggregators meeting the ISOs dispatch

signals. Another metric, i.e., the maximum of total bus phases voltage violation across different time intervals, was also presented in Table. 6.3, wherein the PV units equipped with Volt-VAr support are capable of reducing the maximum of total bus phases violation across different time intervals by 12.7 %, 26.65 %, and 41.68 % for PV penetrations of 15 %, 30 %, and 45 %, respectively. These results can be translated as using volt-var controller helps with higher qualification of DER services during transmission-level uncertain events.

6.5.3. Study 2; Architecture II Versus Architecture I

In this study, the goal is to compare the performance of architecture II against architecture I. In this study, the number of PV units with Volt-VAr support is five for both architectures, and the penetration of PV units is the same as the original data from the local utility in Arizona (~15% penetration). Also, hundred transmission-level uncertain event scenarios are generated in the validation phase for both frameworks.

Table 6.4. Results of DA Wholesale Market under Different Architectures.

Metric	Architecture I	Architecture II
Total operating costs (k$)	2601.38	2602.74
Gen. total cost (k$)	2598.76	2600.31
Gen. energy cost (k$)	2580.01	2581.60
Gen. reserve cost ($)	16191.3	16282.2
Agg. total cost ($)	2630.2	2425.5
Agg. energy cost ($)	2608.7	2404.9
Agg. reserve cost ($)	21.6	20.7

The DA wholesale market metrics associated with different operating costs are given in Table 6.4. Based on this table, although the total operating cost increases to $ 2602.74k from $ 2601.38k by implementing architecture II, $ 2602.74k is a more realistic operating

cost. The reason is that in architecture I, the aggregators are more involved in supplying the load than architecture II (see Fig. 6.12), which could potentially be beyond the DS OSTN hosting capacity. This can reduce the DA total operating costs but potentially jeopardize the DS network security and reliability. Also, based on Table 6.4, architecture II respectively increases and decreases the total generators and aggregators costs compared to architecture I, while the aggregators reserve costs are almost the same for both architectures.

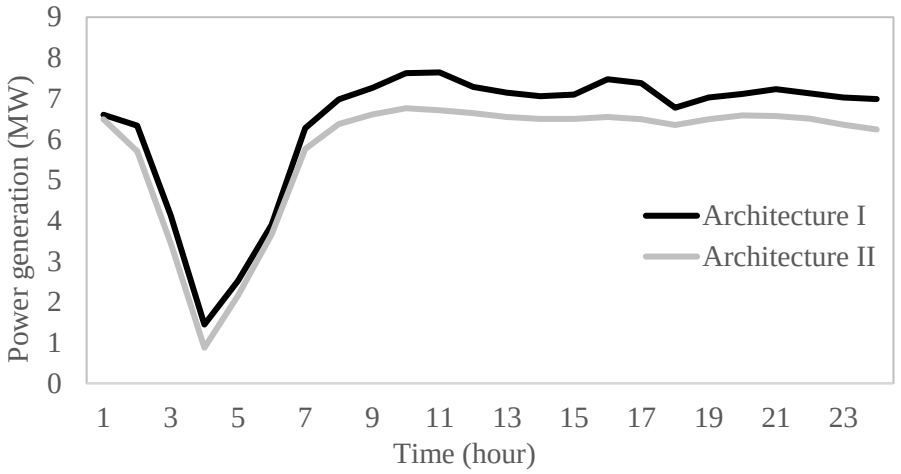

Fig. 6.12. Total Energy Awards to Aggregators in the DA Wholesale Market.

Fig. 6.13 illustrates the power outputs, maximum available capacity, and maximum qualified capacity for aggregators 4, 5, 13, and 14. These aggregators are assumed to manage different DERs (e.g., solar generation, dispatchable distributed generation, and energy storage system), making their maximum available capacity time-varying. Based on these figures, architecture I leads to the aggregators energy awards being beyond the DS OSTN hosting capacity. More specifically, any energy award beyond the dashed red line, i.e., maximum qualified capacity (translatable into the DS OSTN hosting capacity), is not consistent with the DS reliable and safe operation. However, in Fig. 6.13,

architecture II awards energy products to the aggregators lower than the maximum qualified capacity.

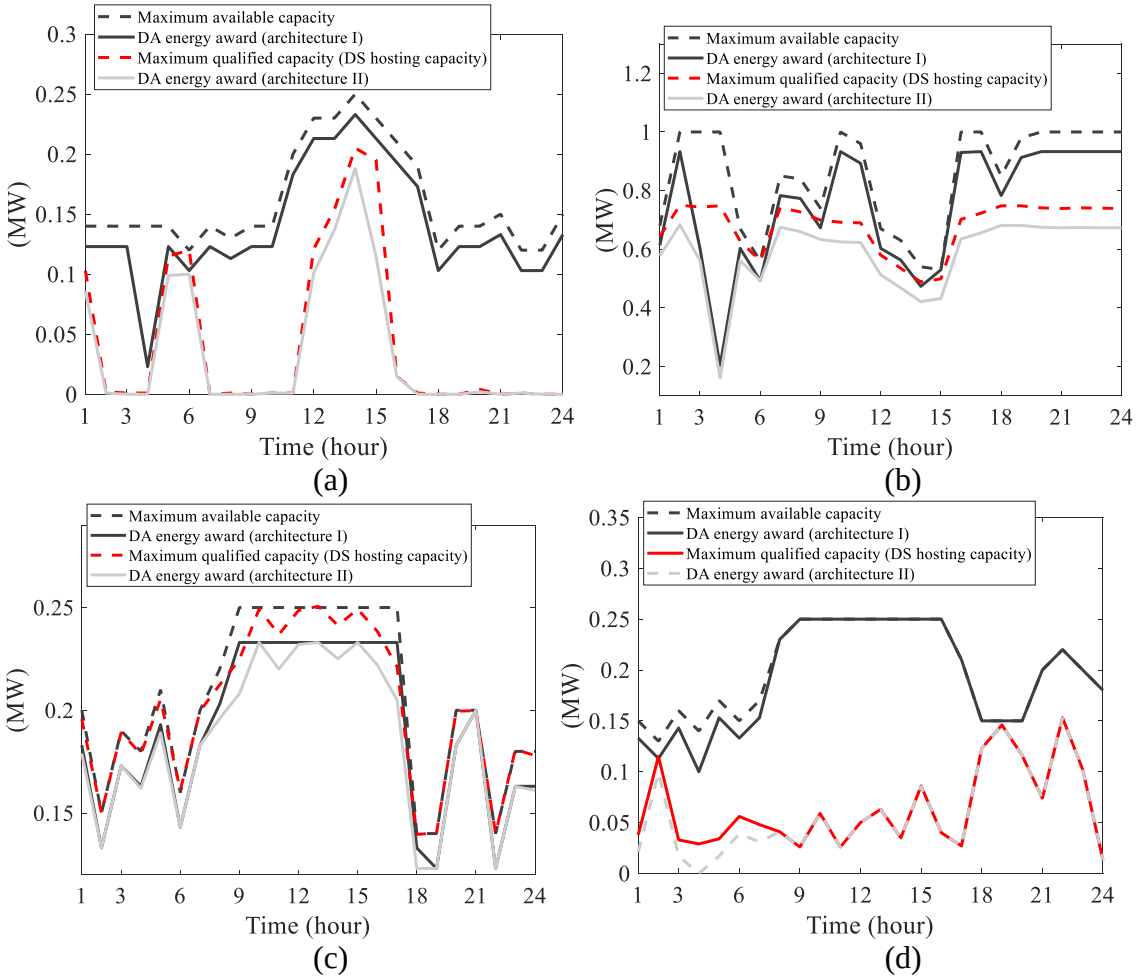

Fig. 6.13. Power Outputs, Maximum Available Capacity, and Maximum Qualified Capacity of: (a) Aggregators # 4, (b) Aggregators # 5, (c) Aggregators # 13, and (d) Aggregators # 14.

Table 6.5. Cases with Non-zero Voltage Violation; Total # of Cases= 1101600, i.e., 100 (# of Uncertain Events) × 459 (# of Bus-Phases) × 24 (# of Time Intervals).

	Architecture I	Architecture II
Total cases of voltage violation (passing maximum)	111755	151
Total cases of voltage violation (passing minimum)	0	0
Total cases of current violation	0	0

Table 6.5 lists the number of cases in which each architecture leads to non-zero voltage violation while evaluating DS operational limits during uncertain events. The total number of cases is 1101600, which is obtained through multiplying the number of bus phases, i.e., 459, by the number of time intervals, i.e., 24, and by the number of uncertain event scenarios, i.e., 100. Based on this table, the number of cases with a non-zero value for architecture I is 111755, which is considerably higher than that of architecture II, which is 151. This reduction is because architecture II preemptively and dynamically considers the DS OSTN hosting capacity effects on the products (i.e., energy and reserve) awarded to the aggregators located in the DS network; therefore, the resulting awards considerably less frequently cause voltage violation in DS. Also, Table 6.5 shows that there was no current thermal violation for this case study. The corresponding histogram of the voltage violations with non-zero value is given in Fig. 6.14 for both architectures. From Fig. 6.14(a), it can be seen that the voltage violation issue happens more frequently for architecture I, with a maximum value around 0.013 pu. In comparison, this value for architecture II equals 0.0005 pu with much less occurring frequency. These results show that the proposed data-driven distribution system operator and ISO coordination framework is effectively capable of awarding energy and reserve products within the hosting capacity of the DS network to the aggregators, which consequently leads to the reliable and safe operation of DS while allowing the aggregators to participate in the wholesale markets. Furthermore, Fig. 6.15 provides one example of how the voltage magnitude looks across 100 transmission-level uncertain scenarios at bus # 1009, phase 3, and time 10 for architectures I and II. As it can be seen,

the voltage histogram entirely falls behind the voltage magnitude limit for architecture II; however, the voltage histogram passes the voltage magnitude limit for architecture I.

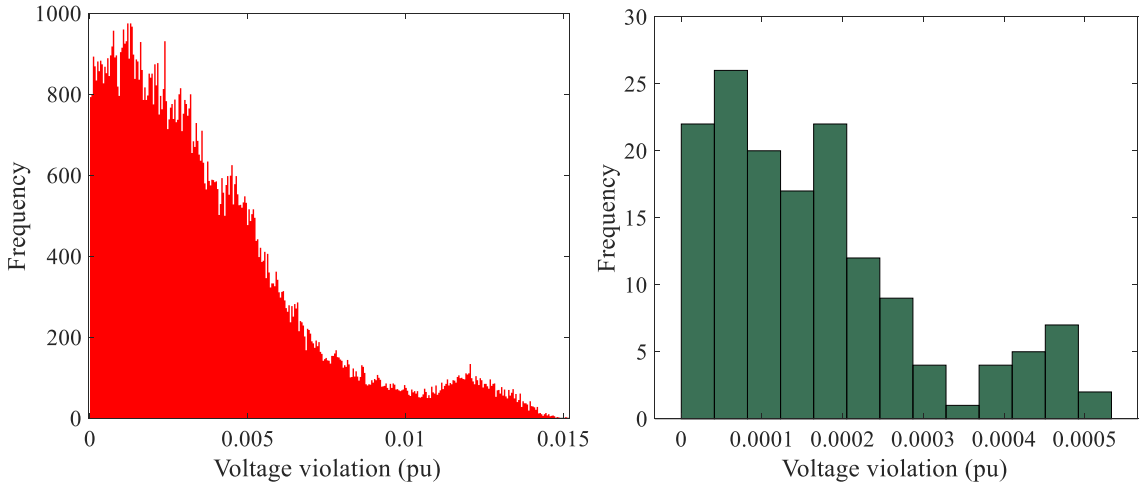

(a) (b)

Fig. 6.14. Histogram of Voltage Violations with Non-Zero Value: (a) Architecture I (111755 Cases), and (b) Architecture II (151 Cases).

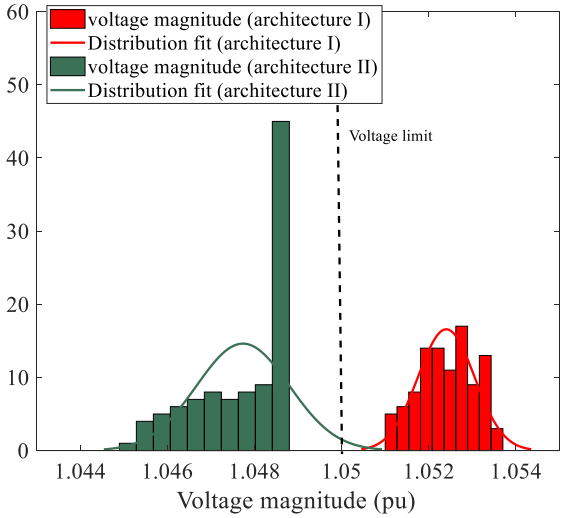

Fig. 6.15. Histogram of Voltage Magnitudes and Associated Distribution Fit at Bus # 1009, Phase 3, Time 10 for Architecture I and II Over 100 Scenarios.

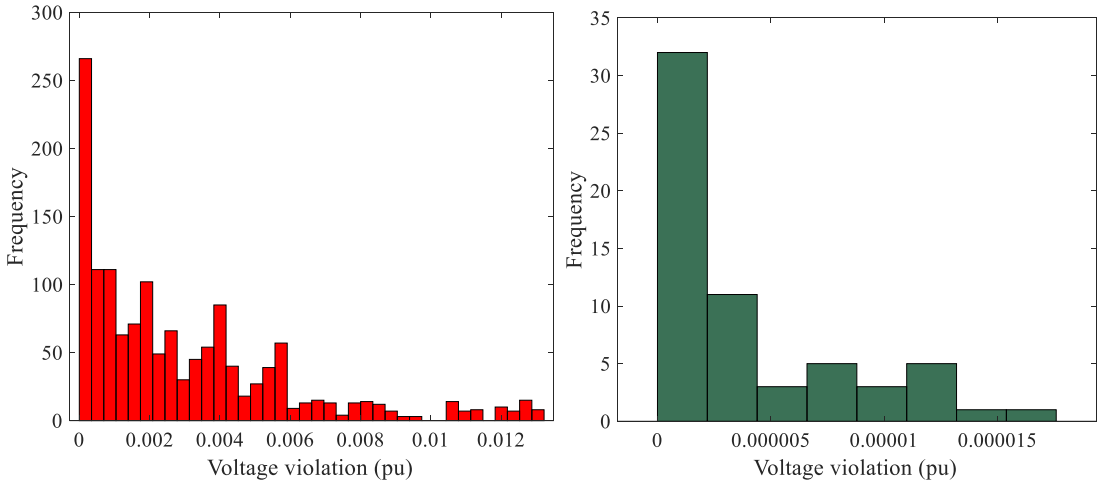

(a) (b)

Fig. 6.16. Histogram of Voltage Violations with Non-Zero Value: (a) Architecture I (1409 Cases), and (b) Architecture II (61 Cases).

Table 6.6. Cases with Non-zero Expected Voltage Violation; Total # of Cases= 11016, i.e., 459 (# of Bus-phases) × 24 (# of Time Intervals).

	Architecture I	Architecture II
Total cases of voltage violation (passing maximum)	1409	61
Total cases of voltage violation (passing minimum)	0	0
Total cases of current violation	0	0

Table 6.6 lists the number of cases where each architecture leads to non-zero expected voltage violation while evaluating DS operational limits during uncertain events. The total number of cases is 11016, which is obtained through multiplying the number of bus phases, i.e., 459, by the number of time intervals, i.e., 24. To clarify, the expected voltage violation value for each bus phase and time is obtained from averaging the corresponding voltage violation over 100 scenarios. Based on Table 6.6, the number of cases with a non-zero expected value for architectures I and II is 1409 and 61, respectively. The corresponding histogram of the expected voltage violations with non-zero value is given in Fig. 6.16 for both architectures. Finally, Table 6.7 tabulates the expected total bus phase voltage violations for different time intervals. Based on Table 6.6, Table 6.7, and

Fig. 6.16, it is clear that the proposed architecture II outperforms architecture I concerning producing wholesale market awards for aggregators that will not pose reliable and safety issues for DS.

Table 6.7. Expected Total Bus-phase Voltage Violations.

Time #	Architecture I	Architecture II	Time #	Architecture I	Architecture II
1	0.112	0	13	0.280	0
2	0.025	0	14	0.380	0.000021
3	0	0	15	0.276	0
4	0	0	16	0.409	0.000030
5	0	0	17	0.200	0
6	0	0	18	0.097	0.000113
7	0.060	0	19	0.056	0.000001
8	0.223	0	20	0.037	0
9	0.380	0	21	0.171	0.000014
10	0.368	0.000073	22	0.110	0
11	0.378	0	23	0.156	0
12	0.275	0	24	0.166	0
Architecture I, average (pu)		0.173	Architecture I, max (pu)		0.409
Architecture II, average (pu)		0.000010	Architecture II, max (pu)		0.000113

6.6. Conclusion

Concerning the ever-growing trend towards more and more utilization of DERs, the ISOs were mandated by FERC order No. 2222 to create proper coordination frameworks between the ISO, aggregators, distribution system operators to ensure safe power system operation. One possible coordination framework is DERs directly participate in the wholesale market through the role of aggregators. At the same time, the distribution system operator is primarily responsible for the safe and reliable operation of the DS network. In this option, if the DS OSTN hosting capacity effects are not preemptively considered on the aggregators bids submitted to the wholesale market, deploying services awarded to aggregators may not be possible without posing significant risks to the DS

operation. The reason is that the aggregators participate in the transmission-level wholesale market and receive dispatch instructions directly from ISOs while locating at the DS network.

In this work, two distribution system operator and ISO coordination frameworks (architectures I and II) were proposed along with the corresponding distinction and definition of the participants roles and the required information exchange in the market management systems. Architectures II enable the ISO to preemptively and dynamically have visibility over the DS limits and accordingly allow the aggregators to participate in the organized wholesale electric market based on the time-varying DS OSTN hosting capacity. To this end, architectures II employed the statistical information obtained using different DS conditions and NN algorithms to predict the hosting capacity with the most-updated DS information and loading conditions before running the DA wholesale market processes. Finally, the validation phase was presented based on the IVACOPF formulation to compare the performance of architectures II with architectures I (wherein the DS limitations are not considered during wholesale market decision-making). The validation phase goal is to mimic the DS condition during a transmission-level uncertain event. In addition, the Volt-VAr support provided by distributed PV smart inverters was leveraged to minimize DS violation.

The simulation results showed that the Volt-VAr support from the distributed PV units could mitigate the DS voltage issues due to the aggregators following ISO dispatch instructions even if the aggregators are allowed to participate in the wholesale market beyond minimum DS OSTN hosting capacity limits. This reduction was due to precisely modeling and using bi-directional utility-interactive inverters and optimally

injecting/absorbing reactive power into DS. Furthermore, the proposed architecture II outperforms architecture I concerning producing wholesale market awards for aggregators that fall within the DS OSTN hosting capacity and consequently will not impose reliable and safety issues for the DS.

Chapter 7.

FUTURE WORK

In this Section, the future work associated with the research performed in chapters 3-6 is described in detail.

7.1. Strategic Reserve Biding

Existing market models rely on approximations to the underlying stochastic program to avoid computational hurdles. These approximated market structures inadequately determine which resources are more eligible to provide reserve concerning network limits. For example, for the market model based on the proxy reserve requirement, the total contingency reserves across the power system are forced to be greater than a certain threshold. However, the procured reserves are not guaranteed to be deliverable in the post-contingency state. Furthermore, the approaches based on the reserve zone treat every generator in a zone as to have the same reserve deliverability, which is not the actual case (industry example: MISO and its reserve disqualification process after closing its DA market). The generators that provide a reserve product that can be deployed when it is needed should be better compensated for the corresponding service. Future work is needed to analyze whether an adjusted reserve bid can compensate and capture the value of providing reserve when contingencies are not explicitly modeled.

A common argument is that the reserve bid should incorporate the risk premium of carrying the reserve for deployment. The reserve bids will reflect opportunity costs between selling energy versus providing reserve for the generators; it is unclear whether they reflect a risk premium that appropriately influences LMPs such that the LMPs

adequately reflect the value of delivering an MW in the post-contingency state when that post-contingency state is not explicitly modeled. Further research should be conducted to demonstrate that if a strategic reserve bid adequately captures the value of security in comparison to when contingencies are explicitly modeled.

7.2. Extending the DA FRP Formulation

The focus of chapter 4 was to improve DA operational scheduling models to enhance flexibility procurement and ramp-responsiveness from available resources. The future research direction can include (i) incorporating other flexible resources including energy storage systems and adjustable loads in the proposed DA FRP scheduling framework, and (ii) extending the proposed FRP design to the RTUC problem with 15-min granularity to capture 5-min variability and uncertainty in the RT economic dispatch.

7.3. Pricing Implication of the Proposed Deployable FMM FRP Design

Existing electricity market operators model their energy markets with a proxy ramping requirement, which do not account for and guarantee post-deployment of FRPs awards. To compensate for this inability to account for post-deployment of FRPs, the operator may intervene and make adjustments in the market solutions to increase the system ramp capability. Such interventions are referred to as out-of-market corrections or exceptional dispatches which include committing additional generation units or redispatching committed units.

Such market models are unable to account for the true value of ramping capability provided by each generation resource on a nodal basis simply due to the fact that they do not account for and guarantee post-deployment of FRPs awards. Consequently, they

might not properly incentivize resources to do as directed by the market. These inabilities to impact market prices can lead to insufficient compensation received by generation resources and cause a natural unfairness as market participants might not be dispatched fairly with these pricing schemes.

One of the impacts that the proposed data-driven FRP policy in chapter 5 has on pricing is how it impacts the LMPs. Typically, LMP comprises three components, which are the marginal energy, marginal congestion, and marginal loss components. It can be assessed that, by implementing the proposed data-driven FRP policy, what additional amount, e.g., additional congestion component resulted from a post-deployment of FRP awards, are added to LMP and how the generators should be compensated for providing the ramping capabilities. It is expected that since chapter 5 enhance the deployability of FRP awards in FMMs, it will mathematically lead to more precise price signals for FRPs since the market model initially better captures the post-deployment of FRP awards that influences actual market outcome in the first place and consequently less out-of-market corrections or exceptional dispatches are needed. In other words, since the market solution initially captures the post-deployment of FRP awards, the resulting LMPs can potentially be capable of rewarding locations that procure higher-quality FRP awards concerning the transmission line limits.

7.4. Improving ISO, Distribution System Operator, and Aggregators Coordination Frameworks

The features used in the neural network functions in architecture II select the loading conditions as the primary features; however, the hosting capacity of the DS is also affected by other factors, including DS configuration and uncertainties imposed by DERs,

etc. Future work can consider these factors in predicting the DS OSTN hosting capacity. Additionally, the DS flexibility can come from various sources: Volt/VAR support from DERs smart inverters, DS reconfiguration, DS services provided by aggregators, etc. Suppose these flexibilities are used and managed correctly. In that case, it can help mitigate violation in the DS even if aggregators are allowed to participate in the wholesale market beyond the minimum DS OSTN hosting capacity limit. Future work can model these flexibilities in the IVACOPF to mitigate adverse impacts of aggregators power generation beyond the DS OSTN hosting capacity, during the transmission and distribution management in the case of transmission-level uncertain events.

REFERENCES

[1] FERC, “Guide to Market Oversight – Glossary,” 2016. http://www.ferc.gov/market-oversight/guide/glossary.asp

[2] FERC, “Workshop Summary Report: R&D for Dispatchable Distributed Energy Resources at Manufacturing Sites,” Apr. 2016. https://www.energy.gov/sites/default/files/2017/02/f34/AMO%20Dispatchable%20DG%20and%20Manufacturing_Workshop%20Report_FINAL.pdf

[3] National Academy of Engineering, “Modernizing and Protecting the Electricity Grid,” Spring 2010. https://nae.edu/18627/Modernizing-and-Protecting-the-Electricity-Grid (accessed Oct. 16, 2019).

[4] NERC, “Reliability concepts,” Mar. 2016. http://www.nerc.com/files/concepts_v1.0.2.pdf

[5] M. Sahraei-Ardakani and K. W. Hedman, “Day-Ahead Corrective Adjustment of FACTS Reactance: A Linear Programming Approach,” *IEEE Transactions on Power Systems*, vol. 31, no. 4, pp. 2867–2875, Jul. 2016, doi: 10.1109/TPWRS.2015.2475700.

[6] Y. Chen, P. Gribik, and J. Gardner, “Incorporating Post Zonal Reserve Deployment Transmission Constraints Into Energy and Ancillary Service Co-Optimization,” *IEEE Transactions on Power Systems*, vol. 29, no. 2, pp. 537–549, Mar. 2014, doi: 10.1109/TPWRS.2013.2284791.

[7] M. Abdi-Khorsand, M. Sahraei-Ardakani, and Y. M. Al-Abdullah, “Corrective Transmission Switching for N-1-1 Contingency Analysis,” *IEEE Transactions on Power Systems*, vol. 32, no. 2, pp. 1606–1615, Mar. 2017, doi: 10.1109/TPWRS.2016.2614520.

[8] CAISO, “Market Performance Metric Catalog,” Nov. 2019. http://www.caiso.com/Documents/MarketPerformanceMetricCatalogforNovember2019.pdf

[9] B. F. Hobbs, M.-C. Hu, J. G. Inon, S. E. Stoft, and M. P. Bhavaraju, “A Dynamic Analysis of a Demand Curve-Based Capacity Market Proposal: The PJM Reliability Pricing Model,” *IEEE Transactions on Power Systems*, vol. 22, no. 1, pp. 3–14, Feb. 2007, doi: 10.1109/TPWRS.2006.887954.

[10] P. Gribik, W. Hogan, and S. Pope, “Market-Clearing Electricity Prices and Energy Uplift,” 2007. http://www.lmpmarketdesign.com/papers/Gribik_Hogan_Pope_Price_Uplift_123107.pdf

[11] CAISO, “Draft final proposal: Generator contingency and remedial action scheme modeling,” Jul. 2017. https://www.caiso.com/Documents/DraftFinalProposal-GeneratorContingencyandRemedialActionSchemeModeling_updatedjul252017.pdf

[12] F. Bouffard, F. D. Galiana, and A. J. Conejo, “Market-clearing with stochastic security-part I: formulation,” *IEEE Transactions on Power Systems*, vol. 20, no. 4, pp. 1818–1826, Nov. 2005, doi: 10.1109/TPWRS.2005.857016.

[13] S. Wong and J. D. Fuller, “Pricing Energy and Reserves Using Stochastic Optimization in an Alternative Electricity Market,” *IEEE Transactions on Power Systems*, vol. 22, no. 2, pp. 631–638, May 2007, doi: 10.1109/TPWRS.2007.894867.

[14] R. Fernández-Blanco, Y. Dvorkin, and M. A. Ortega-Vazquez, “Probabilistic Security-Constrained Unit Commitment With Generation and Transmission Contingencies,” *IEEE Transactions on Power Systems*, vol. 32, no. 1, pp. 228–239, Jan. 2017, doi: 10.1109/TPWRS.2016.2550585.

[15] C. J. López-Salgado, O. Añó, and D. M. Ojeda-Esteybar, “Stochastic Unit Commitment and Optimal Allocation of Reserves: A Hybrid Decomposition Approach,” *IEEE Transactions on Power Systems*, vol. 33, no. 5, pp. 5542–5552, Sep. 2018, doi: 10.1109/TPWRS.2018.2817639.

[16] V. Guerrero-Mestre, Y. Dvorkin, R. Fernández-Blanco, M. A. Ortega-Vazquez, and J. Contreras, “Incorporating energy storage into probabilistic security-constrained unit commitment,” *IET Generation Transmission Distribution*, vol. 12, no. 18, pp. 4206–4215, 2018, doi: 10.1049/iet-gtd.2018.5413.

[17] J. M. Arroyo and F. D. Galiana, “Energy and reserve pricing in security and network-constrained electricity markets,” *IEEE Transactions on Power Systems*, vol. 20, no. 2, pp. 634–643, May 2005, doi: 10.1109/TPWRS.2005.846221.

[18] J. Wang, M. Shahidehpour, and Z. Li, “Contingency-Constrained Reserve Requirements in Joint Energy and Ancillary Services Auction,” *IEEE Transactions on Power Systems*, vol. 24, no. 3, pp. 1457–1468, Aug. 2009, doi: 10.1109/TPWRS.2009.2022983.

[19] Z. Guo, R. L. Chen, N. Fan, and J. Watson, “Contingency-Constrained Unit Commitment With Intervening Time for System Adjustments,” *IEEE Transactions on Power Systems*, vol. 32, no. 4, pp. 3049–3059, Jul. 2017, doi: 10.1109/TPWRS.2016.2612680.

[20] CAISO, “2018 annual report on market issues & performance,” May 2019. http://www.caiso.com/Documents/2018AnnualReportonMarketIssuesandPerformance.pdf

[21] CAISO, “What the duck curve tells us about managing a green grid,” 2016. www.caiso.com/Documents/FlexibleResourcesHelpRenewables_FastFacts.pdf

[22] CAISO, “Day-Ahead Market Enhancements,” Mar. 2019. http://www.caiso.com/Documents/Presentation-Day-AheadMarketEnhancementsPhases1-2-Mar7-2019.pdf

[23] N. Navid, G. Rosenwald, and D. Chatterjee, “Ramp Capability for Load Following in the MISO Markets,” presented at the MISO Market Development and Analysis, Jul. 2011.

[24] CAISO, “California ISO’s Day-Ahead Market Enhancements under High Renewable Penetration Paradigm,” Jun. 2018. https://www.ferc.gov/CalendarFiles/20180627082516-20180627082014-T2%20-%201%20-%20Tretheway%20-%20CAISO%20Presentation_6-26-18_FERC%20Workshop.pdf

[25] MAISO, “Ramp Capability Modeling in MISO Dispatch and Pricing,” Jun. 2016. https://www.ferc.gov/CalendarFiles/20160629114652-1%20-%2020160621%20FERC%20Technical%20Conference_MISO%20Ramp%20Product.pdf

[26] CAISO, “Discussion on flexible ramping product,” Sep. 2017. https://www.caiso.com/Documents/Discussion_FlexibleRampingProduct.pdf

[27] CAISO, “Flexible Ramping Product: Revised Draft Final Proposal,” Dec. 2015. https://www.caiso.com/Documents/RevisedDraftFinalProposal-FlexibleRampingProduct-2015.pdf

[28] B. Wang and B. F. Hobbs, “Real-Time Markets for Flexiramp: A Stochastic Unit Commitment-Based Analysis,” *IEEE Transactions on Power Systems*, vol. 31, no. 2, pp. 846–860, Mar. 2016, doi: 10.1109/TPWRS.2015.2411268.

[29] B. Wang and B. F. Hobbs, “A flexible ramping product: Can it help real-time dispatch markets approach the stochastic dispatch ideal?,” *Electric Power Systems Research*, vol. 109, pp. 128–140, Apr. 2014, doi: 10.1016/j.epsr.2013.12.009.

[30] N. Nivad, “Ramp Capability Product Design for MISO Markets,” Dec. 2013. https://cdn.misoenergy.org/Ramp%20Capability%20for%20Load%20Following%20in%20MISO%20Markets%20White%20Paper271169.pdf

[31] CAISO, “2020 Draft Three-Year Policy Initiatives Roadmap and Annual Plan,” Sep. 2019. http://www.caiso.com/Documents/2020DraftPolicyInitiativesRoadmap.pdf

[32] CAISO, “Day-Ahead Market Enhancements,” Jun. 2019. http://www.caiso.com/InitiativeDocuments/Presentation-Day-AheadMarketEnhancementsWorkshop-Jun20-2019.pdf

[33] J. Hu, M. R. Sarker, J. Wang, F. Wen, and W. Liu, “Provision of flexible ramping product by battery energy storage in day-ahead energy and reserve markets,” *IET Generation Transmission Distribution*, vol. 12, no. 10, pp. 2256–2264, 2018, doi: 10.1049/iet-gtd.2017.1522.

[34] M. Cui, J. Zhang, H. Wu, and B.-M. Hodge, “Wind-Friendly Flexible Ramping Product Design in Multi-Timescale Power System Operations,” *IEEE Transactions on Sustainable Energy*, vol. 8, no. 3, pp. 1064–1075, Jul. 2017, doi: 10.1109/TSTE.2017.2647781.

[35] X. Zhang, L. Che, M. Shahidehpour, A. Alabdulwahab, and A. Abusorrah, "Electricity-Natural Gas Operation Planning With Hourly Demand Response for Deployment of Flexible Ramp," *IEEE Transactions on Sustainable Energy*, vol. 7, no. 3, pp. 996–1004, Jul. 2016, doi: 10.1109/TSTE.2015.2511140.

[36] M. I. Alizadeh, M. P. Moghaddam, and N. Amjady, "Multistage Multiresolution Robust Unit Commitment With Nondeterministic Flexible Ramp Considering Load and Wind Variabilities," *IEEE Transactions on Sustainable Energy*, vol. 9, no. 2, pp. 872–883, Apr. 2018, doi: 10.1109/TSTE.2017.2764061.

[37] N. Navid and G. Rosenwald, "Market Solutions for Managing Ramp Flexibility With High Penetration of Renewable Resource," *IEEE Transactions on Sustainable Energy*, vol. 3, no. 4, pp. 784–790, Oct. 2012, doi: 10.1109/TSTE.2012.2203615.

[38] X. Ma, D. Sun, and K. Cheung, "Energy and reserve dispatch in a multi-zone electricity market," *IEEE Transactions on Power Systems*, vol. 14, no. 3, pp. 913–919, Aug. 1999, doi: 10.1109/59.780903.

[39] F. A. Campos, A. M. S. Roque, E. F. Sánchez-Úbeda, and J. P. González, "Strategic Bidding in Secondary Reserve Markets," *IEEE Transactions on Power Systems*, vol. 31, no. 4, pp. 2847–2856, Jul. 2016, doi: 10.1109/TPWRS.2015.2453477.

[40] E. Ela and M. O'Malley, "Scheduling and Pricing for Expected Ramp Capability in Real-Time Power Markets," *IEEE Transactions on Power Systems*, vol. 31, no. 3, pp. 1681–1691, May 2016, doi: 10.1109/TPWRS.2015.2461535.

[41] M. Ghaljehei and M. Khorsand, "Representation of Uncertainty in Electric Energy Market Models: Pricing Implication and Formulation," *IEEE Systems Journal*, vol. 15, no. 3, pp. 3703–3713, Sep. 2021, doi: 10.1109/JSYST.2020.3025868.

[42] C. Zhao, J. Wang, J.-P. Watson, and Y. Guan, "Multi-Stage Robust Unit Commitment Considering Wind and Demand Response Uncertainties," *IEEE Transactions on Power Systems*, vol. 28, no. 3, pp. 2708–2717, Aug. 2013, doi: 10.1109/TPWRS.2013.2244231.

[43] M. Doostizadeh, F. Aminifar, H. Ghasemi, and H. Lesani, "Energy and Reserve Scheduling Under Wind Power Uncertainty: An Adjustable Interval Approach," *IEEE Transactions on Smart Grid*, vol. 7, no. 6, pp. 2943–2952, Nov. 2016, doi: 10.1109/TSG.2016.2572639.

[44] J. Bushnell, S. M. Harvey, and B. F. Hobbs, "Opinion on Flexible Ramping Product Refinement," Sep. 2020. http://www.caiso.com/Documents/MSC-OpinionOnFlexibleRampingProductEnhancements-Sep8_2020.pdf

[45] FERC, "FERC Order No. 2222." https://www.ferc.gov/media/ferc-order-no-2222-fact-sheet

[46] P. De Martini and L. Kristov, "Distribution Systems in a High Distributed Energy Resources Future," Oct. 2015. https://eta-publications.lbl.gov/sites/default/files/lbnl-1003797.pdf

[47] Z. Soltani, S. Ma, M. Ghaljehei, and M. Khorsand, “Optimal Scheduling of Distributed Energy Resources Considering Volt-VAr Controller of PV Smart Inverters,” *arXiv:2203.11448 [math]*, Mar. 2022, Accessed: Mar. 22, 2022. [Online]. Available: http://arxiv.org/abs/2203.11448

[48] X. Lu, K. Li, H. Xu, F. Wang, Z. Zhou, and Y. Zhang, “Fundamentals and business model for resource aggregator of demand response in electricity markets,” *Energy*, vol. 204, p. 117885, Aug. 2020, doi: 10.1016/j.energy.2020.117885.

[49] J. Wang *et al.*, “Optimal bidding strategy for microgrids in joint energy and ancillary service markets considering flexible ramping products,” *Applied Energy*, vol. 205, pp. 294–303, Nov. 2017, doi: 10.1016/j.apenergy.2017.07.047.

[50] B. F. Hobbs, M. H. Rothkopf, R. P. O’Neill, and H. Chao, Eds., *The Next Generation of Electric Power Unit Commitment Models*. Springer US, 2001. Accessed: Oct. 13, 2019. [Online]. Available: https://www.springer.com/gp/book/9780792373346

[51] N. P. Padhy, “Unit commitment-a bibliographical survey,” *IEEE Transactions on Power Systems*, vol. 19, no. 2, pp. 1196–1205, May 2004, doi: 10.1109/TPWRS.2003.821611.

[52] Q. P. Zheng, J. Wang, and A. L. Liu, “Stochastic Optimization for Unit Commitment—A Review,” *IEEE Transactions on Power Systems*, vol. 30, no. 4, pp. 1913–1924, Jul. 2015, doi: 10.1109/TPWRS.2014.2355204.

[53] NREL, “Western wind and solar integration study,” May 2010. http://www.nrel.gov/docs/fy10osti/47434.pdf

[54] ERCOT, “Report on Existing and Potential Electric System Constraints and Needs,” Dec. 2007. http://www. ercot.com/news/presentations/2008/35171_ERCOT_2007_Transmission_ Constraints_Needs_Report.pdf

[55] MAISO, “Tariff-Midcontinent Independent System Operator,” 2012. https://www.misoenergy.org/_layouts/ MISO/ECM/Download.aspx?ID=169142

[56] A. J. Wood and B. F. Wollenberg, *Power Generation Operation and Control*, 2nd ed. Hoboken, NJ, USA: Wiley, 1996.

[57] CAISO, “Parameter Tuning for Uneconomic Adjustments in the MRTU Market Optimizations,” May 2008. http://www.caiso.com/1fbf/ 1fbfe3a2498e0.pdf

[58] CAISO, “2012 Annual Report on Market Issues & Performance,” Apr. 2013. Available: http://www.caiso.com/Documents/2012AnnualReport- MarketIssue-Performance.pdf

[59] Y. M. Al-Abdullah, M. Abdi-Khorsand, and K. W. Hedman, “The Role of Out-of-Market Corrections in Day-Ahead Scheduling,” *IEEE Transactions on Power Systems*, vol. 30, no. 4, pp. 1937–1946, Jul. 2015, doi: 10.1109/TPWRS.2014.2353647.

[60] P. A. Ruiz, C. R. Philbrick, E. Zak, K. W. Cheung, and P. W. Sauer, "Uncertainty Management in the Unit Commitment Problem," *IEEE Transactions on Power Systems*, vol. 24, no. 2, pp. 642–651, May 2009, doi: 10.1109/TPWRS.2008.2012180.

[61] A. T. Saric, F. H. Murphy, A. L. Soyster, and A. M. Stankovic, "Two-Stage Stochastic Programming Model for Market Clearing With Contingencies," *IEEE Transactions on Power Systems*, vol. 24, no. 3, pp. 1266–1278, Aug. 2009, doi: 10.1109/TPWRS.2009.2023267.

[62] F. Bouffard, F. D. Galiana, and A. J. Conejo, "Market-clearing with stochastic security-part II: case studies," *IEEE Transactions on Power Systems*, vol. 20, no. 4, pp. 1827–1835, Nov. 2005, doi: 10.1109/TPWRS.2005.857015.

[63] B. Stott, J. Jardim, and O. Alsac, "DC Power Flow Revisited," *IEEE Transactions on Power Systems*, vol. 24, no. 3, pp. 1290–1300, Aug. 2009, doi: 10.1109/TPWRS.2009.2021235.

[64] C. Li, K. W. Hedman, and M. Zhang, "Market pricing with single-generator-failure security constraints," *IET Generation Transmission Distribution*, vol. 11, no. 7, pp. 1777–1785, 2017, doi: 10.1049/iet-gtd.2016.1589.

[65] N. G. Singhal, N. Li, and K. W. Hedman, "A Reserve Response Set Model for Systems with Stochastic Resources," *IEEE Transactions on Power Systems*, vol. 33, no. 4, pp. 4038–4049, Jul. 2018, doi: 10.1109/TPWRS.2017.2776202.

[66] N. G. Singhal, N. Li, and K. W. Hedman, "A Data-Driven Reserve Response Set Policy for Power Systems With Stochastic Resources," *IEEE Transactions on Sustainable Energy*, vol. 10, no. 2, pp. 693–705, Apr. 2019, doi: 10.1109/TSTE.2018.2845895.

[67] C. Wang, P. Bao-Sen Luh, and N. Navid, "Ramp Requirement Design for Reliable and Efficient Integration of Renewable Energy," *IEEE Transactions on Power Systems*, vol. 32, no. 1, pp. 562–571, Jan. 2017, doi: 10.1109/TPWRS.2016.2555855.

[68] M. Khoshjahan, M. Moeini-Aghtaie, and M. Fotuhi-Firuzabad, "Developing new participation model of thermal generating units in flexible ramping market," *IET Generation Transmission Distribution*, vol. 13, pp. 2290–2298, 2019, doi: 10.1049/iet-gtd.2018.6244.

[69] M. Khoshjahan, P. Dehghanian, M. Moeini-Aghtaie, and M. Fotuhi-Firuzabad, "Harnessing Ramp Capability of Spinning Reserve Services for Enhanced Power Grid Flexibility," *IEEE Transactions on Industry Applications*, pp. 1–1, 2019, doi: 10.1109/TIA.2019.2921946.

[70] S. Sreekumar, K. C. Sharma, and R. Bhakar, "Multi-Interval Solar Ramp Product to Enhance Power System Flexibility," *IEEE Systems Journal*, vol. 15, no. 1, pp. 170–179, Mar. 2021, doi: 10.1109/JSYST.2020.3001145.

[71] X. Fang, K. S. Sedzro, H. Yuan, H. Ye, and B.-M. Hodge, "Deliverable Flexible Ramping Products Considering Spatiotemporal Correlation of Wind Generation

and Demand Uncertainties," *IEEE Transactions on Power Systems*, vol. 35, no. 4, pp. 2561–2574, Jul. 2020, doi: 10.1109/TPWRS.2019.2958531.

[72] H. Ye and Z. Li, "Deliverable Robust Ramping Products in Real-Time Markets," *IEEE Transactions on Power Systems*, vol. 33, no. 1, pp. 5–18, Jan. 2018, doi: 10.1109/TPWRS.2017.2688972.

[73] C. Wu, G. Hug, and S. Kar, "Risk-Limiting Economic Dispatch for Electricity Markets With Flexible Ramping Products," *IEEE Transactions on Power Systems*, vol. 31, no. 3, pp. 1990–2003, May 2016, doi: 10.1109/TPWRS.2015.2460748.

[74] B. Zhang and M. Kezunovic, "Impact on Power System Flexibility by Electric Vehicle Participation in Ramp Market," *IEEE Transactions on Smart Grid*, vol. 7, no. 3, pp. 1285–1294, May 2016, doi: 10.1109/TSG.2015.2437911.

[75] E. Heydarian-Forushani, M. E. H. Golshan, M. Shafie-khah, and P. Siano, "Optimal Operation of Emerging Flexible Resources Considering Sub-Hourly Flexible Ramp Product," *IEEE Transactions on Sustainable Energy*, vol. 9, no. 2, pp. 916–929, Apr. 2018, doi: 10.1109/TSTE.2017.2766088.

[76] S. Aggarwal and R. Orvis, "Grid flexibility: methods for modernizing the power grid," Mar. 2016. https://energyinnovation.org/wp-content/uploads/2016/05/Grid-Flexibility-report.pdf

[77] Q. Wang and B. Hodge, "Enhancing Power System Operational Flexibility With Flexible Ramping Products: A Review," *IEEE Transactions on Industrial Informatics*, vol. 13, no. 4, pp. 1652–1664, Aug. 2017, doi: 10.1109/TII.2016.2637879.

[78] R. Chen, J. Wang, A. Botterud, and H. Sun, "Wind Power Providing Flexible Ramp Product," *IEEE Transactions on Power Systems*, vol. 32, no. 3, pp. 2049–2061, May 2017, doi: 10.1109/TPWRS.2016.2603225.

[79] P. De Martini and L. Kristov, "Distribution Systems in a High Distributed Energy Resources Future: Planning, Market Design, Operation and Oversight," Nov. 2015. https://eta-publications.lbl.gov/sites/default/files/lbnl-1003797_presentation.pdf

[80] C. Cano, "FERC Order No. 2222: A New Day for Distributed Energy Resources," Sep. 2020. https://www.ferc.gov/media/ferc-order-no-2222-fact-sheet

[81] M. Mousavi and M. Wu, "A DSO Framework for Market Participation of DER Aggregators in Unbalanced Distribution Networks," *IEEE Transactions on Power Systems*, pp. 1–1, 2021, doi: 10.1109/TPWRS.2021.3117571.

[82] S. Thomas, "Evolution of the Distribution System & the Potential for Distribution-level Markets: A Primer for State Utility Regulators," Jan. 2018. https://www.naruc.org/default/assets/File/201801%20Evolution%20of%20the%20Distribution%20System.pdf

[83] Y. K. Renani, M. Ehsan, and M. Shahidehpour, "Optimal Transactive Market Operations With Distribution System Operators," *IEEE Transactions on Smart Grid*, vol. 9, no. 6, pp. 6692–6701, Nov. 2018, doi: 10.1109/TSG.2017.2718546.

[84] G. Muñoz-Delgado, J. Contreras, and J. M. Arroyo, "Distribution System Expansion Planning Considering Non-Utility-Owned DG and an Independent Distribution System Operator," *IEEE Transactions on Power Systems*, vol. 34, no. 4, pp. 2588–2597, Jul. 2019, doi: 10.1109/TPWRS.2019.2897869.

[85] S. Chen *et al.*, "Forming Bidding Curves for a Distribution System Operator," *IEEE Transactions on Power Systems*, vol. 33, no. 5, pp. 5389–5400, Sep. 2018, doi: 10.1109/TPWRS.2018.2821673.

[86] T. Soares, R. J. Bessa, P. Pinson, and H. Morais, "Active Distribution Grid Management Based on Robust AC Optimal Power Flow," *IEEE Transactions on Smart Grid*, vol. 9, no. 6, pp. 6229–6241, Nov. 2018, doi: 10.1109/TSG.2017.2707065.

[87] S. Wang, B. Sun, X. Tan, T. Liu, and D. H. K. Tsang, "Real-Time Coordination of Transmission and Distribution Networks via Nash Bargaining Solution," *IEEE Transactions on Sustainable Energy*, vol. 12, no. 4, pp. 2238–2254, Oct. 2021, doi: 10.1109/TSTE.2021.3087130.

[88] M. Di Somma, G. Graditi, and P. Siano, "Optimal Bidding Strategy for a DER Aggregator in the Day-Ahead Market in the Presence of Demand Flexibility," *IEEE Transactions on Industrial Electronics*, vol. 66, no. 2, pp. 1509–1519, Feb. 2019, doi: 10.1109/TIE.2018.2829677.

[89] S. I. Vagropoulos and A. G. Bakirtzis, "Optimal Bidding Strategy for Electric Vehicle Aggregators in Electricity Markets," *IEEE Transactions on Power Systems*, vol. 28, no. 4, pp. 4031–4041, Nov. 2013, doi: 10.1109/TPWRS.2013.2274673.

[90] M. González Vayá and G. Andersson, "Optimal Bidding Strategy of a Plug-In Electric Vehicle Aggregator in Day-Ahead Electricity Markets Under Uncertainty," *IEEE Transactions on Power Systems*, vol. 30, no. 5, pp. 2375–2385, Sep. 2015, doi: 10.1109/TPWRS.2014.2363159.

[91] Z. Xu, Z. Hu, Y. Song, and J. Wang, "Risk-Averse Optimal Bidding Strategy for Demand-Side Resource Aggregators in Day-Ahead Electricity Markets Under Uncertainty," *IEEE Transactions on Smart Grid*, vol. 8, no. 1, pp. 96–105, Jan. 2017, doi: 10.1109/TSG.2015.2477101.

[92] S. Ghavidel, M. J. Ghadi, A. Azizivahed, J. Aghaei, L. Li, and J. Zhang, "Risk-Constrained Bidding Strategy for a Joint Operation of Wind Power and CAES Aggregators," *IEEE Transactions on Sustainable Energy*, vol. 11, no. 1, pp. 457–466, Jan. 2020, doi: 10.1109/TSTE.2019.2895332.

[93] C. A. Correa-Florez, A. Michiorri, and G. Kariniotakis, "Optimal Participation of Residential Aggregators in Energy and Local Flexibility Markets," *IEEE Transactions on Smart Grid*, vol. 11, no. 2, pp. 1644–1656, Mar. 2020, doi: 10.1109/TSG.2019.2941687.

[94] H. S. Moon, Y. G. Jin, Y. T. Yoon, and S. W. Kim, "Prequalification Scheme of a Distribution System Operator for Supporting Wholesale Market Participation of a

Distributed Energy Resource Aggregator," *IEEE Access*, vol. 9, pp. 80434–80450, 2021, doi: 10.1109/ACCESS.2021.3085002.

[95] D. Koraki and K. Strunz, "Wind and Solar Power Integration in Electricity Markets and Distribution Networks Through Service-Centric Virtual Power Plants," *IEEE Transactions on Power Systems*, vol. 33, no. 1, pp. 473–485, Jan. 2018, doi: 10.1109/TPWRS.2017.2710481.

[96] University of Washington, "Power systems test case archive," 1999. http://www.ee.washington.edu/research/pstca/index.html

[97] https://drive.google.com/file/d/1G0o2VyWw2tVj8YnMadzoJrTDUpWm7KIz/view?usp=sharing&usp=embed_facebook (Accessed Aug. 04, 2020).

[98] CAISO, "Ancillary Services." https://www.caiso.com/Documents/Sections2_5-2_6.pdf

[99] CAISO, "California Independent System Operator Corporation Fifth Replacement Electronic Tariff," Aug. 2019. http://www.caiso.com/Documents/Section34-Real-TimeMarket-asof-Aug12-2019.pdf

[100] IEEE 118 bus test system, 2015. motor.ece.iit.edu/Data/118bus_ro.xls

[101] CAISO, "Today's Outlook." http://www.caiso.com/TodaysOutlook/Pages/default.aspx (accessed Aug. 25, 2020).

[102] N. G. Singhal, N. Li, and K. W. Hedman, "A Reserve Response Set Model for Systems with Stochastic Resources," *IEEE Transactions on Power Systems*, vol. 33, no. 4, pp. 4038–4049, Jul. 2018, doi: 10.1109/TPWRS.2017.2776202.

[103] S. K, *Probability Random Variables and Stochastic Processes Fourth Edition Papoulis*. Accessed: Nov. 01, 2019. [Online]. Available: https://www.academia.edu/35834044/Probability_Random_Variables_and_Stochastic_Processes_Fourth_Edition_Papoulis

[104] CAISO, "Ancillary services requirements protocol." https://www.caiso.com/Documents/AncillaryServicesRequirementsProtocol_ASRP_03-Feb-98.pdf

[105] W. G. Wood, "Spinning Reserve Constrained Static and Dynamic Economic Dispatch," *IEEE Transactions on Power Apparatus and Systems*, vol. PAS-101, no. 2, pp. 381–388, Feb. 1982, doi: 10.1109/TPAS.1982.317118.

[106] L. T. Anstine, R. E. Burke, J. E. Casey, R. Holgate, R. S. John, and H. G. Stewart, "Application of Probability Methods to the Determination of Spinning Reserve Requirements for the Pennsylvania-New Jersey-Maryland Interconnection," *IEEE Transactions on Power Apparatus and Systems*, vol. 82, no. 68, pp. 726–735, Oct. 1963, doi: 10.1109/TPAS.1963.291390.

[107] R. Sioshansi and W. Short, "Evaluating the Impacts of Real-Time Pricing on the Usage of Wind Generation," *IEEE Transactions on Power Systems*, vol. 24, no. 2, pp. 516–524, May 2009, doi: 10.1109/TPWRS.2008.2012184.

[108] D. Streiffert, R. Philbrick, and A. Ott, "A mixed integer programming solution for market clearing and reliability analysis," in *IEEE Power Engineering Society General Meeting, 2005*, Jun. 2005, pp. 2724-2731 Vol. 3. doi: 10.1109/PES.2005.1489108.

[109] T. Mount *et al.*, "The Economic Implications of Adding Wind Capacity to a Bulk Power Transmission Network," 2008.

[110] J. M. Morales, A. J. Conejo, and J. Perez-Ruiz, "Economic Valuation of Reserves in Power Systems With High Penetration of Wind Power," *IEEE Transactions on Power Systems*, vol. 24, no. 2, pp. 900–910, May 2009, doi: 10.1109/TPWRS.2009.2016598.

[111] J. J. Hargreaves and B. F. Hobbs, "Commitment and Dispatch With Uncertain Wind Generation by Dynamic Programming," *IEEE Transactions on Sustainable Energy*, vol. 3, no. 4, pp. 724–734, Oct. 2012, doi: 10.1109/TSTE.2012.2199526.

[112] R. Jiang, M. Zhang, G. Li, and Y. Guan, "Two-Stage Robust Power Grid Optimization Problem," 2011.

[113] L. Zhao and B. Zeng, "Robust unit commitment problem with demand response and wind energy," in *2012 IEEE Power and Energy Society General Meeting*, Jul. 2012, pp. 1–8. doi: 10.1109/PESGM.2012.6344860.

[114] R. Jiang, J. Wang, and Y. Guan, "Robust Unit Commitment With Wind Power and Pumped Storage Hydro," *IEEE Transactions on Power Systems*, vol. 27, no. 2, pp. 800–810, May 2012, doi: 10.1109/TPWRS.2011.2169817.

[115] C. Zhao and Y. Guan, "Unified Stochastic and Robust Unit Commitment," *IEEE Transactions on Power Systems*, vol. 28, no. 3, pp. 3353–3361, Aug. 2013, doi: 10.1109/TPWRS.2013.2251916.

[116] M. Ghaljehei and M. Khorsand, "Day-ahead Operational Scheduling with Enhanced Flexible Ramping Product: Design and Analysis," *IEEE Transactions on Power Systems*, pp. 1–1, 2021, doi: 10.1109/TPWRS.2021.3110712.

[117] CAISO, "Flexible Ramping Product: Draft Final Technical Appendix," Jan. 2016. http://www.caiso.com/documents/addendum-draftfinaltechnicalappendix-flexiblerampingproduct.pdf

[118] "IEEE Standard for Interconnection and Interoperability of Distributed Energy Resources with Associated Electric Power Systems Interfaces," *IEEE Std 1547-2018 (Revision of IEEE Std 1547-2003)*, pp. 1–138, Apr. 2018, doi: 10.1109/IEEESTD.2018.8332112.

[119] Z. Soltani, S. Ma, M. Khorsand, and V. Vittal, "Simultaneous Robust State Estimation, Topology Error Processing, and Outage Detection for Unbalanced

Distribution Systems," *arXiv:2105.10111 [math]*, May 2021, Accessed: Feb. 27, 2022. [Online]. Available: http://arxiv.org/abs/2105.10111

[120] "Iowa Distribution Test Systems." http://wzy.ece.iastate.edu/Testsystem.html (accessed Apr. 01, 2022).

APPENDIX A

PTDF AND LODF CALCULATION

PTDF and LODF are linear sensitivity factors (LSFs) that can be obtained from the analysis of the Jacobian Matrix from the power flow equations [56]. These factors are calculated for a particular topology of the grid and have been the common practice utilized at different market processes in many U.S. independent system operators. The detailed explanations of these factors are given below. Please note that in these explanations, line k is between buses i and j, and line ℓ is between buses n and m. More information on how to calculate these LSFs can be found in [56].

Power transfer distribution factor ($PTDF_{cnk}^{ref}$): this factor represents the resulting flow on line k due to 1 MW injection at bus n and withdrawal at the reference. For scenario c associated with the generators' contingency (i.e., $c \in C_g$), the PTDF is the same as the one in the base-case scenario since the generators' contingency does not change the topology, ($PTDF_{0nk}^{ref}$ =$PTDF_{cnk}^{ref}$ for $c \in C_g$). On the other hand, for scenario c associated with the transmission lines' contingency (i.e., $c \in C_k$), the PTDF should be recalculated for the new topology resulted from the outage of transmission line ℓ. Mathematically, the PTDF can be calculated through the equation A.1 [56].

$$PTDF_{cnk}^{ref} = \frac{1}{x_k}(X_{cjn} - X_{cin}) \quad \text{(A.1)}$$

Where x_k is the reactance of line k, and X_{cjn} and X_{cin} are the elements in the linear power flow equation $\Delta\theta = [X]\Delta P$. Please note that $\Delta\theta$ and ΔP are the vectors of the voltage angle and MW changes in each bus.

Line outage distribution factor ($LODF_{k\ell}^{ref}$): this factor represents the portion of pre-outage active power flow on the line ℓ that is redistributed to the line k after outage of the

line ℓ. LODF allows the system operator to determine the resulting flow on a particular line k due to the loss of line ℓ. It can be proven that LODF can be calculated using PTDF values via equation A.2 [56].

$$LODF_{k\ell}^{ref} = PTDF_{0nk}^{m}\left(\frac{1}{1-PTDF_{0n\ell}^{m}}\right) \quad \text{(A.2)}$$

APPENDIX B

DERIVATION PROCESSES OF PRIMAL-DUAL FORMULATION AND CS CONDITION FOR DA MARKET WITH PROPOSED FRP DESIGN

In this section, the detailed derivation process for the new market payment (presented in Section 4.3) for the proposed FRP design is elaborated. The DA market model (4.37)-(4.38) is a MILP, and therefore the dual formulation is not well-defined. To derivate the dual variables and dual formulation, the linear programming problem created in the node with the best feasible integer solution in the Branch-and-Bound algorithm can be utilized. After deriving full dual formulation, dual constraints related to variables $ur_{g,t}$ and $ur_{g,t}^{ih}$ can be written as (B1) and (B2), respectively.

$$-\alpha_{gt}^{+} - \beta_{gt}^{+} + \pi_{t}^{+} + \omega_{gt}^{+} \leq 0, \forall g, t \qquad \left(ur_{gt}\right) \tag{B.1}$$

$$\pi_{t}^{ih,+} - \beta_{gt}^{ih,+} - \omega_{gt}^{+} \leq 0, \forall g, t \qquad \left(ur_{gt}^{ih}\right) \tag{B.2}$$

For calculating the new FRP market payment for a generator with up DA FRP award, CS conditions associated with constraints (B2) and (4.29) are respectively implemented as follows.

$$\omega_{gt}^{+} ur_{g,t}^{ih} = \pi_{t}^{ih,+} ur_{g,t}^{ih} - \beta_{gt}^{ih,+} ur_{g,t}^{ih}, \forall g, t \tag{B.3}$$

$$\omega_{gt}^{+} ur_{g,t}^{ih} = \omega_{gt}^{+} ur_{g,t}, \forall g, t \tag{B.4}$$

Then, the substitution of (B4) in (B3) results in (B5).

$$\omega_{gt}^{+} ur_{g,t} = \pi_{t}^{ih,+} ur_{g,t}^{ih} - \beta_{gt}^{ih,+} ur_{g,t}^{ih}, \forall g, t \tag{B.5}$$

Furthermore, the CS condition associated with the constraint (B1) can be written as (B6).

$$\omega_{gt}^{+} ur_{g,t} = \alpha_{gt}^{+} ur_{g,t} + \beta_{gt}^{+} ur_{g,t} - \pi_{t}^{+} ur_{g,t}, \forall g, t \tag{B.6}$$

Finally, by substituting (B6) in (B5) and performing rearrangements, equation (B7) can be derived.

$$\pi_{t}^{+} ur_{g,t} + \pi_{t}^{ih,+} ur_{g,t}^{ih} = \alpha_{gt}^{+} ur_{g,t} + \beta_{gt}^{+} ur_{g,t} + \beta_{gt}^{ih,+} ur_{g,t}^{ih}, \forall g, t \tag{B.7}$$